



National Library
of Canada

Bibliothèque nationale
du Canada

Canadian Theses Service

Service des thèses canadiennes

Ottawa, Canada
K1A 0N4

NOTICE

The quality of this microform is heavily dependent upon the quality of the original thesis submitted for microfilming. Every effort has been made to ensure the highest quality of reproduction possible.

If pages are missing, contact the university which granted the degree.

Some pages may have indistinct print especially if the original pages were typed with a poor typewriter ribbon or if the university sent us an inferior photocopy.

Reproduction in full or in part of this microform is governed by the Canadian Copyright Act, R.S.C. 1970, c. C-30, and subsequent amendments.

AVIS

La qualité de cette microforme dépend grandement de la qualité de la thèse soumise au microfilmage. Nous avons tout fait pour assurer une qualité supérieure de reproduction.

S'il manque des pages, veuillez communiquer avec l'université qui a conféré le grade.

La qualité d'impression de certaines pages peut laisser à désirer, surtout si les pages originales ont été dactylographiées à l'aide d'un ruban usé ou si l'université nous a fait parvenir une photocopie de qualité inférieure.

La reproduction, même partielle, de cette microforme est soumise à la Loi canadienne sur le droit d'auteur, SRC 1970, c. C-30, et ses amendements subséquents.

THE UNIVERSITY OF ALBERTA

**MINERAL TRANSLOCATION AND AUTHIGENESIS IN SELECTED
ALBERTA SOILS**

**by
GRAEME A. SPIERS**



**A THESIS
SUBMITTED TO THE FACULTY OF GRADUATE STUDIES AND
RESEARCH IN PARTIAL FULFILMENT OF THE REQUIREMENTS FOR
THE DEGREE OF
DOCTOR OF PHILOSOPHY
IN**

PEDOLOGY AND SOIL MINERALOGY

DEPARTMENT OF SOIL SCIENCE

**EDMONTON, ALBERTA.
FALL, 1990.**



**National Library
of Canada**

**Bibliothèque nationale
du Canada**

Canadian Theses Service Service des thèses canadiennes

**Ottawa, Canada
K1A 0N4**

The author has granted an irrevocable non-exclusive licence allowing the National Library of Canada to reproduce, loan, distribute or sell copies of his/her thesis by any means and in any form or format, making this thesis available to interested persons.

The author retains ownership of the copyright in his/her thesis. Neither the thesis nor substantial extracts from it may be printed or otherwise reproduced without his/her permission.

L'auteur a accordé une licence irrévocable et non exclusive permettant à la Bibliothèque nationale du Canada de reproduire, prêter, distribuer ou vendre des copies de sa thèse de quelque manière et sous quelque forme que ce soit pour mettre des exemplaires de cette thèse à la disposition des personnes intéressées.

L'auteur conserve la propriété du droit d'auteur qui protège sa thèse. Ni la thèse ni des extraits substantiels de celle-ci ne doivent être imprimés ou autrement reproduits sans son autorisation.

ISBN 0-315-65023-0

THE UNIVERSITY OF ALBERTA

RELEASE FORM

NAME OF AUTHOR GRAEME A. SPIERS

**TITLE OF THESIS MINERAL TRANSLOCATION AND AUTHIGENESIS
IN SELECTED ALBERTA SOILS**

DEGREE FOR WHICH THESIS PRESENTED DOCTOR OF PHILOSOPHY

YEAR THIS DEGREE GRANTED FALL, 1990

Permission is hereby granted to **THE UNIVERSITY OF ALBERTA LIBRARY** to reproduce single copies of this thesis and to lend or sell such copies for private, scholarly or scientific research purposes only.

The author reserves other publication rights, and neither the thesis nor extensive extracts from it may be printed or otherwise reproduced without the author's written permission.

(SIGNED)

PERMANENT ADDRESS:

10453 87th Avenue,
Edmonton, Alberta.
T6E 2P4

DATED *October 5*, 1990.

THE UNIVERSITY OF ALBERTA

FACULTY OF GRADUATE STUDIES AND RESEARCH

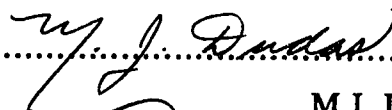
The undersigned certify that they have read, and recommend to the Faculty of Graduate Studies and Research, for acceptance, a thesis entitled **MINERAL TRANSLOCATION AND AUTHIGENESIS IN SELECTED ALBERTA SOILS** submitted by **GRAEME A. SPIERS** in partial fulfilment of the requirements for the degree of **DOCTOR OF PHILOSOPHY** in **PEDOLOGY AND SOIL MINERALOGY**.

.....

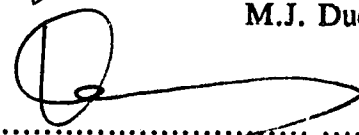
S. Pawluk, Supervisor

.....

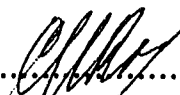
D. Chanasyk

.....

M.J. Dudas

.....

K. Muehlenbachs (Geology)

.....

G.J. Ross, External Examiner

Date .., 1990.

DEDICATION:

Back in 1975, prior to my departure from New Zealand for the frozen wastes of Canada, Professor Harry Gibbs, one of the finest pedologists in New Zealand stated: *'Should you ever have a chance to complete a course with a bloke by the name of Pawluk whilst in Canada, I strongly advise you to do so. He is a pretty good pedologist.'* After many years, I can now claim to have finally followed sound advice.

This thesis is dedicated to the memory Harry Gibbs.

ABSTRACT

Mineral distribution, alteration and authigenesis was studied in a series of pedons of both Luvisolic and Solonetzic soils developed on texturally different tills in Alberta, Canada. The crystalline clay suite, identified by X-ray diffraction analyses and quantified by analyses for cation exchange, surface area and elemental content, of all parent materials consisted of an admixture of smectites, kaolinite, dioctahedral mica, and chlorite. Beidellite, montmorillonite and nontronite were identified as components of the smectite group. The non-crystalline clay component was determined using selective dissolution treatments.

Examination of Solodized Solonetz pedons showed the presence of both crystalline and non-crystalline authigenic minerals in the Ae horizons and the solodized zones of the columnar Bnt horizons. A zeolite mineral with the characteristics of clinoptilolite was detected in the coarse clay (1.0-2.0 μm), fine (2.0-5.0 μm) and medium (5.0-20.0 μm) silt fractions. Selective dissolution analyses indicated that the poorly crystalline minerals were composed predominantly of silicon, aluminum and iron. Differential FT-IR analyses indicated that this phase is a mixture of opaline silica and allophane.

Kaolinite was negatively enriched in the Ae horizons in all clay size separates, whereas mica and smectites were enriched in the Bt (Bnt) horizons as a result of leaching. Although routine chemical and mineralogical characterization suggested apparent neoformation of beidellite in the E horizons of these pedons, the difference in isotopic signature of the detrital crystalline clays from any neoformed clay species disproved the hypothesis. The ^{18}O content of the crystalline clay separates indicated the observed inter-horizon variability in content of the individual phyllosilicate mineral species was a result of physical translocation rather than authigenesis. Analyses of the mobile mineral phases collected by gravity lysimetry demonstrated that kaolinite, mica and smectite are all actively being translocated under the current pedoclimatological environment. Further, changes in measured ^{18}O content of clay separates following selective dissolution indicated that intra-profile variation in the ^{18}O signature of the authigenic poorly crystalline clays could be explained in terms of evaporative enrichment of ^{18}O in the soil water.

An iron oxyhydroxide enriched band at the organic-mineral interface of a Terric Fibrisol formed on calcareous parent material was essentially pure ferrihydrite, with both microbiological and chemical controls on formation from interstitial waters.

ACKNOWLEDGEMENTS

As in any study of this type recognition must be given to many whose names appear to have little relationship to either the author, or to the document being produced. These people have aided by either being present, by aiding and abetting all nefarious activities unrelated to the work in hand, and by actively impeding all concrete progress in a forward direction.

I must thank Dr. S. Pawluk for his assistance and encouragement to finally sit down and complete the task in hand. He rashly decided when he was much younger and more foolish that he could master yet another Ph.D. student; he must have rued the fateful day many a time over the past decade. Drs. Chanasyk, Coen, Dudas, Muehlenbachs, Longstaffe, Pluth, Robertson, Nyborg, Rutter, Smith and McGill all assisted with either advice, or served on the examining committee. I thank Dr. G.J. Ross for serving as an extremely thorough external examiner. For technical assistance, the accolades range from Abley at the head of the alphabet to Yee at the tail. Sandwiched between are people such as Braybrook, Tomlinson, Toerper, Launspach, Hoyle, Swindlehurst, and Hildebrand. Thanks to all, and to the office staff for wielding phone calls and endless paperwork. Professor Michael Abley excelled in the art of scientific program development. The results are evident in the numerous diffractograms in the body of this thesis. The infectious enthusiasm and assistance of Dr. Arocena (to be) helped through the home stretch.

F.O.P., in all its possible permutations, played a role. The role call is long and covers several generations of graduate students. Especially Dave, Cindy, Ted, Charles, Bob, Chuck, Tim, Gary, Jim, Ruth and others whose names are all but lost from memory.

Funding for the adventure was provided in primarily by NSERC, with assistance from the U. of A. Dissertation Fellowship. The U. of Guelph, along with Linda, Ward, Les, Peter and others played a financial, social, and detrimental role in the latter years of this project. Would I do it again? Not bloody likely! At least, not without a large bank account, but it was fun at times, and always interesting.

Allie and Trixie probably must claim full measure of responsibility for starting me on my way to this tome. Thanks Mum and Dad for support, both fiscal and moral. Finally, and most importantly, I must thank three special people: Marie, Rachel and Jude. Gizmo was the perfect black cat.

To those not listed ... my typing finger is ground to the bone. Enough is enough.

TABLE OF CONTENTS

Chapter

1	OVERVIEW TO THE THESIS	11
.1	BACKGROUND	11
.2	OBJECTIVES	43
.3	Bibliography	75
2	AUTHIGENIC MINERAL FORMATION BY SOLODIZATION	18
.1	INTRODUCTION	18
.2	MATERIALS AND METHODS	12
.3	RESULTS AND DISCUSSION	15
.4	CONCLUSIONS	28
.5	Bibliography	30
3	ISOTOPIC EVIDENCE FOR CLAY MINERAL WEATHERING AND AUTHIGENESIS IN LUVISOLIC SOILS	46
.1	INTRODUCTION	46
.2	MATERIALS AND METHODS	47
.3	RESULTS AND DISCUSSION	50
.4	CONCLUSIONS	61
.5	Bibliography	63
4	AN EXAMINATION OF THE MOBILE COLLOIDAL PHASE IN A LUVISOLIC CATENARY SEQUENCE	75
.1	INTRODUCTION	75
.2	MATERIALS AND METHODS	76
.3	RESULTS AND DISCUSSION	78
.1	Static Clay Mineralogy	78
.2	Micromorphological Analysis	85

	.3 Colloidal Suspension Analysis	86
	.4 CONCLUSIONS	92
	.5 Bibliography	95
5	FERRIHYDRITE AT THE MINERAL-ORGANIC INTERFACE: AN EXAMINATION OF COMPOSITION AND FORM	116
	.1 INTRODUCTION	116
	.2 MATERIALS AND METHODS	117
	.3 RESULTS AND DISCUSSION	119
	.1 Water Chemistry	119
	.2 Chemical Analysis	121
	.3 Thermal Analysis	123
	.4 X-ray Diffraction	124
	.5 Infra-red Spectroscopy	125
	.6 Mossbauer and X-ray Photoelectron Spectroscopy	127
	.7 Microscopy	128
	.4 CONCLUSIONS	133
	.5 Bibliography	135
6	OVERVIEW OF THESIS	163
	.1 CONCLUSIONS	
	.1 Authigenic Mineral Formation by Solodization	163
	.2 Isotopic Evidence for Clay Mineral Weathering and Authigenesis in Luvisolic Soils	163
	.3 An examination of the Mobile Colloidal Phase in a Luvisolic Catenary Sequence	165
	.4 Ferrihydrite at the Mineral-Organic Interface: An Examination of Composition and Form	166
	.2 SYNTHESIS	167
	.3 RECOMMENDATIONS FOR RESEARCH	171

LIST OF TABLES

Table

2	.1	Description of the Hemaruka pedon.	12
	.2	Analytical Characteristics of the Hemaruka Pedon.	17
	.3	Titanium and zirconium content of the medium and coarse silt fractions of selected horizons from the Hemaruka pedon.	19
	.4	Crystalline clay mineralogy of the <2.0 um fraction of the genetic horizons of the Hemaruka pedon.	20
	.5	Composition and mineralogy of clay fractions from the solodization region and parent material of The Hemaruka pedon.	23
	.6	Aluminium, iron, and silicon extracted by acid ammonium oxalate and hot potassium hydroxide solutions from the individual clay separates from the horizons of the solodized zone of the Hemaruka pedon.	25
	.7	Si:Al ratios of minerals dissolved from the silt separates of the solodized zone of the Hemaruka pedon.	26
	.8	X-ray diffraction spacings for clinoptilolite separated from the Ae horizon of the Hemaruka pedon.	28
	.9	Solution chemistry of extracts from the major genetic horizons of the Hemaruka pedon.	30
3	.1	Chemical and mineralogical composition of the clay separates from the pedogenic horizons of Cryoboralf pedons from northeast Alberta.	53
	.2	Oxygen isotope (¹⁸ O) geochemistry of clay separates before and after extraction of poorly crystalline material with oxalate and hot (0.5M) KOH solutions.	57
	.3	Oxygen isotope (¹⁸ O) geochemistry of the dissolved poorly crystalline minerals as determined by mass balance calculations.	60
4	.1	Computed Mössbauer parameters at 293 K for the fine clay separates from selected major genetic horizons of an Orthic Grey Luvisol from the upper slope of the catenary sequence.	84

.2	Total chemical analyses of the colloidal leachates from a series of gravity lysimeters installed at three slope positions of a catenary sequence below the AB horizons.	87
.3	Oxalate and pyrophosphate extractable Al, Si, Fe and C contents of the colloidal leachates from a series of gravity lysimeters installed at three slope positions of a catenary sequence below the AB horizons.	88
5 .1	Composition of seasonal interstitial percolating waters from the ferrihydrite band and from an adjacent groundwater discharge spring.	120
.2	Elemental composition of the ferrihydrite material sampled at the peat - mineral interface in late spring.	122
.3	Colour, surface area and some selected chemical values of the fall samples.	123
.4	Computed Mössbauer parameters at 293 K for the ferrihydrite material sampled from the peat-mineral interface in late spring.	128

LIST OF PLATES

Plate		Page
2	.1 Micrographs of selected features from the Ae and Bnt horizons of the Hemaruka pedon.	43
	.2 Scanning electrons micrographs of clinoptilolite grains from the Ae and Ah1 horizons of the Hemaruka pedon.	45
4	.1 Scanning electron micrographs illustrating planar views of cutanic surfaces from the Bt and Ck horizons of an Orthic Grey Luvisol.	111
	.2 Scanning electron micrographs of cross-sections of selected cutanic features observed in the Bt and Ck horizons of an Orthic Grey Luvisol.	113
	.3 Scanning electron micrographs of selected colloidal material collected from a series of gravity lysimeters installed below the Ae and AB horizons of a catenary sequence of Luvisolic soils.	115
5	.1 Scanning electron micrographs of ferrihydrite microstructures within samples from the band sampled from the Terric Fibrisol pedon.	152
	.2 Scanning electron micrographs of material retained on 0.2 μm filters from both spring and fall samples of interstitial waters from within the ferrihydrite band of a Terric Fibrisol pedon.	154
	.3 Scanning electron micrographs of material retained on 0.2 μm filters from both spring and fall samples of interstitial waters from within the ferrihydrite band of a Terric Fibrisol pedon.	156
	.4 Scanning electrons micrographs of microstructures observed in the ferrihydrite material from the band sampled from the Terric Fibrisol pedon following heating to 1000 C for 5 hours in an oxygen atmosphere.	158
	.5 Transmission electron micrographs of both impregnated, stained ferrihydrite and fresh whole mounts of material grown at the water-air interface in the laboratory from interstitial solutions sampled from the band sampled within the Terric Fibrisol pedon.	160

.6	Transmission electron micrographs and electron diffraction patterns of fresh whole mount material grown at the water-air interface in the laboratory from interstitial solutions sampled from the band sampled within the Terric Fibrisol pedon.	162
-----------	---	------------

LIST OF FIGURES

Figure		Page
2 .1	X-ray diffractograms of Ca-and Li-saturated, glycerol and ethylene glycol solvated specimens of 0.2 - 1.0 μm clay separates from the Hemaruka pedon. Diffraction peaks are identified using 2θ values for Cu $K\alpha$ radiation and corresponding d-spacing in nanometers.	39
.2	Infrared spectra obtained for both crystalline and X-ray amorphous clay (0.2 - 1.0 μm) from the solodization region of the Hemaruka pedon. The upper spectrum (a) is for the crystalline phyllosilicate material remaining after both acid oxalate and hot KOH extraction of the X-ray amorphous material of an Ae horizon sample. The spectra (b and c) are differential patterns of the X-ray amorphous minerals extracted from the column top and Ae horizons respectively.	40
.3	Energy dispersive X-ray spectrum of a clinoptilolite crystal separated from the 5 - 20 μm fraction of the Ae horizon of the Hemaruka pedon.	41
3 .1	Location of the study area	70
.2	X-ray diffractograms of clay separates ($<2.0\ \mu\text{m}$) from the C-horizons of the Kinosis and Legend pedons.	72
.3	X-ray diffractograms of the fine clay separates ($<0.2\ \mu\text{m}$) from the major horizons of the Kinosis and Legend pedons.	74
4 1.		101
.2	X-ray diffractograms of magnetic (1.7T) clay separates from selected genetic horizons of an Orthic Grey Luvisol.	103
.3	X-ray diffractograms of the cutanic clay material excised from peds of major genetic horizons of an Orthic Grey Luvisol.	105
.4	X-ray diffractograms of colloidal material collected from a gravity lysimeter installed below the AB horizon of an Orthic Grey Luvisolic pedon.	107

.5	Infra-red spectra of the untreated colloidal material from spring, summer and fall collections filtered from the soil solutions collected by gravity lysimetry below the Ae and AB horizons of a catenary sequence of Luvisolic soils.	109
5 .1	Plot displaying the measured parameters for the site waters displayed on an Eh-pH diagram of selected mineral phases for the system Fe_2O_3 - SiO_2 - H_2O .	140
.2	Differential thermal analysis and thermogravimetric analysis patterns for the ferrihydrite samples, both before and after treatment with H_2O_2 to oxidize organic carbon.	142
.3	X-ray diffractograms of ferrihydrite samples heated to selected temperatures between 25 C and 1000 C: a) 25 C; b) 200 C ; c) 400 C; 600 C; d) 800 C; e) 1000 C. Samples were held at each temperature for 3 hours prior to analysis.	144
.4	Fourier transform infra-red spectra of ferrihydrite samples heated to selected temperatures between 25 C and 1000 C: a) 25 C; b) 200 C ; c) 600 C; d) 800 C; e) 900 C; f) 1000 C. Samples were held at each temperature for 3 hours prior to analysis.	146
.5	Room temperature Mössbauer spectra of size separates of the ferrihydrite material.	148
.6	X-ray photoelectron spectra of ferrihydrite samples obtained following dissolution of the carbonaceous material phases in H_2O_2 .	150

1: OVERVIEW OF THE THESIS

1.1. BACKGROUND:

As the prime mineral groups of interest to the research documented in the current thesis are the phyllosilicate clays and iron oxyhydroxides, it is considered pertinent to review briefly the accepted understanding of the relative distribution of these species in Western Canadian parent materials and related soils. Although information on the controls on phyllosilicate mineral neoformation and weathering in Western Canadian parent materials is sparse, there have been, in recent years, a series of research publications describing pedogenic alteration of sand minerals in Saskatchewan soils (Somasiri et al., 1971; Mermut et al., 1986; Ghabru et al., 1989). These studies, however, generally do not establish the weathering status of the phyllosilicate and/or authigenic mineral species under examination in the Pleistocene glacial parent materials, nor do they consider weathering processes which must have been active in the interglacial epochs of the Quaternary and earlier (Spiers et al., 1989). Such studies have only been completed on the pedogenetically unrelated Pre-Wisconsinian deposits in the Yukon (Smith et al., 1986).

In a literature survey of clay mineralogical data of Canadian soils, the distribution of various clay fraction compositional assemblages was related to major soil-physiographic regions (Kodama, 1979), with the pedons examined in the current study being in the Interior Plains region (Pettapiece, 1976). In general, the mineralogy of the clay sized separates of this region are dominated by smectites and mica, with minor amounts of kaolinite, chlorite and vermiculite (Kodama, 1979). In a regional study by Pawluk and Bayrock (1962), dioctahedral smectite, with a composition between that of nontronite and beidellite, was found to vary in content from about 20% in northern regions of Alberta to in excess of 60% in the south. Although the presence of an interstratified montmorillonite-mica has frequently been documented (Pawluk, 1961; Kodama

and Brydon, 1965; Pawluk and Bayrock, 1969; Dudas and Pawluk, 1970; Kodama, 1979), a re-evaluation based on detailed deterministic analytical pre-treatments suggested that discrete smectite, mica, kaolinite and chlorite, in decreasing order of abundance, comprised the total clay fractions (Dudas and Pawluk, 1982). Further, the smectite component was differentiated into two distinct members, namely montmorillonite and beidellite, with the presence of vermiculite not being recognised. The latter observation is disputed by both Abder-Ruhman (1980) and Howitt (1981) in studies of Luvisol genesis. Abder-Ruhman (1980) documented vermiculite as a component of the parent materials, and not a product of weathering, whereas Howitt (1981) suggested the higher content of soil vermiculite, an Al-OH interlayered dioctahedral smectite, in Ae horizons was a pedogenic product. Enrichment in the Ae clay fraction with a species with similar diffraction behaviour was attributed to additions of aeolian beidellite by Pawluk and Dudas (1982).

The examination of crystalline authigenic mineral phases in the well to imperfectly drained soils of the Interior Plains has primarily focused on the carbonates, with detailed studies of their mineralogical variability (Rostad and St. Arnaud, 1970), micromorphology (Mermut and St. Arnaud, 1981a; Bui and Mermut, 1989), chemical composition (Mermut and St. Arnaud, 1981b) and solution formation control (St. Arnaud, 1979) being primarily completed on Saskatchewan soils. There has been only one study in which stable isotope geochemistry was utilised to provide a definitive separation between allogenic and authigenic phases (Miller et al., 1987).

In soils formed on sodic-alkaline parent materials of the Interior Plains where salinisation processes are still active, there have been a series of examinations of the authigenic secondary salt minerals in soils formed on sodic-alkaline parent materials. In these studies the precipitation of Na-Mg-type evaporite minerals has been described as a surface phenomenon

leading to salt efflorescences (Keller et al., 1986a,b). In contrast Miller et al. (1989) described the formation of authigenic Ca-type evaporites such bassanite and gypsum in upper and lower profile positions respectively for soils in a saline seep in southern Alberta. Although generally precipitating within the solum, authigenic calcite was ubiquitous in all the recent studies of saline soil chemistry and mineralogy (Keller et al., 1986a,b; Miller et al., 1987, 1989; Timpson and Richardson, 1986; Timpson et al, 1986). In an examination of salt fluxes (Fullerton and Pawluk, 1987) in the Bntj horizons of a Black Solonetz the salts NaHCO_3 and Na_2SO_4 were found to be responsible for the solonisation processes.

Although studies documenting the depth distribution of phyllosilicate minerals within the control section of soils of the glaciated terrain of the Interior Plains abound in the literature (Mathieu, 1970; Arshad and Pawluk, 1966; Brunelle et al., 1976; St. Arnaud and Sudom, 1981; Pawluk and Dudas, 1978, 1982; Munn and Boehm, 1983; Howitt and Pawluk, 1985a), there is a paucity of documentation of contemporary dynamic processes. Although Sanborn and Pawluk (1983), in a detailed study of the ongoing processes active in a Gleyed Eluviated Black Chernozemic pedon, documented inorganic carbonates, sulphates and nitrates in freeze-dried gravity lysimeter leachates, there was no evidence of colloidal material mobilisation during the two year sampling period. Howitt and Pawluk (1985b), however, presented evidence for the movement in suspension of discrete crystalline clay mica in leachates sampled from a Gray Luvisolic pedon, with the possible presence of an expandable component. Associated with the mobile crystalline phase in the leachates was a significant component of organically complexed Fe and Al, with the possible presence of X-ray amorphous mineral material.

Although the application of magnetic separation techniques to colloidal minerals (Ghabbru et al., 1987, 1988, 1990) has provided information on the nature of some of the iron-bearing primary and phyllosilicate minerals in Saskatchewan soils, there has been no

information on the pedogenic iron oxyhydroxides such as ferrihydrite, hematite, goethite and lepidocrocite. Studies by Pawluk and Dumanski (1973), and Dudas et al. (1988) are the only documentation of an authigenic maghemite, goethite and hematite known to the author for regional soils. Arshad and St. Arnaud (1980) also described pedogenic ferrromagniferous nodules and Santos et al. (1986) indicated that Fe-bearing clays in Saskatchewan soils are weathering to form unspecified secondary iron oxides.

1.2. OBJECTIVES:

As there are many apparent contradictions pertaining to the mineral distribution within the soils of the Interior Plains, the overall objectives of the current thesis are to describe both the mobility of individual clay mineral species within individual pedons and the nature of selected authigenic minerals in specific soils of Alberta. The four following chapters of the thesis, which are written as independent papers with specific objectives, examine analytical, mineralogical and solution compositional data from pedons selected as being representative of Soil Orders of importance in the regional landscapes of Alberta. The Orders of which the pedons are members are Luvisolic, Organic and Solonetzic, with six individual sampling study sites ranging from 50.5 N to 58 N within the Province of Alberta. The objectives of the individual research chapters are summarized as follows:

Chapter 2. Authigenic Mineral Formation During Solodization. In this chapter the transformations and translocations occurring during pedogenesis within the solodized zones of both a Black and a Brown Solodized Solonetz pedon are examined. Mineralogical, solution chemical and micromorphological data are discussed in terms of preferential translocation of individual phyllosilicate minerals, and neoformation of both crystalline and poorly crystalline aluminosilicate minerals.

Chapter 3. Isotopic Evidence For Clay Mineral Weathering And Authigenesis In Luvisolic Soils. This chapter focuses on the phyllosilicate mineralogy of two Luvisolic pedons with parent materials of different provenance (Spiers et al., 1984). The objectives are to compare and contrast the relative mobilities of the individual phyllosilicate species both within and between the pedons, and to utilise the ^{18}O geochemistry to decipher the possibilities for both crystalline and poorly crystalline aluminosilicate authigenesis.

Chapter 4. An Examination Of The Mobile Colloidal Phase In A Luvisolic Catenary Sequence. Both static and dynamic approaches to the study of soil genesis are combined in this chapter in an endeavour to define the pedogenic mineralogic translocations that have occurred within soils of a Luvisolic catenary sequence, and to establish the exact nature of the contemporary mobile colloidal phase.

Chapter 5. Ferrihydrite At The Mineral-Organic Interface. During a series of field surveys small areas of Terric Fibrisol were mapped on levees several metres above modern drainage channels. Bands of an iron oxyhydroxide material were consistently observed at the interface between the peaty material and the underlying calcareous mineral parent material, an environment not typically described for the occurrence of ferrihydrite. Accordingly the objective of the current chapter is to provide a detailed description of the environment of formation, coupled with the chemistry, morphology and structure of the ferrihydrite deposit.

As suggested by Maulé (1989), the process of research proceeds from hypothesis formulation, through data accumulation and hypothesis testing, to result interpretation. This process moves the researcher from the general to the specific. However, a review of literature,

be it scientific or philosophic, will generally attempt to place the results of any objective specific research into a broad or general framework which attempts to summarize the current understanding of any specific subject. Accordingly the final chapter (Chapter 6) of this thesis will summarize the data presented in the preceding detailed studies and attempt to illustrate how the present research has added to the basic understanding of the genetical processes active in the sola of Western Canada which have formed on either saline or non-saline calcareous parent materials.

1.3. BIBLIOGRAPHY

- Abder-Ruhman, M. (1980). Mineralogical characteristics of soils of east central Alberta. M.Sc. Thesis, University of Alberta, 322pp.
- Arshad, M.A. and S. Pawluk (1966). Characteristics of some solonetzic soils in the Glacial Lake Edmonton basin of Alberta. II. Mineralogy. *J. Soil Sci.* 17: 48-55.
- Arshad, M.A. and St. Arnaud, R.J. (1980). Occurrence and characteristics of ferromagniferous concretions in some Saskatchewan soils. *Can. J. Soil Sci.* 60: 685-695.
- Brunelle, A., S. Pawluk, T.W. Peters (1976) Evaluation of profile development of some solonetzic soils of south central Alberta. *Can. J. Soil Sci.* 56: 149-158.
- Bui, E.N. and Mermut, A.R. (1989). Quantification of soil calcium carbonates by staining and image analysis. *Can. J. Soil Sci.* 69: 677-682.
- Dudas, M.J. and Pawluk, S. (1970). Chernozem soils of the Alberta parklands. *Geoderma* 3: 19-36.
- Dudas, M.J. and Pawluk, S. (1982). Reevaluation of the occurrence of interstratified clays and other phyllosilicates in southern Alberta soils. *Can. J. Soil Sci.* 62: 61-69.
- Dudas, M.J., Warren, C.J. and Spiers, G.A. (1988). Chemistry of arsenic in acid sulphate soils of northern Alberta. *Commun. in Soil Sci. Plant Anal.* 19: 887-895.
- Fullerton S. and Pawluk, S. (1987). The role of seasonal salt and water flakes in the genesis of Solonetzic B horizons. *Can. J. Soil Sci.* 67: 719-730.
- Ghabru, S.K., St Arnaud, R.J. and Mermut, A.R. (1987). Liquid magnetic separation of iron bearing minerals from sand fractions of soils. *Can. J. Soil Sci.* 67: 561-569.
- Ghabru, S.K., St Arnaud, R.J. and Mermut, A.R. (1988). Use of high gradient magnetic separation in detailed clay mineral studies. *Can. J. Soil Sci.* 68: 645-655.
- Ghabru, S.K., Mermut, A.R. and St Arnaud, R.J. (1989). Characterization of garnets in a Typic Cryoboralf (Gray Luvisol) from Saskatchewan, Canada. *Soil Sci. Soc. Am. J.* 53: 575-582.

- Ghabru, S.K., St Arnaud, R.J. and Mermut, A.R. (1990). Association of DCB-extractable iron with minerals in coarse soil clays. *Soil Sci.* 149: 112-120.
- Howitt, R.W. (1980). Dynamics of a Grey Luvisol. M.Sc. Thesis, University of Alberta, 168pp.
- Howitt, R.W. and S. Pawluk (1985) Genesis of a Gray Luvisol in the Boreal Forest zone. I. Dynamic pedology. *Can. J. Soil Sci.* 65: 1-8.
- Howitt, R.W. and S. Pawluk (1985) Genesis of a Gray Luvisol in the Boreal Forest zone. II. Dynamic pedology. *Can. J. Soil Sci.* 65: 9-19.
- Keller, L.P., McCarthy, G.J. and Richardson, J.L. (1986a). Mineralogy and the stability of soil evaporites in North Dakota. *Soil Sci. Soc. Am. J.* 50: 1069-1071.
- Keller, L.P., McCarthy, G.J. and Richardson, J.L. (1986a). Laboratory modelling of Northern Great Plains salt efflorescence mineralogy. *Soil Sci. Soc. Am. J.* 50: 1363-1367.
- Kodama, H. 1979. Clay minerals in Canadian soils: their origin, distribution and alteration. *Can. J. Soil Sci.* 59: 37-58.
- Kodama, H. and Brydon, J.E. (1965). Interstratified montmorillonite-mica from the subsoils of the Prairie provinces, Western Canada. *Clays Clay Min.* 16: 437-447.
- Mathieu, A.L. (1960) The mineralogy of the clay fraction in relation to the genesis of Solodized Solonetz soils. Ph. D. thesis, Univ. of Saskatchewan, Saskatoon. 181 pp.
- Maulé, C.P. (1989). Snowmelt infiltration and seasonal groundwater interactions with the unsaturated zone. Unpubl. Ph.D. thesis, University of Alberta. Edmonton, Alberta.
- Mermut, A.R. and St. Arnaud, R.J. (1981a). A micromorphological study of calcareous soil horizons in Saskatchewan soils. *Can. J. Soil Sci.* 61: 243-260.
- Mermut, A.R. and St. Arnaud, R.J. (1981b). A study of microcrystalline pedogenic carbonates using submicroscopic techniques. *Can. J. Soil Sci.* 61: 261-272.
- Mermut, A.R., Ghebre-Egziabhier, K. and St. Arnaud, R.J. (1986). Quantitative evaluation of feldspar weathering in two Boralfs (Gray Luvisols) from Saskatchewan. *Soil Sci. Soc. Am. J.* 50: 1072-1079.

- Miller, J.J., Dudas, M.J. and Longstaffe, F.J. (1987). Identification of pedogenic carbonate minerals using stable carbon and oxygen isotopes, X-ray diffraction and SEM analyses. *Can. J. Soil Sci.* 67: 953-958.
- Miller, J.J., Pawluk, S. and Beke, G.J. (1989). Evaporite mineralogy, and soil solution and groundwater chemistry of a saline seep from southern Alberta. *Can. J. Soil Sci.* 69: 273-286.
- Munn, L.C. and Boehm, M.M. (1983). Soil genesis in a Natragid-Haplargid complex in northern Montana. *Soil Sci. Soc. Am. J.* 47: 1186-1192.
- Pawluk, S. (1961). Mineralogical composition of some Gray Wooded soils developed from glacial till. *Can. J. Soil Sci.* 41: 228-240.
- Pawluk, S. (1971). Characteristics of Fera-Eluviated Gleysols developed from acid shales in Northwestern Alberta. *Can. J. Soil Sci.* 51: 113-123.
- Pawluk, S. and Bayrock, L.A. (1969). Some characteristics and physical properties of Alberta soils. Research Council of Alberta, Bull. 26. 72 pp.
- Pawluk, S. and Dumanski, J. (1973). Ferruginous concretions in a poorly drained soil of Alberta. *Soil Soc. Am. Proc.* 37: 124-127.
- Pawluk, S. and Dudas, M.J. (1978). Reorganisation of soil materials in the genesis of an acid Luvisolic soil of the Peace River region, Alberta. *Can. J. Soil Sci.* 58: 209-220.
- Pawluk, S. and M.J. Dudas (1982). Pedological investigation of a Gray Luvisol developed from eolian sand. *Can. J. Soil Sci.* 62: 49-60.
- Pettapiece, W.W. (1976). Physiographic map of Alberta. Alberta Inst. of Pedology, Edmonton.
- Rostad, H.P.W. and St. Arnaud, R.J. (1970). Nature of carbonate minerals in two Saskatchewan soils. *Can. J. Soil Sci.* 50: 65-70.
- Sanborn, P. and Pawluk, S. (1983). Process studies of a Chernozemic pedon, Alberta (Canada). *Geoderma* 31: 205-237.
- St. Arnaud, R.J. (1979). Nature and distribution of secondary soil carbonates within landscapes in relation to soluble Mg^{++}/Ca^{++} ratios. *Can. J. Soil Sci.* 59: 87-98.

- St. Arnaud, R.J. and M.D. Sudom (1981) Mineral distribution and weathering in Chernozemic and Luvisolic soils from central Saskatchewan. *Can. J. Soil Sci.* 61: 79-89.
- Santos, M.C.D., St. Arnaud, R.J. and Anderson, D.W. (1986). Iron redistribution in three Boralfs (Luvisols) of Saskatchewan. *Soil Sci. Soc. Am. J.* 50: 1272-1277.
- Santos, M.C.D., St. Arnaud, R.J. and Anderson, D.W. (1986). Quantitative evaluation of pedogenic changes in Boralfs (Gray Luvisols) of east-central Saskatchewan. *Soil Sci. Soc. Am. J.* 50: 1013-1019.
- Smith, C.A.S., Tarnocai, C. and Hughes, O.W. (1986). Pedological investigations of the Pleistocene drift surfaces in the Central Yukon. *Geog. Phys. Quat.* 40: 29-47.
- Somasiri, S., Lee, S.Y. and Huang, P.M. (1971). Influence of certain pedologic factors on potassium reserves of selected Canadian soils. *Soil Sci. Soc. Am. Proc.* 35: 500-505.
- Spiers, G.A., Dudas, M.J., K. Muchlenbachs and Turchenek, L.W. (1984). Mineralogy and oxygen isotope geochemistry of clays from surficial deposits in the Athabasca Tar Sands area. *Can. J. Earth Sci.* 21: 53-60.
- Spiers, G.A., Dudas, M.J. and Turchenek, L.W. (1989). The chemical and mineralogical composition of soil parent materials in northeast Alberta. *Can. J. Soil Sci* 69: 721-738.
- Timpson, M.E. and Richardson, J.L. (1986). Ionic composition and distribution in saline seeps of southwestern North Dakota, U.S.A. *Geoderma* 37: 295-305.
- Timpson, M.E. and Richardson, J.L., Keller, L.P. and McCarthy, G.J. (1986). Evaporite mineralogy associated with saline seeps in southwestern North Dakota. *Soil Sci. Soc. Am. J.* 50: 490-493.

2: AUTHIGENIC MINERAL FORMATION BY SOLODIZATION¹

2.1: INTRODUCTION

Examination of the genesis of Solonetzic soils in Canada has concentrated on description of salt and water movement (Maclean and Pawluk, 1975; Landsburg, 1981) and on describing alteration and translocation of the phyllosilicate minerals (Mathieu, 1960; Arshad and Pawluk, 1966; Brunelle et al, 1976). Although solodization is recognised as a degradation process involving relocation of solum materials, with accompanying alteration of the primary and secondary minerals, there has been little evidence presented for the formation of either amorphous or crystalline authigenic minerals in either the clay or silt fractions of these soils.

Early research on the genetic processes of Solonetzic soils postulated the formation of authigenic calcium and sodium silicates (Kovda, 1939) and amorphous silica (Gedroits, 1927), but there was no evidence of either the mineralogical composition or relative amounts of the species formed. Authigenic analcime was described in the coarse clay and fine silt fractions of alkaline Solonetzic soils from California (Baldar and Whittig, 1968). Acid Solonetzic soils in Utah were shown to have significant amounts of another zeolite mineral, clinoptilolite (Southard and Kolesar, 1978), which was considered responsible for the high levels of ammonium acetate extractable K detected in these soils. The clinoptilolite was detrital, being inherited from the tuffaceous sediments comprising the parent materials of these soils. Detrital clinoptilolite was shown to first alter to zelandite, and then to weather completely, in soils developed on carbonate-rich tuffaceous sediments in Texas (Jacob and Allen, 1983).

The objective of this section of the thesis was to evaluate transformations and translocations within the solodized zone of both a Brown and a Black Solodized Solonetz pedon.

¹Published in Canadian Journal of Soil Science 64: 515-532.

Mineralogical and micromorphological data are discussed in terms of preferential translocation of different phyllosilicate minerals, and formation of the authigenic minerals.

2.2: MATERIALS AND METHODS

Soil samples used in this study were collected from both a Brown Solodized Solonetz representative of the Hemaruka Soil Series (Table 1) and a Black Solodized Solonetz of the Camrose Series (Bowser et al, 1962) from central Alberta. The parent material of the pedons is a loam till. The location of the Hemaruka pedon is NE 1/4 section 22, township 30, range 14 west of the fourth meridian and that of the Camrose pedon is NE 1/4 section 9, township 50, range west of the fourth meridian. The soil was sampled by genetic horizon.

Table 2.1: Description of the Hemaruka Pedon

	cm.	
Ah ₁	0-13	Brown (10YR5/3(d)); sandy loam; strong fine granular; friable; clear smooth boundary.
Ah ₂	13-24	Brown (10YR5/3(d)); sandy loam; weak coarse prismatic to strong fine and medium granular; mxiable; clear smooth boundary.
Ahe	24-32	Yellowish brown (10YR5/4(d)); sandy loam; moderate coarse prismatic to weak coarse platy and moderate fine granular; friable; clear smooth boundary.
Ae	32-39	Light brownish gray (10YR6/2(d)); sandy loam; moderate coarse prismatic to moderate coarse and fine platy; friable; abrupt wavy boundary.
Bnt	39-50	Pale brown (10YR6/3(d)); clay loam; strong coarse and medium columnar to strong medium subangular blocky; very firm; clear smooth boundary.
Bntk	50-61	Pale brown (10YR6/3(d)); clay loam; moderate coarse columnar to moderate medium subangular blocky; very firm; abrupt smooth boundary.
BCsak	61-78	Pale brown (10YR6/3(d)); loam; pseudo-blocky; firm; gradual smooth boundary.
Csak	78-100	Pale brown (10YR6/3(d)); loam; pseudo-blocky to massive; firm.

Composite samples were obtained by bulking sub-samples from three walls of the pit. Samples from the active solodization zone of the upper column were obtained by transferring intact columns to the laboratory, and there carefully scraping the thin ($<0.5\text{cm}$) eluviated zone from the apices of the columns.

Soil monoliths were air-dried in the laboratory, impregnated with epoxy resin and cut into 7×5 cm thin sections using procedures described by Brewer and Pawluk (1975). The microfabric of unimpregnated structural units from the solodization zone at the top of the Bnt columns was examined by scanning electron microscopy.

Collected samples were air-dried in the laboratory, ground with a mortar and pestle to pass a 2 mm sieve, and stored for subsequent analyses. The following analyses were conducted according to the procedures recommended by McKeague (1978): cation exchange (1.0M NH_4OAc , pH 7.0); exchange acidity (0.5M BaOAc); pH (H_2O , 0.01M CaCl_2) and 1.0M NaF ; organic carbon (dry combustion); total nitrogen (Kjeldahl); particle size distribution (pipet). Content of titanium and zirconium in the silt fraction ($20\text{-}50\text{ }\mu\text{m}$) was determined by X-ray fluorescence (Drees and Wilding, 1973).

Clay ($< 2.0\text{ }\mu\text{m}$) was extracted by dispersing 50 g of air-dried soil in distilled water by ultrasonification using a probe type vibrator at 400 watts for 5 minutes. This was followed by repetitive extractions according to the gravity separation technique outlined by McKeague (1978), with further separation of the clay into four sub-fractions (0-0.08, 0.08-0.2, 0.2-1.0 and 1.0-2.0 μm) by centrifugation techniques (Jackson, 1975). Saturation of 50 mg portions of the clay with Ca^{++} , Li^+ and K^+ was accomplished by three washings with the appropriate 1M salt solutions followed by distilled water washings and centrifugation to remove the excess electrolyte. Oriented specimens for X-ray diffraction analysis were prepared on glass slides using the paste method (Thiesen and Harward, 1962). The remaining portions of the clay fractions were Ca-

saturated, washed free of excess electrolyte, freeze-dried and used for subsequent analysis.

Diffraction patterns of the oriented specimens were obtained with a Philips diffractometer equipped with a LiF curved crystal monochromator using $\text{CuK}\alpha$ radiation generated at 40 kV and 20 mA. Diffraction patterns of Ca-saturated specimens were obtained for 54% RH, glycerol, and ethylene glycol pretreatments while patterns for K-saturated specimens were obtained for 105 C heated samples analysed at 0% RH, then again after equilibration at 54% RH and for 300 and 500 C heated samples maintained at 0% RH during the analysis. Diffraction patterns of Li-saturated specimens were obtained for 200 C heated samples both before and after saturation with glycerol vapour (Greene-Kelley, 1953). Analysis of Ca-saturated samples for elemental composition by inductively coupled plasma emission spectroscopy following HCl-HF dissolution followed the techniques described by Spiers et al (1983). The surface area of the clay separates was determined by solvation with ethylene glycol monoethyl ether (Carter et al, 1965). Cation-exchange capacity was determined by extraction of Ca-saturated clays with 2M KOAc, and measurement of displaced Ca^{++} (CaEC) by atomic absorption spectroscopy. Quantitative determination of the crystalline phyllosilicates in the various clay fractions separated from the horizons of the solodized zone is based on the analytical data for exchange capacity, surface area, and potassium content. Content of kaolinite+chlorite is estimated by difference.

Sub-samples of the freeze-dried clay separates were sequentially extracted with Na-pyrophosphate, acid ammonium oxalate (McKeague, 1978) and boiling 0.5 M KOH (Dudas and Harward, 1971). The content of Si, Al, and Fe in the supernatant solutions as determined by atomic absorption spectroscopy was utilized to obtain an estimate of amorphous clay materials in the individual fractions. Infrared analyses were conducted on these subsamples, both before and after the chemical extractions, using a Nicolet Fourier transform infrared spectrometer (FT-IR). Pellets were prepared by dispersing 2 mg clay in 200 mg KBr. The KBr pellets were

heated to 150 C for 12 hours prior to analysis. Infrared spectra of the material dissolved by the chemical extraction procedures were obtained by computing the differential spectra from the above patterns.

The silt separates were also fractionated using gravity separation techniques (Jackson, 1975) into 2.0-5.0, 5.0-20.0 and 20.0-50.0 μm fractions. These fractions were further processed with heavy liquids to obtain a light mineral fraction (S. G. <2.35). The purified light mineral fractions were examined with a Cambridge Stereoscan 250 scanning electron microscope equipped with a Kevex 7000 energy dispersive X-ray micro-analysis system.

A 300 g sample from each horizon was incubated at approximately field capacity for two months at 25 C under aerobic conditions in order to obtain steady-state pore water conditions. The solutions subsequently extracted under vacuum were analysed by inductively-coupled plasma atomic emission spectroscopy to obtain concentrations of dissolved constituents. Carbonate, bicarbonate, and chloride were determined by the methods recommended by McKeague (1978). The activities of the ionic species and the saturation state of the extracted solutions for different minerals were estimated using the computer model SOLMNEQ (Kharaka and Barnes, 1973). Free energy data for clinoptilolite calculated by Cosgrove and Papavassilou (1979) were added to the SOLMNEQ data-base.

2.3: RESULTS AND DISCUSSION

Examination of the particle size distribution within the profile (Table 2) revealed a definite accumulation of both coarse and fine clay in the Bnt horizons. The negative enrichment of sand in the A horizons is a consequence of clay translocation to the lower profile. The decrease in amount of silt in the eluviated horizons may reflect either physical comminution of sand and silt particles (Brunelle et al, 1970), or actual physical translocation of silt to lower horizons (Howitt

and Pawluk, 1984). The former possibility is more plausible in view of the constancy of content of silt in both B and C horizons.

The total cation-exchange capacity is a function of both clay and organic matter content. The CEC bulge in the Bnt horizon paralleled the increase in clay content and the smaller bulge in the Ah horizons was attributed to distribution of organic matter. The dominant exchangeable cations varied with depth. In the A horizons, Ca^{++} was dominant with lesser amounts of Mg^{++} and Na^+ . In the upper Bnt horizon the order was reversed as a result of the displacement and translocation of Na^+ in solution during desalinization. The exchange complex in the lower B and the C horizons was dominated by Mg^{++} . Sodium occupied approximately 25% of the exchange complex in these latter horizons. The overall dominance of divalent cations on the exchange complex is similar to that described for solodized solonchic soils by MacGregor and Wyatt (1945) and Whittig (1959). The dominance of Mg^{++} in the lower pedon is similar to that described for a Mg-solonch (Ellis and Caldwell, 1935; Rost and Mahl, 1943).

The changes in pH values from the upper to the lower horizons (Table 2) reflect the changes induced in the parent materials during the processes of solodization. The acid pH in the upper pedon results from the leaching of soluble salts to the lower horizons, with subsequent hydrolysis of both primary and secondary aluminosilicate minerals, whereas the alkaline pH of the lower horizons is a result of the presence of soluble carbonate salts. The pH(NaF) indicates there is a significant component of reactive Al-OH groups in the Ahe and Ae horizons (Fieldes and Perrot, 1966). An alkaline pH(NaF) is often interpreted as implying the presence of allophane-like minerals.

Micromorphological examination of the solodization zone of the profile indicated that the banded porphyric fabric of the Ae horizon (Plate 1a) consisted of a dense porphyric fabric between well developed horizontal joint planes.

Table 2.2: Analytical Characteristics of the Hermaruka Pedon.

	Sand	Silt	Clay	Fine Clay	H ₂ O (1:1)	CaCl ₂ (1.01M)	NaF (1.0M)	me 100 g ⁻¹			CEC	Exchange Acidity
								Ca	K	Na		
Ab ₁	61	30	9	7	5.8	4.5	8.5	4	0.5	0.4	1.7	5
Ab ₂	64	25	11	5	6.5	4.6	8.7	3	0.5	0.8	1.6	3
Abc	68	24	8	7	6.4	4.9	8.8	3	0.3	0.9	1.9	2
Ac	76	20	3	1	6.5	5.6	9.4	1	0.4	1.2	2.4	1
B _{ut}	50	28	23	16	7.0	6.4	10.1	5	0.9	5.2	3.1	<1
B _{nk}	48	32	20	10	8.0	7.1	n.d.*	<1	0.6	3.3	9.7	<1
BC _{stk}	44	36	21	12	8.4	7.0	n.d.	<1	0.6	3.3	9.7	<1
C _{stk}	44	34	22	12	8.3	7.0	n.d.	<1	0.7	1.0	8.3	<1

* n.d. = not determined

This fabric is similar to the isoband fabric described by Dumanski and St. Arnaud (1966) for the Ae horizons of Luvisols. The plasma fabric was skelsepic to weak insepic, with a significant proportion of an isotropic noncrystalline or amorphous groundmass present in the numerous vughs. Examination of selected domains by energy dispersive X-ray microanalysis demonstrated that this groundmass was comprised primarily of Al and Si, with minor amounts of K. The Si:Al ratio was between 1.5:1 and 2.1:1. There were common aggotubules containing mullgranic units (35-45 μm diameter), and common iron oxide concentrations of varying size. There were sporadic zones of organic plasma concentration, with a weak humic component throughout the plasma. Electron optical examination of the structural units indicated that the skeletal grains were loosely packed, with a minor amount of clay material bridging and binding the individual grains (Plate 1b, 1c).

The banded porphyric fabric of the Ae graded into a dense porphyric fabric in the upper Bnt horizon, with common vughs and widely spaced vertical joint planes (Plate 1a). The plasma fabric was comprised dominantly of omnisepic zones randomly intermixed with skel-mosepic zones. The well-developed void argillans observed in the channels, but not in vughs, resulted from the translocation of clay material from the overlying horizons. These argillans were observed electron optically to consist of concentric clay layers deposited on the surrounding matrix. The proportion of K, Mg and Fe in these translocated clays suggested a dominance of smectites, with lesser amounts of mica. Active translocation of mica suspended in the soil solution has been described in the upper Bt horizons of Luvisols (Howitt and Pawluk, 1984). The skeletal grains in the f-matrix of the Bnt horizon were bridged and cemented by a dense groundmass of well-oriented clay material (Plate 1d, 1e). This strong orientation of the clay comprising the plasma probably accounts for the well-developed structure and hardness observed in these horizons in the field.

Evaluation of pedogenic alteration and/or translocation requires that the initial parent material be lithologically uniform. The content of Ti and Zr in the 5-20 and 20-50 μm fractions and the ratio between these two relatively immobile elements (Table 2.3) displayed little variability among horizons. This lack of variability in the Ti/Zr ratio indicated that the soil developed within a lithologically uniform deposit. Thus any mineralogical variation observed among the individual horizons in the solodization zone of this pedon can be most likely ascribed to pedogenic processes.

Table 2.3: Titanium and zirconium content of the medium and coarse silt fractions of selected horizons from the Hemaruka pedon.

Horizon	Size fraction (μm)	Ti (%)	Zr (%)	Ti/Zr
Ae	5-20	0.55	0.034	16.18
	20-50	0.55	0.079	6.96
Column Top	5-20	0.50	0.031	16.13
	20-50	0.55	0.76	7.24
Bnt	5-20	0.60	0.038	15.79
	20-50	0.50	0.072	6.94
Csak	5-20	0.57	0.035	16.29
	20-50	0.54	0.80	6.75

Clay mineral assemblages varied in composition throughout the depth of the pedon. The phyllosilicate suite was comprised of admixtures of mica, smectite, kaolinite and chlorite. On the basis of the intensities of the x-ray diffraction peaks mica was estimated to be the dominant mineral in the A horizons (Table 2.4). Content of kaolinite was also highest in the A horizons which reflected negative enrichment (Arshad and Pawluk, 1966b) through translocation of the

smectite-enriched finer clay fractions to horizons lower in the profile. Chlorite was present in only trace amounts in the A horizons and was not detected in the B and C horizons. The highest content of smectite was observed in the Bntk horizon, perhaps reflecting the preferential translocation of components of the finer clay ($<0.2 \mu\text{m}$) fractions (Table 2.5). The content of micaceous and kaolinite minerals displayed a concomitant decrease in the lower profile as a result of the dilution effect induced by the preferential translocation of the smectite-rich fine clay fractions.

Table 2.4 Crystalline clay mineralogy of the $<2.0 \mu\text{m}$ fraction of the genetic horizons of the Hemaruka pedon.

Horizon	Mica	Smectite	Kaolinite	Chlorite	Zeolite
Ah1	++++	++	++	(+)	+
Ah2	++++	++	++	(+)	+
Ahe	++++	++	++	(+)	+
Ae	++++	++	++	(+)	+
Column Top	+++	++	++		+
Bnt	+++	+++	++		(+)
Bntk	+++	++++	+		
BCsak	+++	++++	+		
Csak	+++	++++	+		

+ is equivalent to approximately 10%

Contents of individual phyllosilicate minerals were relatively constant within the individual fractions throughout both the zone of active solodization and the parent material. This indicates that the eluviation/illuviation processes described previously as an important component of solodization (Brunelle et al, 1976) involve merely the movement of individual size fractions and not distinct mineral species. Individual minerals may, however, actually be concentrated

in a narrow particle size range. Thus the enrichment of smectite minerals in the Bnt horizons (Table 2.4) is a result of preferential translocation of the fine clay fractions ($<0.2 \mu\text{m}$), which incidently have smectite as a dominant component (Table 2.5). The lower contents of hydrous mica in the 0.2-1.0, 0.08-0.2, and the $<0.08 \mu\text{m}$ fractions from the Ae do not follow the trend for the underlying solodized zone, indicating possible depotassification of this mineral in the Ae horizon.

Diffraction analyses indicated that the expandable components were comprised of a mixture of distinct smectite species. The presence of 1.43 and 1.7 nm spacings for glycerol solvated specimens (Figure 2.1), and only a 1.7 nm spacing for the ethylene glycol solvated specimens is characteristic of a mixture of montmorillonite and a beidellite-like mineral (Harward et al, 1969). The X-ray diffraction patterns (Figure 2.1) indicate that this beidellite-like species dominates in the Ae horizon, whereas the montmorillonite is the major species in both the Bnt and Csak horizons. This variability with depth can be explained by either preferential translocation of the individual species, by alteration of montmorillonite, or by neoformation of the beidellite-like species in the Ae horizon.

The partial re-expansion of the 0.95 nm spacing of Li-saturated specimens (Greene-Kelly, 1953) following glycerol solvation to spacings of 1.38 and 1.7 nm in the Ae and Bnt horizons respectively confirmed the presence of both octahedrally and tetrahedrally substituted smectites (Schultz, 1969). The differentiation of the 1.38 and 1.7 nm spacings with depth (Figure 2.1) suggests a change in the distribution of the beidellite-like phase within the profile. The beidellite phase with the 1.3 nm spacing is dominant in the Ae horizon, and present in only minor amounts in the Csak horizon. The phase with the 1.7 nm spacing, on the other hand, is dominant in the Csak horizon. Based on the criteria defined by Schultz (1969), approximately 60% of the net layer charge of the beidellite-like species of the Ae is in the tetrahedral layers, whereas

approximately 25% of the net charge is in the tetrahedral layer for the expandable species in samples from the C horizon. This high charge beidellite-like species of the Ae horizon may have formed by the weathering of the micaceous minerals (Somasiri et al, 1971; Churchman, 1980; St Arnaud and Sudom, 1981), while the low charge montmorillonite species in the lower pedon is an inherited mineral. The beidellite species may also have formed by partial desilication of the tetrahedral layer of the montmorillonite, with subsequent incorporation of Al in tetrahedral coordination in the clay structure (Schultz, 1969). A model for the transformation of montmorillonite to beidellite has been proposed by Karathanasis and Hajek (1983).

Infrared absorption spectra (Figure 2.2a) obtained for crystalline clay minerals of the 0.2-1.0 μm separate from the Ae and Bnt horizons display strong Al-O-Al vibrations in the 910-920 cm^{-1} region. This 910-920 cm^{-1} band indicates the presence of a tetrahedrally-substituted mineral and is characteristic of beidellite (Farmer, 1974). The intensity of the band is stronger in the separates from the upper Ae horizon and thus confirms the interpretation based on XRD analysis which indicated a higher proportion of beidellite. The presence of strong absorption bands in the 810-820 cm^{-1} region in the infrared spectra from all horizons is indicative of Fe substitution in the octahedral layer of minerals in the smectite-rich 0.2-1.0 μm separates. This Fe substitution suggests that the octahedrally-substituted smectite, indicated by the 0.95 nm spacing in the diffraction patterns of the Li^+ -saturated samples (Figure 2.1), is probably an Fe-rich montmorillonite. The presence of a significant content of Fe in the various clay fractions (Table 2.5) supports this suggestion. This Fe-rich inherited smectite was detected in clay separates throughout the sola, and has previously been documented in Alberta soils (Arshad and Pawluk, 1966b; Pawluk and Bayrock, 1969).

Table 2.5: Composition and mineralogy of clay fractions from the solodization region and parent material of the Hermaruka pedon.

Sample (μm)	K	Mg		Fe $\text{m}^2 \text{g}^{-1}$	S.A.	CEC ¹	Mica		S.A.	Smectite CEC	Kaol. +Chl.		Amorph.
		%						%					
<u>Ae horizon</u>													
1.0-2.0	2.51	1.33		4.44	170	30	30	21	29	31		10	
0.2-1.0	1.19	1.02		5.01	282	36	23	35	34	33		10	
0.08-0.2	1.78	1.18		8.04	412	55	21	52	52	28		9	
<0.08	1.08	0.96		6.70	516	79	13	65	75	2		10	
<u>Column Top</u>													
1.02-2.0	2.81	1.03		4.40	142	28	34	18	27	34		5	
0.2-1.0	2.69	1.49		6.84	387	46	33	48	44	13		11	
0.08-0.2	2.50	1.59		6.85	520	57	30	65	54	6		10	
<0.08	1.78	1.73		7.72	689	73	21	86	70	0		12	
<u>Bnt Horizon</u>													
1.0-2.0	2.67	1.25		4.78	178	29	32	22	28	36		4	
0.2-1.0	2.43	1.79		6.00	442	46	29	55	44	21		6	
0.08-0.2	2.03	1.69		6.48	525	57	24	66	54	11		10	
<0.08	1.44	1.78		6.39	694	75	17	87	71	0		12	
<u>Csak Horizon</u>													
1.0-2.0	2.74	1.19		5.51	188	31	33	24	30	34		3	
0.2-1.0	2.20	1.61		6.08	474	49	27	59	47	22		4	
0.08-0.2	2.06	1.64		6.98	565	61	26	69	57	11		5	
<0.08	1.48	1.72		5.61	682	78	18	85	74	5		4	

¹Expressed as $\text{cmol}(+) 100 \text{ g}^{-1}$

The higher levels of acid oxalate extractable Fe in clay separates from Ae and column top samples (Table 2.6) may have resulted from the products of either the weathering of Fe^{++} in the octahedra of Fe-containing smectites (Rozenson and Heller-Kallai, 1978), or the weathering of ferromagnesian minerals. Oxidation of octahedral iron, and subsequent migration from the crystal lattice, would have only very minor effects on the b-axis spacings of the smectite minerals (Rozenson and Heller-Kallai, 1978), although it would cause a decrease in the exchange capacity. Any effect on the c-axis spacing would require a concomitant partial desilication of the tetrahedral layers of the lattice (Karathanasis and Hajek, 1983). X-ray powder diffractograms of clay separates (0.08-0.2 μm) dominated by Fe-containing montmorillonite (data not shown) showed that b-axis spacings remained unchanged for samples from throughout the profile.

The content of amorphous material (Table 2.5) is estimated from the sum of the oxides of Al, Fe, and Si extracted by the oxalate and hot KOH solutions. Content of this amorphous component comprises approximately 10% by weight of all clay fractions analysed from the solodized zone, but dropped to a maximum of 5% in the fractions separated from the Csak horizon. The higher levels in the upper profile result from the hydrolysis of the crystalline alumino-silicate minerals. The acid oxalate reagent dissolves allophane, imogolite and poorly-ordered iron oxides such as ferrihydrite and maghemite (Parfitt and Henmi, 1982). The Al/Si ratios reported in Table 2.6 range from 1.3 to 2.9, with most between 1.9 and 2.6. These ratios are typical for allophane-like constituents (Parfitt et al, 1980; Parfitt and Henmi, 1980; Russell et al, 1981; Anderson et al, 1982) formed from a range of parent materials. The oxalate extractable iron levels were highest from Ae horizon clay samples, and may result from the dissolution of the zones of iron oxide concentrates observed in the plasma fabrics during the

Table 2.6: Aluminium, iron, and silicon extracted by acid ammonium oxalate and hot hydroxide solutions from the horizons of the solodized zone of the Hemenruka pedon.

Sample (μm)	Oxalate extraction				Hot KOH extraction			
	Al	Si	Fe	Al/Si	Al	Si	Al/Si	
								%
<u>Ac Horizon</u>								
1.0-2.0	0.54	0.47	1.18	1.2	0.81	1.70	0.48	
0.2-1.0	0.33	0.16	0.93	2.1	1.24	2.43	0.51	
0.08-0.2	0.60	0.26	1.19	2.3	0.97	1.86	0.52	
<0.08	0.77	0.32	1.03	2.4	0.42	1.30	0.32	
<u>Column Top</u>								
1.0-2.0	0.21	0.08	0.67	2.6	0.30	1.10	0.27	
0.2-1.0	0.42	0.15	0.91	2.8	0.96	2.47	0.39	
0.08-0.2	0.46	0.20	0.86	2.3	0.92	2.39	0.39	
<0.08	0.57	0.25	0.53	2.3	1.22	3.23	0.38	
<u>Bnt Horizon</u>								
1.0-2.0	0.18	0.08	0.84	2.3	0.20	0.77	0.26	
0.2-1.0	0.32	0.14	0.59	2.3	0.45	1.44	0.31	
0.08-0.2	0.42	0.22	0.90	2.1	0.79	2.55	0.31	
<0.08	0.49	0.24	0.79	2.0	0.94	3.13	0.30	

micromorphological examination. Substitution of iron by aluminium in the poorly crystalline minerals of these plasma concentrates (Nakai and Yoshinaga, 1980) may contribute to the higher Al/Si ratios calculated for the Ae horizon samples.

Subsequent extraction of the clay separates with hot KOH dissolved a siliceous component, as is demonstrated by the calculated Al/Si ratios. The range in ratios is fairly narrow, being between 0.3 and 0.5, and falls within the range documented for opaline silica (Higashi, 1982). Maximum levels of the KOH-soluble amorphous material were measured in the separates from the column top and Bnt.

Table 2.7: Si:Al ratios of minerals dissolved from the silt separates of the solodized zone of the Hemaruka pedon.

Horizon	Fraction (μm)	Si:Al
Ae	2-5	5.96
	5-20	7.69
	20-50	*10.80
Column top	2-5	5.03
	5-20	4.77
	20-50	4.69

* Plant opal was observed in the 5-20 and 20-50 μm fractions from the Ae horizon.

The differential FT-IR spectra presented in Figure 2.2b and 2.2c were calculated for the samples analysed before and after the selective dissolution treatments. The upper spectrum was calculated for the 0.2-1.0 μm separate from the column top. The material dissolved in the separate had an Al/Si (KOH) ratio of 0.39:1. The absorption maxima at 1075 cm^{-1} are due to Si-O vibrations (Higashi, 1982). The additional absorptions at 780 and 460 cm^{-1} indicated that

much of the material dissolved by the hot KOH was opaline silica. The differential spectrum (c) calculated for the sample from the Ae horizon displayed bands which suggested that the dissolved material was a mixture of two distinct amorphous mineral phases. The absorption maxima at 980 and 915 cm^{-1} are Si(Al)-O vibrations. The associated absorption bands at the 700, 570 and 480 cm^{-1} regions indicate dissolution of a mineral with the infrared characteristics of imogolite (Higashi, 1982). The absorption maximum at 1050 cm^{-1} , with associated bands at 570 and 430 cm^{-1} are characteristic of allophane minerals (Parfitt and Henmi, 1980; Higashi, 1982).

Diffraction analyses of coarse clay and silt fractions from the upper section of the solodized zone consistently produced a spacing at about 0.89 nm which was stable following heating to 550 C for 12 hours. This spacing, which was not present in samples from the Csak horizon, disappeared when the samples were treated with hot alkali solutions (80 C). The 0.89 nm spacing was, however, stable following treatment with hot 2M HCl. The Si/Al ratio of the material dissolved from the silt and coarse clay separates with the hot alkali ranged from 4.6 to 10.8 (Table 2.7). Plant opal observed by light microscopy of the silt fractions probably accounts for some of the dissolved Si, but opal could not explain the high levels of dissolved Al. Specific gravity separations enabled preconcentration of the material with the 0.89 spacing in the 2.35-2.53 separate. Powder diffraction analysis (Table 2.8) indicated that this authigenic material has the diffraction characteristics of clinoptilolite (Boles, 1972).

Such siliceous zeolite minerals commonly precipitate from saline solutions (Boles and Wise, 1978) of hydrogen ion activity of 10^{-7} - 10^{-8} moles litre⁻¹ and a dissolved silica concentration of 20-40 ppm (Gieskes and Kastner, 1975). The reported Na^+ concentration of solutions in equilibrium with these zeolites is generally 6-10 times that of the K^+ concentration, although K is the dominant alkali metal incorporated into the zeolite structure (Cosgrove and Papavassilou,

1979; Kastner, 1979).

Table 2.8: X-ray diffraction spacings for clinoptilolite* separated from the Ae horizon of the Hemaruka pedon.

(hkl)	d (nm)	I/I ₀
020	0.894	100
200	0.794	16
111	0.681	9
220	0.595	8
131	0.465	14
400	0.397	50
330	0.391	33
151	0.298	33
161	0.273	10

* Mineral preconcentrated in the 2.35-2.53 S.G. separate.

Electron optical examination of the specific gravity separates indicated that the clinoptilolite was comprised of euhedral crystals composed of stacked euhedral plates each 1-5 μm thick and commonly 5-25 μm across (Plate 2.2c). Crystals exhibited monoclinic symmetry. The observed morphology is similar to that documented for clinoptilolite of both marine and freshwater origin (Mumpton and Ormsby, 1978; Desprairies, 1981). The size and crystallinity of the zeolite suggested precipitation directly from the soil pore fluids (Boles and Wise, 1978). Crystals separated from the Ah1 horizon appeared to be etched (Plate 2.2b, 2.2c), indicating that the mineral has possibly undergone partial dissolution in this horizon. Energy-dispersive x-ray microanalysis (Figure 2.3) of the individual crystals confirmed that the clinoptilolite is siliceous, with an Si/Al ratio of between 4.8:1 to 5.2:1. The high K content of the the clinoptilolite separated from these samples and the solubility of the mineral in alkaline but not in acid media

is typical of characteristics described for clinoptilolite species (Vaughan, 1978).

The solution chemistry of the aqueous extracts from the Ae and Ahe horizons (Table 2.9) are similar to those described for the pore waters of siliceous clinoptilolite-bearing sediments (Gieskes and Kastner, 1975). This similarity, coupled with the obvious lack of this mineral in the parent material, prompted examination of the solution chemistry with the SOLMNEQ solution-mineral equilibrium model to determine the predicted reaction state of the aqueous solutions with respect to the solid clinoptilolite phase. The free energy estimates calculated by Cosgrove and Papavassilou (1979) assuming both smectite and kaolinite as precursors to the formation of clinoptilolite were utilized as input to the model data base. The predictions indicated that clinoptilolite would not form by the weathering of kaolinite. This supports the thermodynamic predictions for the stability of kaolinite minerals in soil horizons with a pH between 5.5 and 7.0 (Lindsay, 1979).

However, the thermodynamic calculations within the SOLMNEQ model predicted precipitation of clinoptilolite from the solutions extracted from the Ah₂, Ahe and Ae horizons assuming dissolution of a smectite precursor. Precipitation of clinoptilolite was thought to require a source of soluble silica such as opal or volcanic glass (Mumpton and Ormsby, 1978). Volcanic glass in the Hemaruka and Camrose soils would be silt-sized, and from either the Mazama or St. Helens-Y plumes (Westgate et al, 1969). Microscopic examination also indicated the presence of plant opal grains in the 5-20 and 20-50 μm separates from the A horizons of the pedons. However, the silica concentrations (Table 2.9) were in the range for equilibrium solutions with smectite minerals (Kittrick, 1969), rather than the aforementioned silica minerals. Thus, desilication of smectites may have provided the source of silicon for the neoformation of clinoptilolite. The prediction that clinoptilolite would not be stable in the Ah₁ horizon is in agreement with the electron optical observations of solution pitting on the zeolite

grains separated from this horizon. Dissolution of clinoptilolite may be a result of the lower Si concentrations in the Ah1 horizon (Waterman et al, 1972). Furthermore, the model predicted that clinoptilolite is thermodynamically unstable in the pore solutions extracted from the lower solum.

Table 2.9: Solution chemistry of extracts from the major horizons of the Hemaruka pedon.

Horizon	pH	Al	Ca	Fe	K	Mg	Na	Si	HCO ₃ ⁻	PO ₄ ³⁻
----- ug ml ⁻¹ -----										
Ah ₁	6.9	3	37	32	13	11	58	11	94	<1
Ah ₂	6.1	2	5	5	3	2	27	23	37	<1
Ahe	7.0	4	7	6	3	3	43	13	205	<1
Ae	8.2	2	6	4	4	5	94	18	244	<1
Bnt	7.4	1	35	2	12	50	454	5	80	<1
Bntk	7.4	1	529	1	28	230	668	7	231	<1
BCsak	7.2	1	99	1	17	66	432	6	329	<1
Csak	7.4	1	712	1	31	263	240	4	218	<1

2.4. CONCLUSIONS

Although the data presented in this paper have been drawn from the analyses of samples of a

Brown Solodized Solonetz pedon, the pedogenic translocations and transformations described herein were also observed in the Black Solodized Solonetz pedon characterized in the course of the current study. The results of the current study describe three major mineralogical consequences of pedogenesis which add to the understanding of the processes active during the solodization of saline soils in Western Canada.

The translocations and transformations of smectite present in the sola comprised the first pedogenic processes described in detail in this study. The two dominant smectites found were an Fe-rich montmorillonite and a beidellite. The Fe-rich montmorillonite, an inherited mineral, was translocated by processes of lessivage of the fine clay fractions ($<0.2\ \mu\text{m}$) from the Ae and column top regions of the solodized zone to the Bnt horizons of the solum. The beidellite, a high charge smectite species, was concentrated in the fine clay fractions ($<0.2\ \mu\text{m}$) of the Ae horizon and is either an alteration/degradation product of another inherited phyllosilicate mineral or an authigenic species. Evidence for depotassification of micas in the upper solum suggested the beidellite could form as a degradation product of the micaceous minerals.

The recognition of significant amounts of pedogenically formed amorphous aluminosilicate minerals in the A horizons of the sola confirms suggestions made in earlier studies of solodized sola (Gedroits, 1927; Brunelle et al, 1976). Extraction chemistry and differential infrared analyses indicate that these authigenic minerals have characteristics reported for imogolite and allophane. Opaline silica was also detected in the zone of solodization on the upper Bnt columns. Plant opal was observed in the light mineral (S.G. <2.35) separates from the Ah and Ae horizons.

The major finding of the study was the recognition of the neoformation of significant amounts of clinoptilolite as a precipitate of the pore waters in the Ae and column top region of

the zone of active solodization. This mineral is concentrated in the light mineral separate (S.G. <2.35) of the silt fractions. Examination of the aqueous chemistry of pore waters extracted from the major genetic horizons indicated that the clinoptilolite may form as a result of the weathering of smectites and is thermodynamically stable in only the Ahe and Ae horizons. Although unstable in pore waters of the Ah horizons, the relatively short periods of field saturation of these horizons enable its persistence as an important mineralogical component. The observed solubility of clinoptilolite in alkaline solutions may explain the lack of previous recognition of the mineral in Solodized Solonetz soils from Western Canada. The use of an alkaline dispersant, calgon, prior to mineralogical analyses may have dissolved the zeolite.

Both the amorphous mineral phases and the authigenic zeolite described in this paper are known to have high cation/anion exchange and retention properties. An understanding of the effects of these properties may prove to be of major importance in the understanding of the unique fertility problems, such as plant responses to phosphate and nitrate fertilization, associated with Solodized Solonetz soils.

BIBLIOGRAPHY

- Anderson, H.A., M.L. Berrow, V.C. Farmer, A. Hepburn, J.D. Russell and A.D. Walker (1982) A reassessment of podzol formation processes. *J. Soil Sci.* 33: 125-136.
- Arshad, M.A. and S. Pawluk (1966a) Characteristics of some solonetzic soils in the Glacial Lake Edmonton basin of Alberta. I. Physical and chemical. *J. Soil Sci.* 17: 36-47.
- Arshad, M.A. and S. Pawluk (1966b) Characteristics of some solonetzic soils in the Glacial Lake Edmonton basin of Alberta. II. Mineralogy. *J. Soil Sci.* 17: 48-55.
- Baldar, N.A. and L.D. Whittig (1968) Occurrence and synthesis of soil zeolites. *Soil Sci. Soc. Am. Proc.* 32: 235-238.
- Boles, J.R. (1972) Composition, optical properties, cell dimensions, and thermal stability of some heulandite-group zeolites. *Am. Mineral.* 57: 1463-1493.
- Boles, J.R. and W.S. Wise (1978) Nature and origin of deep-sea clinoptilolite. In: Sand, L.B. and F.A. Mumpton (eds), *Natural Zeolites: occurrence, properties, use*. Pergamon Press, London.
- Bowser, W.E., A.A. Kjarsgaard, T.W. Peters and R.E. Wells (1962) Soil Survey of the Edmonton Sheet (83-H). Alberta Soil Survey Report No. 21. University of Alberta SS-4, Edmonton, Alberta.
- Brewer, R. and S. Pawluk (1975) Investigations of some soils developed in hummocks of the Canadian Sub-Arctic and Southern Arctic regions. *Can. J. Soil Sci.* 55: 301-309.
- Brunelle, A., S. Pawluk, T.W. Peters (1976) Evaluation of profile development of some solonetzic soils of south central Alberta. *Can. J. Soil Sci.* 56: 149-158.
- Carter, D.L., M.D. Heilman and C.L. Gonzales (1965) Ethylene glycol monoethyl ether for determining surface area of silicate minerals. *Soil Sci.* 100: 356-360.
- Churchman, G.J. (1980) Clay minerals formed from chlorites and micas in some New Zealand soils. *Clay Min.* 15: 59-75.

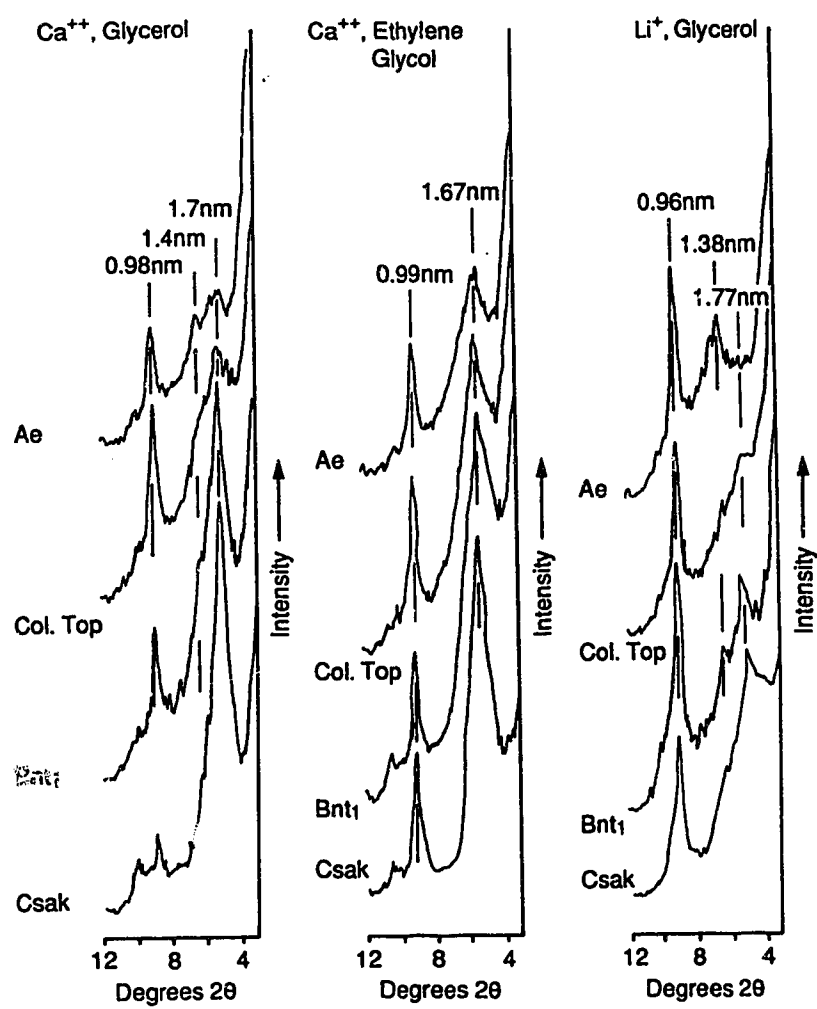
- Cosgrove, M.E. and C.Th. Papavassiliou (1979) Clinoptilolite in DSDP sediments of the Indian Ocean (Site 223, Leg 23): its stability conditions and estimation of its free energy. *Marine Geol.* 33: M77-M84.
- Desprairies, A. (1981) Authigenic minerals in volcanogenic sediments cored during Deep Sea Drilling Project Leg 60. In: Hussong, D.M. and S. Uyeda., et al. (1981) Initial Reports of the Deep Sea Drilling Project, vol 60: 455-465.
- Drees, L.R. and L.P. Wilding (1973) Elemental variability within a sampling unit. *Soil Sci. Soc. Am. Proc.* 37: 82-87.
- Dudas, M.J. and M.E. Harward (1971) Effects of dissolution treatments on standard soil clays. *Soil Sci. Soc. Am. Proc.* 35: 134-140.
- Dumanski, J. and R.J. St. Arnaud (1966) A micropedological study of eluvial soil horizons. *Can. J. Soil Sci.* 46: 287-292.
- Ellis, J.H. and O.G. Caldwell (1935) Magnesium clay solonetz. *Trans. 3rd Int. Soil Sci. Congress, Oxford.* 1: 348-350.
- Farmer, V.C. (ed) (1974) *The Infrared Spectra of Minerals.* Mineralogical Society, Monograph 4, London. 539 pp.
- Fieldes, M. and K.W. Perrot (1966) The nature of allophane in soils: III. Rapid field and laboratory tests for allophane. *N.Z. J. Sci.* 9: 623-629.
- Gedroits, K.K. (1927) Genetic soil classification based on the absorptive soil complex and absorbed soil cations. Israel Program for Scientific Translations, 1966. IPST Cat. No. 1628.
- Giekes, J.M. and M. Kastner (1975) Evidence for extensive diagenesis, Madagascar Basin, Deep Sea Drilling Site 245. *Geochim. Cosmochim. Acta* 39: 1385-1393.
- Greene-Kelley, R. (1953) The identification of montmorillonoids. *J. Soil Sci.* 4: 233-237.
- Harward, M.E., D.D. Carstea and A.H. Sayegh (1969) Properties of vermiculites and smectites: expansion and collapse. *Clays Clay Min.* 16: 437-447.

- Higashi, T. (1982) Amorphous inorganic constituents under prominent accumulation of humus in volcanic ash soils. *Pedologie*, XXXII: 5-18.
- Howitt, R.W. and S. Pawluk (1985) Genesis of a Gray Luvisol in the Boreal Forest zone. II. Dynamic pedology. *Can. J. Soil Sci.* 65: 9-19.
- Jackson, M.L. (1975) *Soil Chemical Analysis: an advanced course*. University of Wisconsin, Madison, Wisconsin.
- Jacob, J.S. and B.L. Allan (1983) Persistence of a zeolite in tuffaceous soils of southwest Texas. *Agron. Abstr.*, p. 219.
- Karathanasis, A.D. and B.F. Hajek (1983) Transformation of smectite to kaolinite in naturally acid soil systems: structural and thermodynamic considerations. *Soil Sci. Soc. Am. J.* 47: 158-163.
- Kastner, M. (1979) Zeolite Minerals. In: Burns, R.G., ed. *Marine Minerals. Reviews in Mineralogy*, vol 6. Mineralogical Society of America. pp. 111-122.
- Kharaka, Y.K. and I. Barnes (1973) SOLMNEQ: solution-mineral equilibrium computation. U.S. Department of Commerce, National Technical Information Service, PB 215 899.
- Kittrick, J.A. (1969) Minerals in the Al_2O_3 - SiO_2 - H_2O system and a theory of their formation. *Clays Clay Min.* 17: 157-167.
- Kovda, V.A. (1939) *The Solonetz Soils*. Israel Program for Scientific Translations, 1961. IPST Cat. No. 254.
- Landsburg, S. (1981) Salt and Water Fluxes in Solonetzic B Horizons. M.Sc. thesis, University of Alberta, Edmonton. 181 pp. Accession no. 51526, National Library of Canada, Ottawa, Ontario.
- Lindsay, W.L. (1979) *Chemical Equilibria in Soils*. Wiley, New York, N.Y., 439 pp.
- MacGregor, J.M. and F.A. Wyatt (1945) Studies on solonetz soils of Alberta. *Soil Sci.* 59: 419-435.
- Maclean, A.H. and S. Pawluk (1975) Soil genesis in relation to groundwater and soil moisture near Vegreville, Alberta. *J. Soil Sci.* 26: 278-293.
- McKeague, J.A. ed. (1978) *Manual of soil sampling and methods of analysis*. Soil Research Institute, Ottawa, 212 pp.

- Mathieu, A.L. (1960) The mineralogy of the clay fraction in relation to the genesis of Solodized Solonetz soils. Ph. D. thesis, Univ. of Saskatchewan, Saskatoon. 181 pp.
- Mumpton, F.A. and W.C. Ormsby (1978) Morphology of zeolites in sedimentary rocks by scanning electron microscopy. In: Sand, L.B. and F.A. Mumpton, (eds). Natural Zeolites: occurrence, properties, use. Pergamon Press, London.
- Nakai, M. and N. Yoshinaga (1980) Fibrous goethite in some soils from Japan and Scotland. *Geoderma* 24: 143-158.
- Parfitt, R.L. and T. Henmi (1980) Structure of some allophanes from New Zealand. *Clays Clay Min.* 28: 285-294.
- Parfitt, R.L., R.J. Furkett and T. Henmi (1980) Identification and structure of two types of allophane from volcanic ash soils and tephra. *Clays Clay Min.* 28: 328-334.
- Parfitt, R.L. and T. Henmi (1982) Comparison of an oxalate extraction method and infrared spectroscopic method for determining allophane in soil clays. *Soil Sci. Plant Nutr.* 28: 183-190.
- Pawluk, S. and L.A. Bayrock (1969) Some characteristics and physical properties of Alberta soils. Research Council of Alberta, Bull. 26. 72 pp.
- Rost, C.O. and K.A. Mahl (1943) Some solodized soils of the Red River Valley. *Soil Sci.* 55: 301-312.
- Rozenson, I. and L. Heller-Kallai (1978) Reduction and oxidation of Fe^{3+} in dioctahedral smectites. III: Oxidation of octahedral iron in montmorillonites. *Clays Clay Min.* 26: 88-92.
- Russell, M., R.L. Parfitt and G.C. Claridge (1981) Estimation of the amounts of allophane and other materials in the clay fraction of an Egmont loam profile and other volcanic ash soils, New Zealand. *Aust. J. Soil Res.* 19: 185-195.
- St. Arnaud, R.J. and M.D. Sudom (1981) Mineral distribution and weathering in Chernozemic and Luvisolic soils from central Saskatchewan. *Can. J. Soil Sci.* 61: 79-89.
- Schultz, L.G. (1969) Li and K absorption, dehydroxylation temperature and structural water content of aluminous smectites. *Clays Clay Min.* 17: 115-150.

- Somasiri, S., S.Y. Lee and P.M. Huang (1971) Influence of certain pedologic factors on potassium reserves of selected Canadian soils. *Soil Sci. Soc. Am. Proc.* 35: 500-505.
- Southard, A.R. and P.T. Kolesar (1978) An exotic source of extractable potassium in some soils of northern Utah. *Soil Sci. Soc. Am. J.* 42: 528-530.
- Spiers, G.A., M.J. Dudas and L.W. Hodgins (1983) Instrumental conditions and procedure for multielement analysis of soils and plant tissue by ICP-AES. *Comm. Soil Sci. Plant Anal.* 14: 629-644.
- Thiesen, A.A. and M.E. Harward (1962) A paste method for preparation of slides for clay mineral identification by X-ray diffraction. *Soil Sci. Soc. Am. Proc.* 26: 90-91.
- Vaughan, D.E.W. (1978) Properties of natural zeolites. In: Sand, L.B. and F.A. Mumpton, (eds). *Natural Zeolites: occurrence, properties, uses*. Pergamon Press, London. pp. 113-132.
- Waterman, L.S., L.S. Sayles and F.T. Manheim (1972) Interstitial water studies on small core samples, leg 14. In: Hayes, D.E., et al., (eds). *Initial Reports of the DSDP, vol 14*: U.S. Govt Printing Office, Washington, pp. 753-762.
- Westgate, J.A., D.G.W. Smith and H. Nichols (1969) Late Quaternary pyroclastic layers in the Edmonton area, Alberta. In: Pawluk, S., ed. *Pedology and Quaternary Research*. pp. 179-186. University of Alberta, Edmonton, Alberta.
- Whittig, L.D. (1959) Characteristics and genesis of a Solodized Solonetz of California. *Soil Sci. Soc. Am. Proc.* 23: 469-473.

Figure 2.1. X-ray diffractograms of Ca^{++} -saturated and Li^+ -saturated, glycerol and ethylene glycol solvated specimens of 0.2 to 1.0 μm clay separates from the Hemaruka pedon. Diffraction peaks are identified using 2θ values for Cu $K\alpha$ radiation and corresponding d-spacing in nanometers.



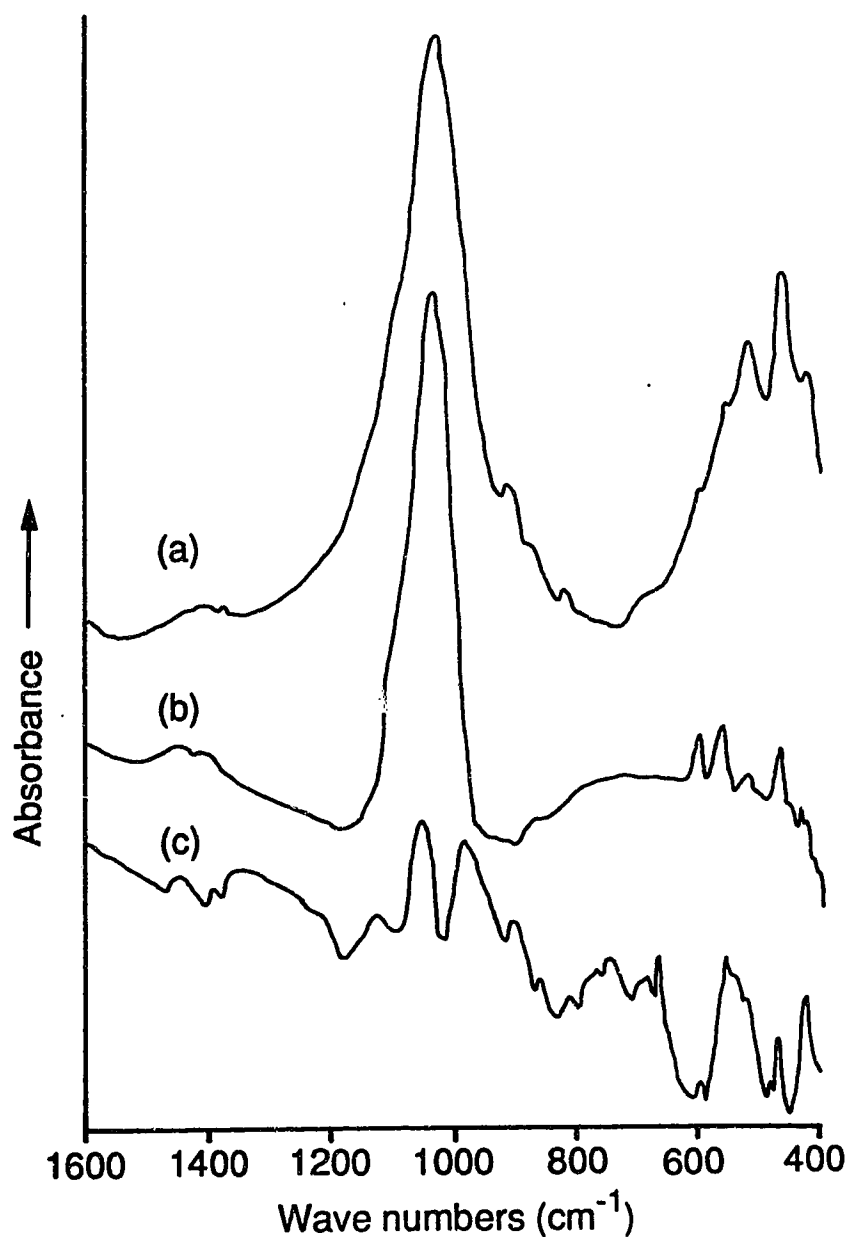


Figure 2.2. Infrared spectra obtained for both crystalline and X-ray amorphous clay (0.2-1.0 μm) from the solodization region of the Hemaruka pedon. The upper spectrum (a) is for the crystalline phyllosilicate material remaining after both acid oxalate and hot KOH extraction of the X-ray amorphous material of an Ae horizon sample. The spectra (b) and (c) are differential patterns of the X-ray amorphous minerals extracted from the column top and Ae horizons respectively.

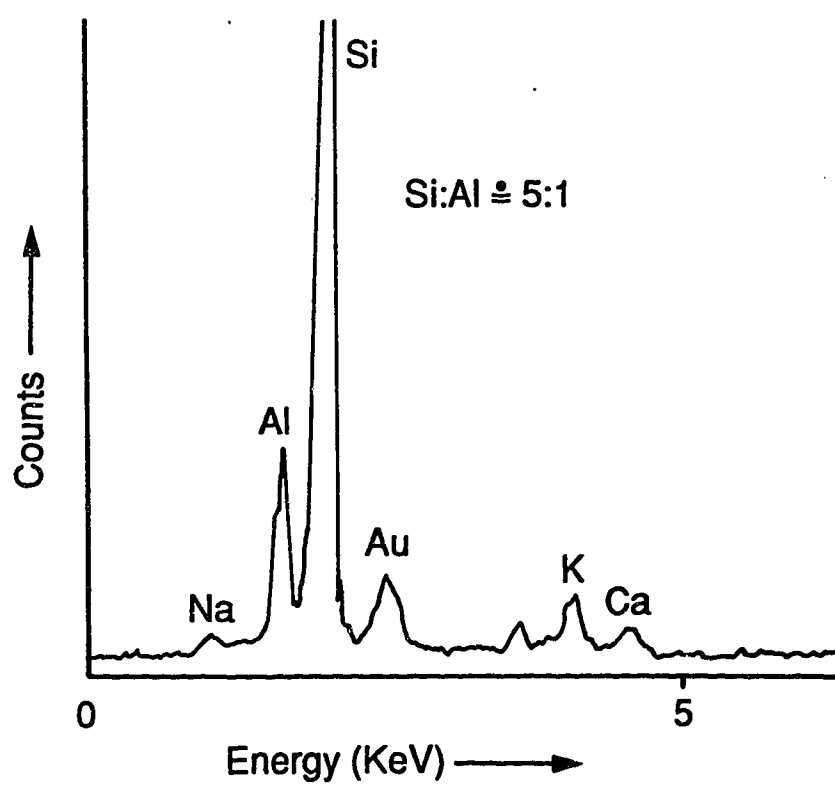


Figure 2.3. Energy dispersive X-ray spectrum of a clinoptilolite crystal separated from the 5- to 20- μm fraction of the Ae horizon of the Hemaruka pedon.

Plate 1: Micrographs of selected features from the Ae and Bnt horizons of the Hemaruka pedon.

(a) Fabric of the Ae and upper Bnt horizons. The zones represented by numbers (1, 2, 3, 4) represent the location of the following scanning electron micrographs (b, c, d, e, respectively).

Frame width = 1cm.

(b) Morphology of the incipient platy structure forming in the zone of active solodization at the top of the Bnt column.

(c) Plan view of the solodization zone at the top of the column illustrating the absence of clay material binding the skeletal sand and silt grains. (d) Clay matrix cementing the the skeletal grains in the upper Bnt horizon.

(e) Clay bridge cementing silt grains in the intertextic spaces in the upper Bnt horizon.

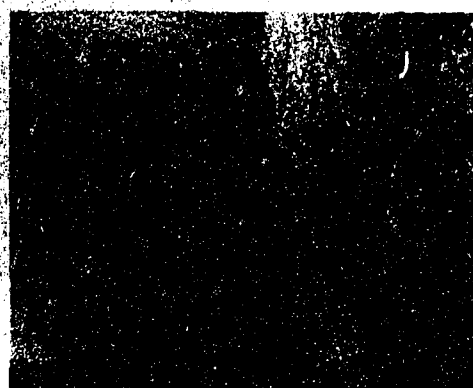
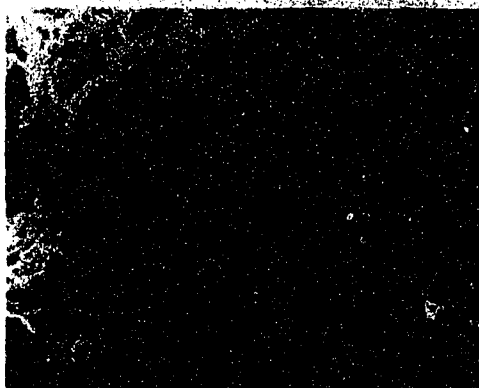
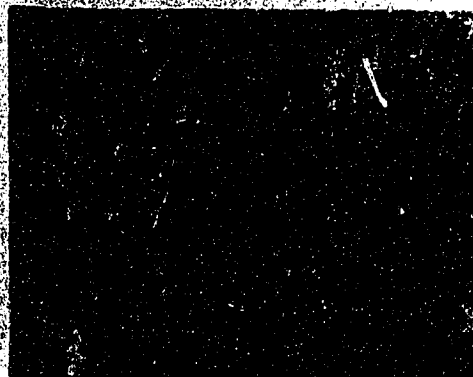
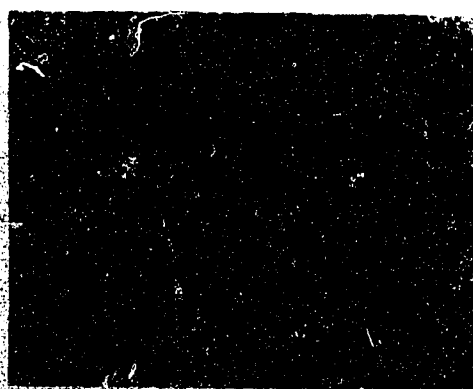
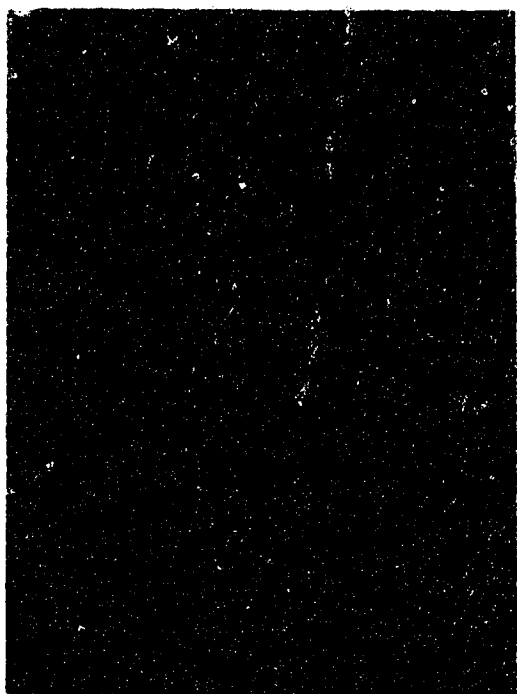


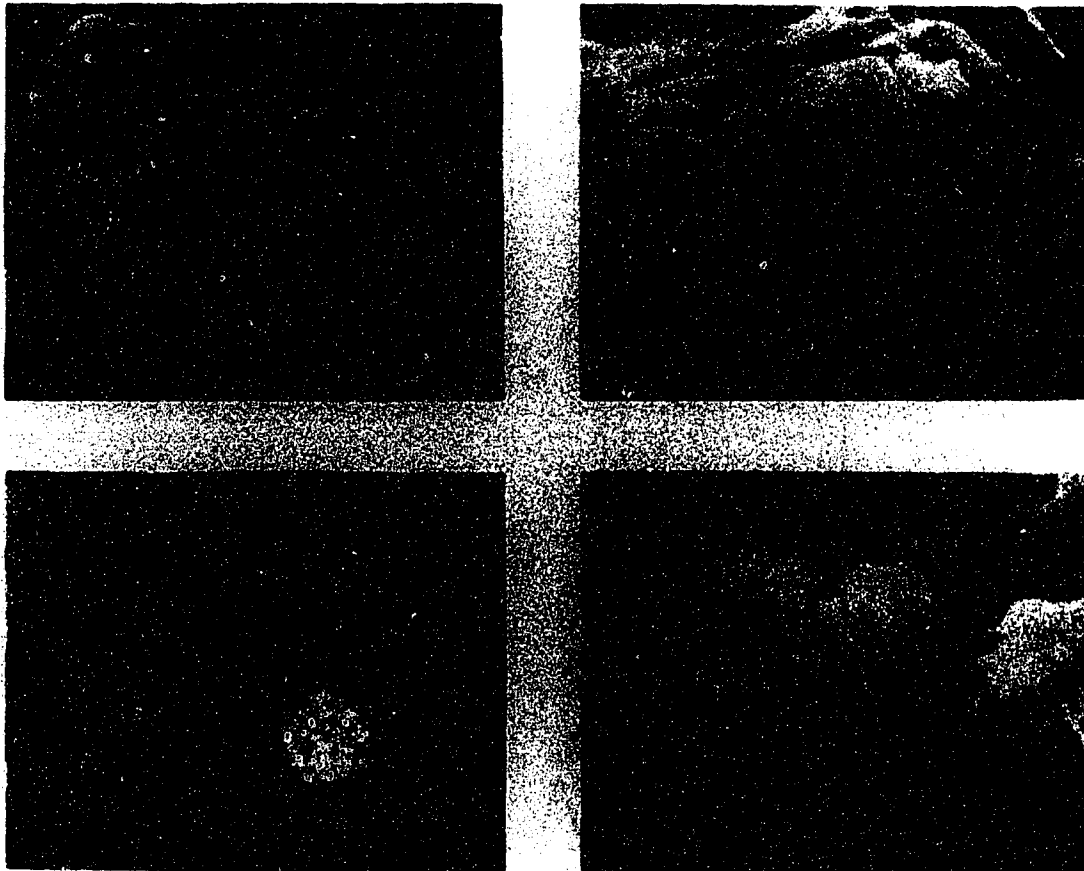
Plate 2.2. Scanning electron micrographs of clinoptilolite grains from the Ae and Ah1 horizons of the Hemaruka pedon.

(a) Unweathered clinoptilolite grain separated from the Ae horizon.

(b) Weathered clinoptilolite grain separated from the Ah1 horizon.

(c) Enlargement of (b) illustrating the distinctive crystal morphology of the clinoptilolite. Solution pitting is obvious on the grain surface.

(d) Fine grained clinoptilolite crystals formed in situ in the eluviated zone of active solodization on the column top.



3: ISOTOPIC EVIDENCE FOR CLAY MINERAL WEATHERING AND AUTHIGENESIS IN LUVISOLIC SOILS ¹

3.1: INTRODUCTION

Recognition of mineral formation and clay mineral weathering in soils is often confounded by the presence of admixed inherited or detrital components mineralogically similar to the authigenic phases. Further complications in identifying authigenic minerals arise with stratified soils containing lithologic discontinuities (Wang and Arnold, 1973), with soils affected by eolian additions (Coen and Arnold, 1972), and in soils containing eluviated/illuviated horizons.

The difficulties in unambiguous identification of authigenic minerals is particularly apparent in soils developed from glacially-derived materials. For example, the authigenic formation of smectite with associated transformations of chlorite, mica and kaolinite was reported for Podzolic soils of Canadian Shield-derived sediments (Nicholson and Moore, 1977), whereas the presence of smectite in the albic horizons of similar Spodosols in New York was attributed to eolian additions (Coen and Arnold, 1972). Somasiri et al (1971) describe alteration of mica to an expandable phyllosilicate in Luvisolic (Cryoboralf) pedons but, in a study of similar soils, Pawluk and Dudas (1982) consider physical processes, including eolian additions, account for the heterogeneous clay distribution within the profile.

These conflicting interpretations indicate routine methods of analysis (X.R.D., D.T.A., elemental composition) may not adequately differentiate between authigenic and detrital components. In recent years oxygen isotopic composition has been used to determine formation conditions of secondary silicate minerals in sedimentary rocks (Lawrence and Taylor, 1971; Yeh and Savin, 1976; Longstaffe, 1983). Theoretical considerations and geologically oriented studies

¹Published in Soil Science Society of America Journal 49: 467-474.

suggest oxygen isotope geochemistry may also provide clear identification of authigenic phases in soils. The oxygen isotopic composition of any authigenic phyllosilicates formed during pedogenesis is controlled by the formation temperature, the isotopic composition of meteoric waters percolating through the soil, the oxygen mass balance between meteoric water and the mineral phase, the stable isotope equilibrium fractionation factor between the authigenic mineral and the fluid phase, and the extent of isotopic exchange between the mineral and the water following crystallization. The oxygen isotope partitioning between clay and water is large at low temperatures (Savin and Epstein, 1970; Lawrence and Taylor, 1971). For example, smectite, formed in isotopic equilibrium with meteoric water of $\delta^{18}\text{O} \approx -20\text{‰}$ (per mil) at 15 C will have an $^{18}\text{O}/^{16}\text{O}$ of about $+7\text{‰}$ while detrital smectites originally formed in marine environments ($\delta^{18}\text{O} = 0\text{‰}$) would have an $^{18}\text{O}/^{16}\text{O}$ of about $+26\text{‰}$ (Savin and Epstein, 1970). For normal soil temperatures there would not be significant isotopic exchange between the soil water and the oxygen of the structural sites in inherited crystalline clay minerals (James and Baker, 1976). Isotopic exchange would require considerable mineral dissolution and reprecipitation (Lawrence and Taylor, 1971, 1972).

Authigenic mineral formation in Cryoboralfs (Luvisols) requires clarification. Various clay mineral weathering sequences and products have been reported for these and associated soils (Kodama, 1979); however, most investigators have not clearly differentiated between authigenic and inherited phases. Accordingly, the objectives of this section of the thesis are to present detailed clay mineralogical data for Cryoboralfs in northern Alberta, and to assess authigenic clay formation by conventional methods of mineral analyses in conjunction with measurement of the oxygen isotopic geochemistry of the structural framework of the clay fraction minerals.

3.2: MATERIALS AND METHODS

The sites selected for this study were located on till deposits of Wisconsinan age in northeastern

Alberta within the Boreal Forest Region (Rowe, 1972). The soils comprising the parent materials (Figure 1) of the sampled pedons are derived from two distinct lithologies; one (Legend) is derived largely from Cretaceous sediments and the other (Kinosis) is derived from the preweathered surfaces of the Canadian Shield (Spiers et al, 1984).

Composite samples were collected from the major pedogenic horizons of two Cryoboralf pedons, air-dried and ground to pass a 2 mm sieve. Routine analyses and soil descriptions are documented elsewhere (Turchenek and Lindsay, 1982). Clay ($< 2 \mu\text{m}$) was separated by dispersing 50 g of air-dried soil in distilled water by ultrasonification using a probe type vibrator at 400 watts for 5 minutes. This was followed by repetitive extractions according to the gravity separation technique outlined by McKeague (1978). Content of titanium and zirconium in the silt fraction (5 - 50 micron) was determined by X-ray fluorescence (Drees and Wilding, 1973).

Saturation of 50-mg portions of the clay with Ca^{++} , Li^+ and K^+ was accomplished by three washings with the appropriate 1 M salt solutions followed by distilled water washings and centrifugation to remove the excess electrolyte. Oriented specimens for X-ray diffraction analysis were prepared on glass slides using the paste method (Thiesen and Harward, 1962). The remaining portions of the clay fractions were Ca-saturated, washed free of excess electrolyte, freeze-dried and used for subsequent analysis.

Diffraction patterns of the oriented specimens were obtained with a Philips diffractometer equipped with a LiF curved crystal monochromator using $\text{CuK}\alpha$ radiation generated at 40 kV and 20 mA. Diffraction patterns of Ca-saturated specimens were obtained for 54 % RH, glycerol, and ethylene glycol pretreatments while patterns for K-saturated specimens were obtained for 105 C heated samples analyzed at 0 % RH, then again after equilibration at 54 % RH and for 300 and 550 C heated samples maintained at 0 % RH during the analysis. Diffraction patterns of Li-saturated specimens were obtained for 200 C heated samples both before and after saturation with

glycerol vapour (Greene-Kelley, 1953). Dissolution of Ca-saturated samples and analysis for mica-K by inductively coupled plasma emission spectroscopy following HCl-HF dissolution followed the techniques described by Spiers et al (1983). The surface area of the clay separates was determined by solvation with ethylene glycol monoethyl ether (Carter et al, 1965). Cation-exchange capacity was determined by extraction of Ca-saturated clays with 2N KOAc, and measurement of displaced Ca^{++} (CaEC) by AAS. After washing with water / alcohol mixtures, the sample was further extracted with 2N NaOAc and the displaced K^+ measured to provide an estimate of KEC (Coffman and Fanning, 1975).

Quantitative determination of phyllosilicates in the fine and coarse clay separates was based on data for exchange capacity, surface area, and potassium content. The amount of smectite was calculated on the basis of the potassium exchange capacity (KEC), assuming pure smectite to have an exchange capacity of 110 $\text{cmol(p+)} \text{ kg}^{-1}$. The amount of vermiculite was calculated from the difference between the CaEC and KEC, assuming pure vermiculite to have an interlayer exchange capacity of 154 $\text{cmol(p+)} \text{ kg}^{-1}$ (Coffman and Fanning, 1975). Mica content was calculated assuming an ideal end-member muscovite composition of 8.3 $\text{g } 100\text{g}^{-1} \text{ K}$ (Jackson, 1975). The balance was assigned to kaolinite and chlorite. Chlorite was not detected in any of the fine clay separates, and estimated at a maximum of 8 $\text{g } 100\text{g}^{-1}$ in the Kinosis and 5 $\text{g } 100\text{g}^{-1}$ in the Legend parent materials respectively, using empirical relationships based on relative peak intensities at 0.359 and 0.352 nm (Griffin, 1971).

Sub-samples of the freeze-dried clay separates were further purified for isotopic analyses by oxidation of the organic matter with NaOCl (Lavkulich and Wiens, 1970) and dissolution of poorly crystalline minerals with acid ammonium oxalate and boiling 0.5 N KOH (Dudas and Harward, 1971). The content of Si, Al and Fe in the supernatant solutions was determined by atomic absorption spectroscopy. Oxygen for isotopic analyses was extracted from the clay

separates, both before and after removal of the poorly crystalline component by the BrF_3 method (Clayton and Mayeda, 1963), passed over hot carbon to form CO_2 and analysed on a double collecting, double inlet mass spectrometer. The results are reported in the usual δ -notation with respect to the SMOW standard (Craig, 1961), assuming that a $\text{CO}_2\text{-H}_2\text{O}=1.0407$. The standard deviation of replicate analyses calculated from the pooled residual variance was ± 0.12 .

3.3: RESULTS AND DISCUSSION

Both pedons have well-developed E horizons, with clay-enriched B horizons with both argillans and zones of oriented illuvial clay which meet the requirements for a textural B (Canada Soil Survey Committee, 1978) or an argillic horizon (Soil Survey Staff, 1975). These soils are classified as Orthic Grey Luvisols (Canada Soil Survey Committee, 1978) or Cryoboralfs (Soil Survey Staff, 1975). The difference in clay content between the two pedons (Table 1) reflects the different provenance of the glacial deposits forming the parent materials of the two soils (Spiers et al, 1984).

Diffraction analyses indicated clay separates from both parent materials consisted primarily of admixtures of smectite, mica, kaolinite, and chlorite. Diffractograms illustrating the diffraction characteristics of these parent materials are depicted in Figure 2. The presence of 1.43 and 1.7 nm spacings for glycerol solvated specimens and only 1.7 nm spacings for ethylene glycol solvated specimens is characteristic of a mixture of beidellite and montmorillonite (Harward et al, 1969). The micaceous component of both soils is dominated by dioctahedral species as indicated by the strong (002) reflections at 0.5 nm relative to the first order basal reflections (1.0 nm). A weak (060) reflection at 0.154 nm for Ca-saturated samples heated to 550 C (not shown) indicates the presence of minor amounts of trioctahedral mica in the Kinosis samples only (Fanning and Keramidas, 1977). Diffraction peaks for chlorite were weak, and only clearly evident after samples were heated to 550 C. The increase in intensity of the (001)

chlorite reflection (1.4 nm) on heating and the location of the (060) reflection at 0.156 nm indicates that the mineral is an iron-rich chlorite (Brown and Brindley, 1980). The collapse of the strong 0.7 nm peak after heating to 550 C indicates the presence of kaolinite. Treatment of subsamples of Ca-saturated clay overnight with 2N HCl to selectively dissolve chlorite followed by X-ray analysis confirmed the presence of kaolinite.

Diffraction patterns of K-saturated specimens heated to 105 C and then equilibrated at 54 % R.H. indicated complete rehydration of collapsed layers for the Legend parent material, and only partial rehydration of the collapsed layers of the Kinosis parent material. For the Kinosis sample, the ratio of the intensity of the 1.0 nm to the 0.7 nm peaks for the K-saturated sample was greater than the same ratio for the Ca-saturated sample and there was a distinct shoulder in the 1.04 nm region and broad peaks in the 1.2 - 1.4 nm region. Such rehydration behaviour indicated the presence of minor amounts of vermiculite in the Kinosis parent material. Thus, although the till matrix of these sola is of different lithologic origin, the phyllosilicate composition of both parent materials was similar.

Evaluation of pedogenic alteration, neoformation and/or translocation requires an assessment of the lithological uniformity of the parent material of the solum (Drees and Wilding, 1973; Wang and Arnold, 1973). The constancy of the Ti/Zr ratios of these separates (data not shown) with solum depth for both pedons indicated that the original geological deposits in which the pedons developed were reasonably uniform (Drees and Wilding, 1973). Thus any mineralogical changes observed in the clay separates were attributed to pedological processes.

Contents of individual mineral species in both the fine and coarse clay fractions from the sola of the Kinosis and Legend pedons displayed considerable variability among the different horizons, and between the two fractions within each pedon (Table 3.1). Content of micaceous minerals increased with depth in both size separates, indicative of either weathering of this

species in the upper pedon or preferential translocation by lessivage. In the Kinosis pedon the levels of micaceous species is greater in the coarse clay separates whereas levels are similar in both separates for the Legend pedon. Content of smectite was also lowest in the E horizons and, especially in the fine clay fractions, reached a maximum in the Bt for both pedons. The Bt horizon also has the highest content of both fine and coarse clay. This indicated enrichment either through preferential translocation or, perhaps, authigenesis of the smectite minerals in the upper B horizons (Douglas, 1982).

Kaolinite shows a different relative distribution within the profiles than the other phyllosilicate species. The greatest amounts of kaolinite in both separates occurred in the E horizon (Table 3.1). The high levels of kaolinite in the E horizon may indicate either enrichment as a result of the translocation of the smectite and micaceous species, or authigenic formation (Nicholson and Moore, 1977). A proposed mechanism for the transformation of smectite to kaolinite in naturally acid soils has been outlined by Karathanasis and Hajek (1983). In all samples levels of vermiculite, calculated from the difference between the CEC and KEC, were highest in the E horizons. The levels are relatively low (< 10 %), and may merely represent fixation of the potassium by edge weathered mica. The apparent crystallinity of the phyllosilicate minerals is lowest in the Bt1 horizon based on the high background levels of the diffractograms (Fig 3). This may represent either partial weathering of the crystals or coating with x-ray amorphous sesquioxides which induce a scattering and/or absorption of the X-radiation (Munn and Boehm, 1983). The higher levels of poorly crystalline minerals (Table 1) extracted from the clay separates of the Bt1 horizons are consistent with the concomitant reduction in intensity of the (001) peaks of the phyllosilicate species in these horizons.

Diffraction analyses indicated that the expandable component of the fine clay separates were comprised of a mixture of distinct smectite species.

Table 3.1. Chemical and mineralogical composition of the clay from the pedogenic horizons of Cryoboralf pedons from northeast Alberta.

Horizon	Clay g 100g ⁻¹	K	CaEc cmol(p ⁺)kg ⁻¹	KEC	S.A. m ² g ⁻¹	Smect. ¹	Mica	Kaol + Chl.	Verm.	Poorly Cryst.
LEGEND PEDON										
_____ gm 100 gm ⁻¹ _____										
Coarse Clay										
E	8	1.55	46.9	43.5	238	39	22	37	2	3.0
Bt1	26	2.15	53.3	47.8	324	43	29	25	4	4.2
Bt2	27	2.33	48.4	45.2	288	44	31	27	2	4.7
Bt3	24	2.55	56.6	49.5	277	44	34	18	5	4.8
BC	26	2.54	57.3	52.6	64	47	34	16	3	4.9
C	430	2.53	50.5	49.5	253	49	33	18	<1	5.8
Fine Clay										
E	4	1.63	46.2	35.3	342	32	23	37	8	4.9
Bt1	12	1.97	63.1	59.8	471	55	26	18	2	7.8
Bt2	20	2.30	63.8	61.3	493	56	30	13	2	6.2
Bt3	26	2.37	54.7	52.6	474	47	31	20	1	5.6
BC	18	2.37	59.2	57.8	430	52	32	15	1	7.7
C	12	2.62	55.7	55.6	528	50	35	16	<1	7.7

Table 3.1. Continued.

Horizon	Clay g 100g ⁻¹	K	CaEc cmol(p ⁺)kg ⁻¹	KEC	S.A. m ² g ⁻¹	Smect. ¹	Mica	Kaol + Chl.	Verm.	Poorly Cryst.*
<hr/>										
										gm 100 gm ⁻¹
<hr/>										
KINOSIS PEDON										
<hr/>										
Coarse Clay										
E	<1	0.98	23.2	16.2	230	13	19	63	5	3.3
Bt1	11	1.59	35.3	29.1	253	26	23	48	4	7.5
Bt2	14	1.73	40.1	36.2	306	32	24	41	3	5.0
BC	10	1.90	38.7	34.4	348	30	28	40	3	3.8
<hr/>										
Fine Clay										
E	<1	1.14	57.4	45.6	446	41	15	36	8	8.0
Bt1	3	1.23	70.8	65.8	586	61	16	20	3	12.1
Bt2	6	1.36	74.7	70.0	581	65	17	15	3	7.7
BC	4	1.44	72.7	65.1	581	61	18	17	5	8.3
C	5	1.74	76.3	67.7	683	62	22	10	6	8.9

* Poorly crystalline minerals based on extractable levels of Fe, Al and Si, assuming 20% water (Jackson, 1975).

¹ Estimated as percent of the crystalline mineral phase.

The x-ray diffractograms (Fig 3.3) indicated that a beidellite-like species dominated the fine clay separates from the E horizon, whereas montmorillonite was the major species in the C horizons. This depth variability has previously been described for Luvisolic soils (Cryoboralfs) in Alberta (Pawluk and Dudas, 1982), Gley-podzolic soils in Russia (Kuznetsova and Sokolova, 1983) and Solodized Solonetz soils (Natroborolls) in Alberta (Spiers et al, 1984). The variability with depth may be explained by either eolian additions (Pawluk and Dudas, 1982), preferential translocation of the individual species (Spiers et al, 1984), by alteration and/or decomposition of montmorillonite (Munn and Boehm, 1983), or by neoformation of the beidellite-like species in the upper pedon (Kuznetsova and Sokolova, 1983). The latter two possibilities are consistent with the transformation pathway outlined by Karathanasis and Hajek (1983) in which montmorillonite alters to beidellite through local dissolution and recrystallization reactions (Sridhar and Jackson, 1974). The subsequent formation of kaolinite would then be a result of dissolution of the beidellite and recrystallisation, with a net loss of silica from the system either in percolating solutions or as neoformed poorly ordered silica-rich gels (Karathanasis and Hajek, 1983). Micaceous minerals, the content of which was lowest in the E horizons, have also been shown to weather to beidellite in soil systems (Churchman, 1980; Gjems, 1970; Kapoor, 1973; Malcolm et al, 1969).

in equilibrium with the soil solution, which reflects the isotopic composition of the meteoric water of the region. As there is little oxygen isotopic exchange between soil water and the structural oxygen of crystalline phyllosilicates at low temperatures (James and Baker, 1976), the oxygen isotopic geochemistry of any authigenic crystalline clays in the Kinosis and Legend pedons should be different from that of the detrital clays of both Shield and Cretaceous sediment origin (Lawrence and Taylor, 1971). Even if the transformations of the mineral species are a result of within crystal isomorphous substitution and local dissolution and reprecipitation

reactions (Karathanasis and Hajek, 1983), the exchange of the oxygen component of the crystal lattice would be sufficient to alter the content of ^{18}O in the clay separates (Clauer et al, 1982). Such alteration within the clay lattices would be measurable because the detrital clays of these pedons formed in equilibrium with solutions with a $\delta^{18}\text{O}$ distinct from that of the modern precipitation (-23 to -25 ‰, as measured by Schwartz, 1979). The sensitivity of the ^{18}O technique was demonstrated in an examination of the natural weathering of biotite in a granodiorite in which a 2 ‰ change in ^{18}O content of the biotite was observed with no corresponding change observed by x-ray diffraction (Clauer et al, 1982). This isotopic change was interpreted to be caused by a 13 % alteration of the mica structure to kaolinite.

If the changes in profile distribution of specific clay species (Table 3.1 and Fig 3.3) observed in the Kinosis and Legend pedons are a result of either authigenesis or crystal alteration, analysis of the oxygen isotopic geochemistry would provide the required discriminant. The oxygen isotope analyses (Table 3.2) of the crystalline phyllosilicate minerals indicate a large difference between the pedons, and a smaller difference between the size separates within the pedons. The difference in oxygen isotopic composition of the treated separates between the Legend (16-18 ‰) and Kinosis (13-14 ‰) pedons reflects the source lithologies comprising the till parent materials (Spiers et al, 1984). The minor differences in isotopic composition, both between size separates and for a given separate with depth, merely reflect the variability in relative amounts of the individual mineral species within the separates.

The similarity in ^{18}O content of the individual clay separates with depth (Table 2) indicated there was little or no exchange of structural oxygen within the lattice of the individual phyllosilicate minerals with local meteoric waters. Assuming a kaolinite-water fractionation of 1.026 and a smectite-water fractionation of 1.027 (Lawrence and Taylor, 1971), authigenic kaolinite, for example, would have a $\delta^{18}\text{O}$ of +3 ‰ and authigenic smectite would have a $\delta^{18}\text{O}$

value of +4 ‰. For the 20 % enrichment of kaolinite recorded in the fine clay separate of the E horizon of the Legend pedon to be a result of neoformation, a simple mass balance calculation (Salomons and Mook, 1976; Rabenhorst et al, 1984) indicates that the $\delta^{18}\text{O}$ value should be 13.7 ‰ instead of the 16.4 ‰ measured (Table 3.2).

Table 3.2. Oxygen isotope (^{18}O) geochemistry of clay separates before and after extraction of poorly crystalline material with oxalate and hot (0.5M) KOH solutions. Data reported in ‰ (SMOW).

Horizon	Fine	Clay	Coarse	Clay
	Untreated	Treated Legend Pedon ($\delta^{18}\text{O}$)	Untreated	Treated
Ae	16.5	16.6	16.8	16.9
Bt1	15.4	16.4	16.8	17.1
Bt2	15.6	16.4	17.3	17.4
Bt3	14.7	16.5	16.0	17.5
BC	14.9	16.6	16.5	17.8
C	14.3	16.1	16.5	17.6
Kinosis Pedon				
Ae	13.2	13.5		
Bt1	12.8	13.3	13.3	13.8
Bt2	12.8	13.5	12.3	14.1
BC	11.7	13.6	13.0	14.1
C	11.5	13.5	12.8	13.4

If the 23% relative enrichment of smectite in the Legend Bt1 was authigenic, the measured $\delta^{18}\text{O}$ would have to be 13.3 ‰. Similarly, the kaolinite enrichment observed in the fine and coarse clay separates of the E horizon of the Kinosis pedon would require $\delta^{18}\text{O}$ values of 11.9 ‰ and

12.3 ‰, respectively, if the observed enrichment was a result of authigenesis. Examination of the oxygen isotope content of the crystalline clay separates indicated that interpretations of either authigenesis and/or alteration of the crystalline clay species of these pedons are unlikely. Such alteration and/or authigenesis would require at least local dissolution and reprecipitation reactions. The reactions would require at least partial exchange with the oxygen of the soil solutions, with a resultant change in the ^{18}O content of the clay separates. A change in ^{18}O content in favour of any authigenic crystalline species is not apparent in the samples analysed from either the Legend or Kinosis pedons (Table 3.2).

The isotopic data do not, however, preclude the possible depotassification reactions removing K from the ditrigonal positions of the clay mica structures to form either a hydroxy-interlayer vermiculite or beidellite with no exchange of tetrahedral or octahedral structural oxygen. X-ray diffraction analyses following K^+ fixation at 105 °C, however, indicate that there is little, if any, neoformation of a vermiculite species.

Data for the clay separates from both pedons prior to the partial dissolution of poorly crystalline material with acid ammonium oxalate and 0.5N KOH showed a decrease in ^{18}O content relative to the purified crystalline phyllosilicate minerals (Table 3.2). The data in Table 1 indicate material was dissolved from the separates of all horizons. These poorly crystalline materials were postulated to be authigenic, in which case their ^{18}O content would reflect that of their formation waters. Although the fractionation factors between poorly crystalline minerals and water are not well known, it has been demonstrated that authigenic soil oxy-hydroxides are isotopically distinct from crystalline primary and secondary soil minerals, with fractionation factors being estimated to range between 1.015 and 1.020 (Lawrence and Taylor, 1971). Any authigenic poorly crystalline components would thus have a $\delta^{18}\text{O}$ value less than that of the detrital crystalline clays. The differences observed between the crystalline phyllosilicates and

the clay separates prior to the selective dissolution treatments merely reflected the presence of isotopically distinct poorly crystalline minerals. The signature of these oxalate and KOH soluble phases, being lower than that of the crystalline materials, lowers the bulk ^{18}O content of the untreated clays relative to that of the treated clays.

The decrease in $\delta^{18}\text{O}$ of the untreated clay separates with increasing profile depth indicated either increasing levels of authigenic material in the lower sola, or differences in the isotopic composition of the soil solutions from which these minerals precipitated. The levels of poorly crystalline minerals were shown, however, to be highest in the B horizons (Table 3.1). Thus the second hypothesis, namely that there is a variation in the ^{18}O content of the soil solution in the different horizons of the pedons under study, must be invoked to explain the observed depth trends in ^{18}O content of the authigenic clays. Precipitation of the poorly crystalline minerals can only occur once their solubility product has been exceeded and the solution becomes supersaturated with respect to that particular mineral phase. This supersaturation can be expected to occur as a result of the removal of water from the soil by either plant uptake or evaporation.

Although plant transpiration has been demonstrated to have no effect on the isotopic content of the soil solution (Zimmerman et al, 1967), evaporative processes and subsequent removal of water in the vapour phase cause large enrichments in both ^{18}O and deuterium in soil solutions (Lloyd, 1966; Matsubaya and Sakai, 1978; Barnes and Allison, 1983; Dever et al, 1983). The enrichment of ^{18}O in soil solutions at 1 m relative to a datum at 4 m was shown to be between +2 and +6 ‰ (Allison and Hughes, 1982), while enrichments in the upper 5 cm of sand columns due to evaporation were as high as +18 ‰ (Allison, 1982; Allison et al, 1983). Thus minerals formed in evaporative zones (upper parts of the pedon) will appear to be significantly out of equilibrium with local meteoric waters, while those precipitated in the lower

pedon, where transpiration processes dominate over evaporative processes, will have an isotopic enrichment reflecting that of the infiltrated meteoric waters.

Table 3.3. Oxygen isotope (^{18}O) geochemistry of the dissolved poorly crystalline minerals as determined by mass balance (reported in ‰ [SMOW]).

Horizon	Fine Clay	$\delta^{18}\text{O}$	Coarse Clay
	Legend Pedon		
Ae	12.5		14.1
Bt1	3.6		4.2
Bt2	3.6		5.3
Bt3	-13.7		-11.7
BC	-3.1		-9.0
C	-10.8		-4.6
	Kinosi Pedon		
Ae	10.9		
Bt1	8.4		6.0
Bt2	6.0		-1.9
BC	-7.0		-9.7
C	-5.5		-5.6

Meteoric waters in the study region have a $\delta^{18}\text{O}$ of between -23 and -25 ‰ (Schwartz, 1979). Consequently, any authigenic material formed in equilibrium with this precipitation should have a $\delta^{18}\text{O}$ content of between -3 and -10 ‰. The estimated $\delta^{18}\text{O}$ content of the poorly crystalline clays were calculated using the mass balance approach described by Salomons and Mook (1976) and Rabenhorst et al. (1984). The trend with depth (Table 3.3) can best be explained in terms of the behaviour of soil solution $\delta^{18}\text{O}$ contents as a result of evapotranspiration processes. Although the isotopic enrichments calculated for the poorly crystalline clays of the lower B and C horizons from both Kinosi and Legend pedons are within

or close to the range estimated for authigenic oxy-hydroxide materials formed in equilibrium with local meteoric waters, the isotopic enrichments for similar materials in the A and upper B horizons suggest either disequilibrium conditions of formation or that the soil solutions had an $\delta^{18}\text{O}$ enrichment of between -6 and -17 ‰. These conditions would require evaporative enrichment of the soil solutions of between +18 and +7 ‰ relative to meteoric water. These enrichments are within the extremes documented for soil and sand columns as a consequence of evaporative processes and vapour phase transport of isotopically depleted vapours from the soil (Allison, 1982; Allison and Hughes, 1982; Allison et al, 1983). Thus the authigenic material in the upper pedons likely precipitated from soil solutions isotopically enriched in ^{18}O by evaporation, whereas similar materials in the lower pedons precipitated from non-enriched percolating meteoric waters.

3.4: CONCLUSIONS

Although chemical and x-ray diffraction analyses of clays in Cryoboralfs (Luvisolic soils) from northeastern Alberta suggest that pedogenic processes are responsible for a combination of structural alteration, neoformation and preferential translocation of crystalline phyllosilicates, oxygen isotope geochemistry of the same separates indicated there is no variation in the composition of the structural oxygen associated with the tetrahedra or octahedra of the minerals with pedon depth. Such lack of variability suggests there is little or no structural alteration or neoformation of the crystalline phyllosilicates in these pedons, and that the observed depth segregation of individual minerals is simply a result of leaching. The oxygen isotope data do not, however, preclude removal of K from the ditrigonal structural positions of the clay mica to form either a dioctahedral beidellite-like mineral or hydroxy-interlayer species. The interlayer structural water is removed by the drying and outgassing procedures prior to sample analysis. Further, in mica weathering processes oxidation of small amounts of Fe^{++} , or substitution of

Al by Si in the lattice structure could alter the layer charge density with no influence on the oxygen isotope geochemistry.

The isotopic chemistry of the authigenic poorly crystalline minerals dissolved from the clay separates was estimated by calculation. The poorly crystalline constituents dissolved with a combination of oxalate and hot KOH displayed profile trends in oxygen isotopic composition related to evaporative processes. The authigenic minerals in the upper pedon precipitated from soil solutions that were enriched in ^{18}O by evaporation, whereas those in the lower pedons precipitated from solutions with isotopic chemistry similar to that of the meteoric waters of the region. Any crystalline minerals forming in a soil profile would likewise reflect the isotopic chemistry of the pore waters as influenced by evaporative processes.

3.5: BIBLIOGRAPHY

- Allison, G.B. 1982. The relationship between ^{18}O and D in water in sand columns undergoing evaporation. *J. Hydrol.* 55: 163-169.
- Allison, G.B., and M.W. Hughes 1982. The use of natural tracers as indicators of soil-water movement in a temperate semi-arid region. *J. Hydrol.* 60: 157-173.
- Allison, G.B., C.J. Barnes and M.W. Hughes 1983. The distribution of D and ^{18}O in dry soils. 2. Experimental. *J. Hydrol.* 64: 377-397.
- Barnes, C.J. and G.B. Allison 1983. The distribution of D and ^{18}O in dry soils. 1. Theory. *J. Hydrol.* 60: 141-156.
- Brown, G.E. and G.W. Brindley 1980. X-ray diffraction procedures for clay mineral identification. In: Brindley, G.W., and G.E. Brown, editors. *Crystal structures of clay minerals and their X-ray identification*. Mineralogical Society, London. Monograph 5, pp 305-359.
- Canada Soil Survey Committee 1978. The Canadian system of soil classification. Can. Dep. Ag. Publ. 1646. Supply and Services Canada, Ottawa, Ontario. 164pp.
- Carter, D.L., M.D. Heilman and C.L. Gonzales 1965. Ethylene glycol monoethyl ether for determining surface area of silicate minerals. *Soil Sci.* 100: 356-360.
- Churchman, G.J. 1980. Clay minerals formed from chlorites and micas in some New Zealand soils. *Clay Min.* 15: 59-75.
- Clauer, N., J.R. O'Neil and C. Bonnot-Courtois 1982. The effect of natural weathering on the chemical and isotopic compositions of biotites. *Geochim. Cosmochim. Acta* 46: 1755-1762.
- Clayton, R., and T.K. Mayeda 1963. The use of bromine pentafluoride in the extraction of oxygen from oxides and silicates for isotope analysis. *Geochim. Cosmochim. Acta* 27: 43-52.
- Coen, G.M. and R.W. Arnold 1972. Clay mineral genesis of some New York Spodosols. *Soil Sci. Soc. Am. Proc.* 36: 342-350.
- Coffman, C.B. and D.S. Fanning 1975. Maryland soils developed in residuum from chloritic basalt having high amounts of vermiculite in sand and silt fractions. *Soil Sci. Soc. Am. Proc.* 39: 723-732.

- Craig, H. 1961. Standard for reporting concentration of deuterium and ^{18}O in natural waters. *Science* 133: 1702-1703.
- Dever, L., R. Durand, J.Ch. Fontes and P. Vacher 1983. Etude pedogenetique et isotope des neoformations de calcite dans un sol sur craie. Caracteristiques et origines. *Geochim. Cosmochim. Acta* 47: 2079-2090.
- Douglas, L.A. 1982. Smectites in acid soils. In *Developments in Sedimentology*, Vol. 35. International Clay Conference. Edited by: H. van Olphen and F. Veniale. Elsevier, New York. Pp. 635-640.

- Drees, L.R. and L.P. Wilding 1973. Elemental variability within a sampling unit. *Soil Sci. Soc. Am. Proc.* 35: 134-140.
- Dudas, M.J. and M.E. Harward 1971. Effect of dissolution treatment on standard and soil clays. *Soil Sci. Soc. Am. Proc.* 35: 134-140.
- Fanning, D.S. and V.Z. Keramidas 1977. Micas. In: *Minerals in Soil Environments*. Edited by: J.B. Dixon and S.E. Weed. Soil Science Society of America. Madison, WI.
- Gjems, O 1970. Mineralogical composition of pedogenic weathering of the clay fraction in podzol soil profiles Zalesine, Yugoslavia. *Soil Sci.* 110: 237-243.
- Greene-Kelley, R. 1953. The identification of montmorillonoids. *J. Soil Sci.* 4: 233-237.
- Griffin, G.M. 1971. Interpretation of X-ray diffraction data. In: Carver, R.F., editor. *Procedures in sedimentary petrology*. Wiley Interscience. New York, NY, pp. 541-569.
- Harward, M.E., D.D. Carslea, and A.H. Sayegh 1969. Properties of vermiculites and smectites: expansion and collapse. *Clays and Clay Min.* 16: 437-447.
- Jackson, M.L. 1975. *Soil chemical analysis: an advanced course*. University of Wisconsin, Madison, WI. 895 p.
- James, A.T. and D.R. Baker 1976. Oxygen isotope exchange between illite and water at 22 C. *Geochim. Cosmochim Acta* 40: 235-239.
- Kapoor, B.S. 1973. The formation of 2:1-2:2 intergrade clays in some Norwegian Podzols. *Clay Min.* 10: 79-86.
- Karathanasis, A.D. and B.F. Hajek 1983. Transformation of smectite to kaolinite in naturally acid soil systems: structural and thermodynamic considerations. *Soil Sci. Soc. Am. J.* 47: 158-163.
- Kodama, H. 1979. Clay minerals in Canadian soils: their origin, distribution and alteration. *Can. J. Soil Sci.* 59: 37-58.
- Kuznetsova, Ye.G. and T.A. Sokolova 1983. Mineral composition of the clay fraction in Gley-Podzolic soils of the Komi ASSR. *Soviet Soil Sci.* 14: 84-92.
- Lavkulich, L.M. and J.H. Wiens 1970. Comparison of organic matter destruction by H_2O_2 and $NaOCl$

- and its effect on selected mineral constituents. *Soil Sci. Soc. Am. Proc.* 34: 755-758.
- Lawrence, J.R. and H.P. Taylor 1971. D and ^{18}O correlation: clay minerals and hydroxides in Quaternary soils compared to meteoric waters. *Geochim. Cosmochim. Acta* 35: 993-1003.
- Lawrence, J.R. and H.P. Taylor 1972. Hydrogen and oxygen isotope systematics in weathering profiles. *Geochim. Cosmochim. Acta* 36: 1377-1393.
- Lloyd, R.M. 1966. Oxygen isotope enrichment of sea water by evaporation. *Geochim. Cosmochim. Acta* 30: 801-814.
- Longstaffe, F.J. 1983. Stable isotope studies in diagenesis in clastic rocks. *Geosci. Can.* 10: 43-58.
- McKeague, J.A., Editor. 1978. Manual on soil sampling and methods of analysis. Soil Research Institute, Ottawa, Ontario. 212 pp.
- Malcolm, R.L., W.D. Nettleton and R.J. McCracken 1969. Pedogenic formation of montmorillonite from 2:1-2:2 intergrade clay minerals. *Clays Clay Min.* 16: 405-414.
- Matsubaya, O. and H. Sakai 1978. D/H and $^{18}\text{O}/^{16}\text{O}$ fractionation factors in evaporation of water at 60 and 80 C. *Geochem. J.* 12: 121-126.
- Munn, L.C. and M.M. Boehm 1983. Soil genesis in a Natragid-Haplargid complex in northern Montana. *Soil Sci. Soc. Am. J.* 47: 1186-1192.
- Nicholson, H.M. and T.R. Moore 1977. Pedogenesis in a subarctic iron-rich environment: Schefferville, Quebec. *Can. J. Soil Sci.* 57: 35-45.
- Pawluk, S. and M.J. Dudas 1982. Pedological investigation of a Gray Luvisol developed from eolian sand. *Can. J. Soil Sci.* 62: 49-60.
- Rabenhorst, M.C., L.P. Wilding and L.T. West 1984. Identification of pedogenic carbonates using stable carbon isotope and microfabric analyses. *Soil Sci. Soc. Am. J.* 48: 125-132.
- Rowe, J.S. 1972. Forest regions of Canada. Dept. of Environment, Can. Forest Service, Publ. No. 1300. Ottawa, Ontario. 172 pp.
- Salomons, W. and W.G. Mook 1976. Isotope geochemistry of carbonate dissolution and reprecipitation in soils. *Soil Sci.* 122: 15-24.

- Savin, S.M. and S. Epstein 1970. The oxygen and hydrogen isotope geochemistry of clay minerals. *Geochim Cosmochim Acta* 34: 25-42.
- Schwartz, F.W. 1979. Interim report on hydrogeological investigation of the Muskeg River basin, Alberta. Prepared for the Alberta Oil Sands Environmental Research Program by Dep. of Geology, University of Alberta. AOSERP Rep. 48, 104 pp.
- Soil Survey Staff 1975. Soil Taxonomy. Agric. Handb. No. 18, USDA. U.S. Government Printing Office, Washington, DC.
- Somasiri, S., S.Y. Lee and P.M. Huang 1971. Influence of certain pedologic factors on potassium reserves of selected Canadian soils. *Soil Sci. Soc. Am. Proc.* 35: 500-505.
- Spiers, G.A., M.J. Dudas and R.W. Hodgins 1983. Instrumental conditions and procedure for multielement analysis of soils and plant tissue. *Comm. Soil Sci. Plant Anal.* 14: 629-644.
- Spiers, G.A., M.J. Dudas, K. Muehlenbachs and L.W. Turchenek 1984. Mineralogy and oxygen isotope geochemistry of clays from surficial deposits in the Athabasca Tar Sands area. *Can. J. Earth Sci.* 21: 53-60.

- Sridhar, K. and M.L. Jackson 1974. Layer charge decrease by tetrahedral cation removal and silicon incorporation during natural weathering of phlogopite to saponite. *Soil Sci. Soc. Am. Proc.* 38: 847-851.
- Thiesen, A.A. and M.E. Harward 1962. A paste method for the preparation of slides for clay mineral identification by X-ray diffraction. *Soil Sci. Soc. Am. Proc.* 26: 90-91.
- Turchenek, L.W. and J.D. Lindsay 1982. Soils inventory of the Alberta Oil Sands Environmental Research Programme study area. Prepared for the Alberta Oil Sands Environmental Research Program by Alberta Research Council. AOSERP Rep. 122. 220 pp.
- Wang, C. and R.W. Arnold 1973. Quantifying pedogenesis for soils with discontinuities. *Soil Soc. Sci. Am. Proc.* 37: 271-278.
- Yeh, H. and S.M. Savin 1976. The extent of oxygen isotope exchange between clay minerals and sea water. *Geochim. Cosmochim. Acta* 40: 743-748.
- Zimmerman, U., D. Ehhalt and K.O. Munnich 1967. Soil-water movement and evapotranspiration changes in the isotopic composition of the water. *Proc. Symp. Isotopes in Hydrology, Vienna, 1966.* Int. At. Energy Agency, Vienna, pp. 567-584.

Figure 3.1. Location of the study area.

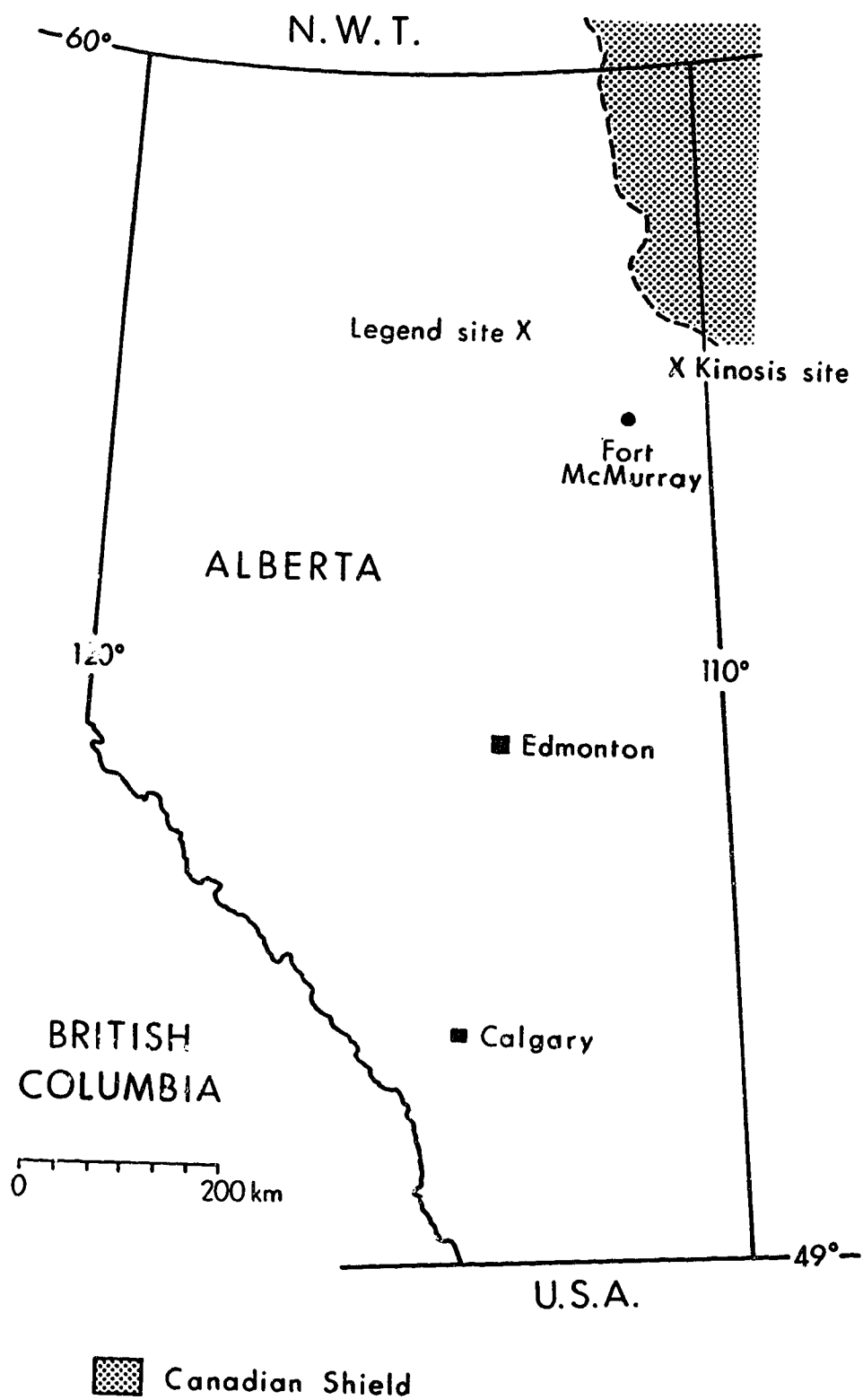


Figure 3.2. X-ray diffractograms of clay separates (<2.0 μm) from the C-horizons of the Kinosis and Legend pedons.

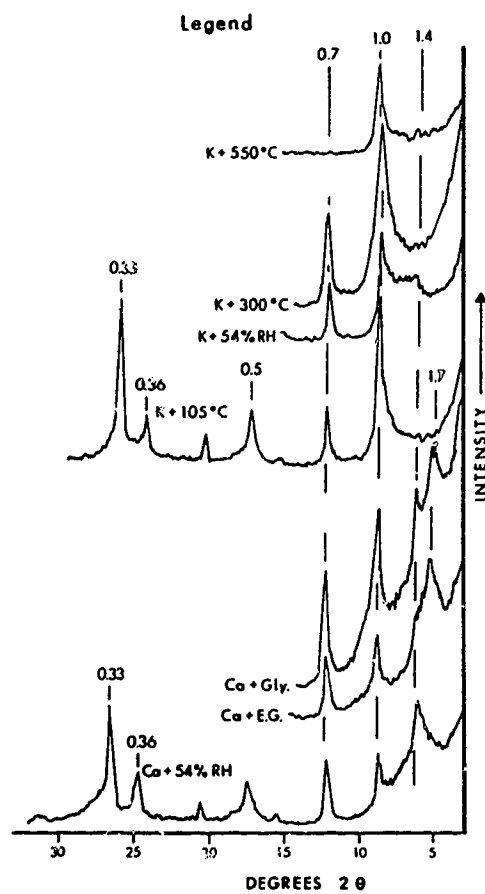
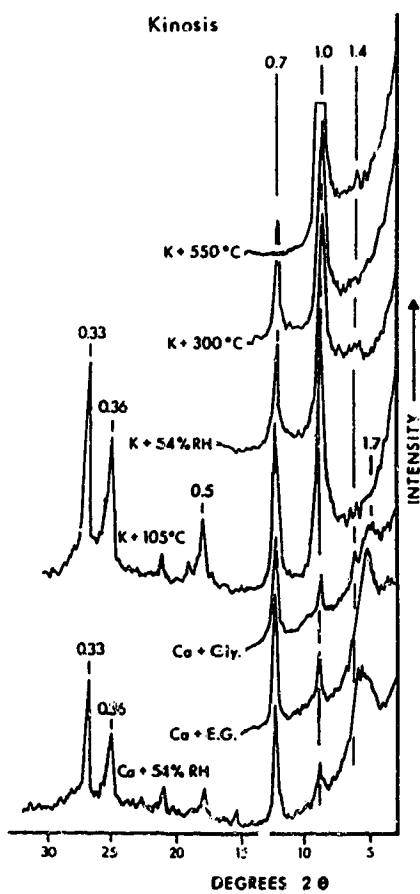
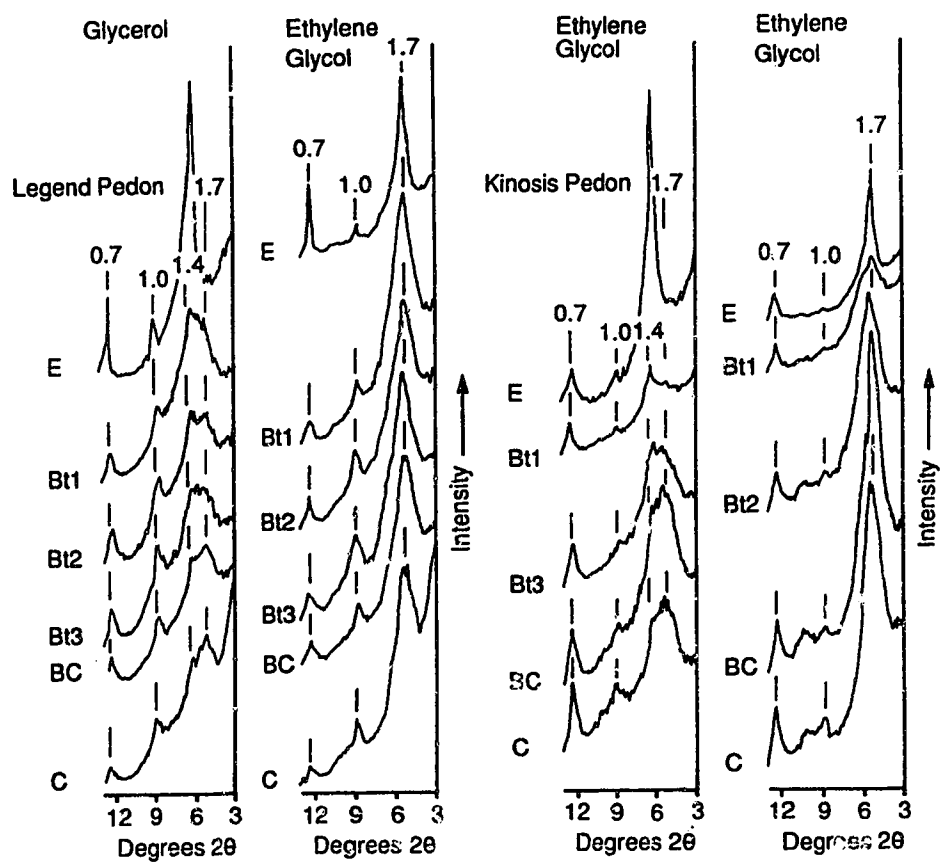


Figure 3.3. X-ray diffractograms of the fine clay separates ($<0.2\text{ }\mu\text{m}$) from the major horizons of the Kinosis and Legend pedons.



4. AN EXAMINATION OF THE MOBILE COLLOIDAL PHASE IN A LUVISOLIC CATENARY SEQUENCE

4.1. INTRODUCTION

The texturally differentiated profiles of the Orthic Grey Luvisols of the Boreal Forest Region of Alberta are characterized by well-developed, platy Ae horizons overlying Bt horizons with strong blocky mesostructure, and calcareous C horizons. Downward migration of colloidal material, primarily phyllosilicates, in suspension without mineral dissolution from the A to the B horizon is generally considered to be responsible for the vertical textural differentiation of such soils (Jenny and Smith, 1935; Brewer and Haldane, 1957; Gagarina and Chizokova, 1984; Howitt and Pawluk, 1985a). Static (Singer et al, 1978) pedological studies have described the vertical zonation of the individual minerals of the phyllosilicate groups within the Grey Luvisolic soils (Pawluk, 1961; St. Arnaud and Sudom, 1981; Pawluk and Dudas, 1978, 1982; Howitt and Pawluk, 1985a; Santos et al, 1986b). These studies have shown that the smectite group minerals are enriched in the Bt horizons, with negative enrichment of kaolinite, clay mica and chlorite in the Ae horizons. Total iron enrichment in the Bt horizon has been shown to be strongly correlated with the intra-pedon translocation of smectite minerals (Santos et al, 1986a).

The process mechanisms considered responsible for clay translocation fall into two main groups. The first process group is mainly physical, with the clay and fine silt particles being disaggregated from the soil structural units by either freeze-thaw or wetting-drying cycles prior to pedotranslocation through macropores by the soil solution, with particle sieving in zones of decreasing pore size (Bound, 1986) such as Bt horizons. The second suggests that organic compounds complex with clays, producing a higher net surface negative charge (Dixit, 1978) which promotes particle dispersion and subsequent mobilisation (Davis, 1971). To understand

the dynamics of these mobilisation processes in pedogenesis, data are required on the volume, solute concentration, ionic speciation and time dependent variability of solutions moving through soil (McKeague, 1979). There have been a series of publications describing particle migration in suspension in the throughflow within Podzolic soils (Singer et al, 1978, Ugolini et al., 1977a,b; Ugolini et al., 1987) formed on acidic parent materials. However, there has been only one similar dynamic study of particle migration in conjunction with detailed soil solution analysis for both organic and inorganic components in soils formed on calcareous tills (Howitt and Pawluk, 1985b). The conclusions of the latter study indicate that major processes active in Luvisolic soils are translocation of Al, Fe and organic constituents both in solution and colloidal form, with associated movement of micaceous clays in soil solutions with pH near neutral. Such conclusions support the hypothesis that clay-oxyhydroxide complexes migrate down a soil profile together when solution pH is above 6.0 (Gagarina and Chizokova, 1984).

Elucidation of the ongoing genetical processes within selected soils of a catenary sequence of Luvisolic soils, specifically as related to the mobile colloidal phase, is the objective of this section of the thesis. Specifically, the mineralogy of the colloidal material of the sola was examined by a combination of static and dynamic pedological techniques.

4.2. MATERIALS AND METHODS

The study site was within the Cooking Lake Moraine east of the city of Edmonton, Alberta. Uncultivated soils representative of members of a catenary sequence were sampled for static pedological examination, namely an Orthic Grey Luvisol, and a Gleyed Grey Luvisol. Upper slope sola developed under a *Populus tremuloides* canopy, whilst the lower slope canopy was comprised of *Populus balsamifera* grading into *Salix* spp. Bulk samples were collected on a depth increment basis within the genetic horizons, with increment thickness being 1.0 cm in the Ae and AB horizons, 5.0 cm in the Bt1, Bt2 and BC horizons, and 10.0 cm to a depth of 2.0

m. Samples were air-dried, ground to pass a 2 mm sieve and stored for analysis. Soil monoliths to a depth of 1.5 m were air-dried, impregnated with epoxy resin for the manufacture of 7 x 5 cm thin sections (Pawluk and Brewer, 1975). Regions of the impregnated blocks were selected following preliminary micromorphic examination to produce 1.0 cm diameter highly polished sections for quantitative electron microprobe analysis of selected argillans and cutans. The microfabric of intact peds, excised cutanic material and thin sections was examined by electron optical and microchemical analytical techniques (SEM-EDS).

The clay fraction was separated ($<2.0 \mu\text{m}$) from the bulk samples (Spiers et al, 1984), with separation into three sub-fractions (<0.2 , $0.2 - 1.0$ and $1.0 - 2.0 \mu\text{m}$) for subsequent mineralogical and chemical analyses. The paramagnetic minerals of selected fractions were purified by high gradient magnetic separation (HGMS) (Schulz and Dixon, 1979; Russell et al, 1984; Ghabru et al, 1988) at a magnetic field strength of 1.75 Tesla (T) following selective dissolution of iron oxyhydroxide coatings (Mehra and Jackson, 1960). X-ray diffractograms of oriented specimens were obtained by step-scan (Meunier and Velde, 1982) with a Philips PW1730-PW1710 diffractometer-microprocessor equipped with a curved crystal monochromator using $\text{CoK}\alpha$ radiation generated at 50 kV and 25 Ma. Diffractograms of Ca-saturated specimens were obtained for 54% R.H., glycerol and ethylene glycol treatments while those for K-saturated specimens were obtained for 105 C heated samples analyzed at 0% R.H., then again following equilibration at 54% R.H., and for 300 C and 500 C heated samples, with the humidity maintained at 0% R.H. during analysis. The resultant digital data was processed using specialized software written in-house for clay mineralogical analyses on an IBM-PC. The clay component of cutanic material from the Bt1, Bt2, BC and Ck horizons was also analyzed. The clay separates were also analyzed by Fourier Transform Infra-red spectroscopy (FTIR).

Powder diffraction patterns of selected fine clay ($<0.2\mu\text{m}$) samples, obtained with a

Debye-Scherrer camera, enabled measurement of non-basal reflections. Samples of the $<0.2\mu\text{m}$ clay fraction were analyzed by Mössbauer spectroscopy on a 512-channel Cryophysics microprocessor-based instrument with a constant acceleration drive system and a sawtooth waveform. A ^{57}Co -in-Rh α -ray source was used and sample sizes were chosen to give about 10 mg Fe cm^{-2} or less in the beam. Velocity scales were calibrated with respect to natural iron at 293 K, with the midpoint of the magnetic hyperfine spectrum defining zero velocity. Spectra were deconvoluted, assuming overlapping Lorentzian peak lineshapes, using an iterative nonlinear regression X^2 minimization procedure (Cardile and Johnston, 1986).

A series of gravity lysimeters of 300 cm^2 cross-sectional area were installed in selected slope positions under the LFH, Ae and AB horizons in 1982, and were sampled continuously throughout spring, summer and fall until 1988. Leachates were analyzed for pH, electrical conductivity and oxidation-reduction potential immediately on collection, and frozen prior to subsequent analysis. Colloidal material retained on 0.2 μm filters was composited on a seasonal basis for individual lysimeters for chemical, mineralogical and SEM-EDS examination. The colloidal residues were treated with selective reagents (Loveland and Digby, 1984; Mehra and Jackson, 1960; Parfitt, 1989) to ascertain the nature of both organically complexed and poorly crystalline components.

4.3. RESULTS AND DISCUSSION

4.3.1. Static Clay Mineralogical Analysis

Diffraction analyses indicated clay separates from the parent materials consisted primarily of admixtures of smectite, mica, kaolinite, and chlorite (Figure 4.1). The presence of 1.43 and 1.7 nm spacings for glycerol solvated specimens and only 1.7 nm spacings for ethylene glycol solvated specimens is characteristic of a mixture of beidellite/nontronite and montmorillonite (Harward et al, 1969). The micaceous component of both sola is dominated by dioctahedral

species, with only minor amounts of trioctahedral mica. Diffraction peaks for chlorite in total clay separates were weak, and only clearly evident after samples were heated to 550 C. Separates (1.0 - 2.0 μm) refined by magnetic separation at 1.75 T were dominated by chlorite, with the increase in intensity of the (001) chlorite reflection (1.4 nm) on heating coupled with the location of the (060) reflection at 0.156 nm indicating that the chlorite is iron-rich (Brown and Brindley, 1980). The collapse of the strong 0.7 nm peak in untreated clay separates after heating to 550 C indicates the presence of kaolinite, confirmed by selective dissolution of chlorite by overnight treatment with 2M HCl followed by X-ray analysis. Diffractograms of K-saturated specimens heated to 105 C and then equilibrated at 54 % R.H. indicated partial rehydration of the collapsed layers of the parent material. The ratio of the intensity of the 1.0 nm to the 0.7 nm peaks for the K-saturated sample was greater than the same ratio for the Ca-saturated sample and there was a distinct shoulder in the 1.04 nm region and broad peaks in the 1.2 - 1.4 nm region. Such rehydration behaviour indicated the presence of minor amounts of vermiculite.

Clay mineral (<2.0 μm) assemblages varied in composition on an inter-horizon basis throughout the depth of the pedon (Table 4.1). On the basis of the intensities of the X-ray diffraction peaks content of kaolinite was highest in the Ae horizon, reflecting negative enrichment (Arshad and Pawluk, 1966) through translocation of the smectite-enriched finer clay fractions to horizons lower in the profile. Vermiculite levels, calculated from the difference between the CEC and KEC, were highest in the Ae horizons. However, the levels are relatively low (<10%), and may merely represent fixation of the potassium by edge weathered mica. Mica was estimated to be the next dominant mineral of the Ae and AB horizons, with chlorite present in only trace amounts in all horizons. Smectite species contents were highest in the Bt horizons, with a slight decrease in relative content in the parent material. The smectite maxima

in the Bt horizons reflects the preferential translocation of components of the finer clay ($<0.2 \mu\text{m}$) fractions (Table 4.1), with the content of micaceous and kaolinite minerals displaying a concomitant decrease in the lower profile as a result of the dilution effect induced by the preferential translocation of the smectite-rich fine clay fractions.

Content of individual phyllosilicate mineral groups were relatively constant within the individual size fractions throughout the entire sola to the parent material. This indicates that the eluviation/illuviation processes of lessivage involve merely the movement of individual size fractions and not distinct mineral species. Individual minerals may, however, actually be concentrated in a narrow particle size range. Thus the enrichment of smectite minerals in the Bt horizons is a result of preferential translocation of the fine clay fractions ($<0.2 \mu\text{m}$), which incidently have smectite as a dominant component.

Diffraction analyses indicated that the expandable component of the fine clay separates were comprised of a mixture of distinct smectite species. The X-ray diffractograms indicate that a species exhibiting the diffraction behaviour of beidellite or nontronite dominated the fine clay separates from the Ae horizon, whereas montmorillonite was the major species in the Ck horizons. This depth variability has previously been described for Luvisolic soils (Cryoboralfs) in Alberta (Pawluk and Dudas, 1982; Spiers et al, 1985), Gley-podzolic soils in Russia (Kuznetsova and Sokolova, 1983) and Solodized Solonetz soils (Natroborolls) in Alberta (Spiers et al, 1984). Such vertical differentiation of diffraction behaviour in fine clays separated from an Aqualf with glycerol solvation has been attributed to weathering of micaceous minerals (Ransom et al, 1988) to form vermiculite. However, fixation of K^+ into any vermiculite present by heating to clay separates 105°C , followed by resaturation with Ca^{++} and glycerol vapour solvation, produced the identical diffraction behaviour to that described above. These results indicate that weathering of mica may not be a major process in the well to imperfectly drained

soils of the catena. Further the variability with depth may be explained by either eolian additions (Pawluk and Dudas, 1982), preferential translocation of the individual species (Spiers et al, 1984), by alteration and/or decomposition of montmorillonite (Munn and Boehm, 1983), or by neoformation of the tetrahedrally substituted species in the upper pedon (Kuznetsova and Sokolova, 1983). The latter two possibilities, based on an isotopic examination of the crystalline phyllosilicates in Northern Alberta soils (Spiers et al, 1984), are not probable in the soils under examination.

The partial re-expansion of the 0.95 nm spacing of Li-saturated specimens (Greenery, 1953) following glycerol solvation to spacings of 1.38 and 1.7-1.8 nm (Figure 4.1) respectively confirmed the presence of distinct smectite phases. The 1.38 nm phase may be attributed to a tetrahedrally substituted smectite species with the diffraction characteristics of beidellite or nontronite, whereas the 1.7 - 1.8 nm phase has the characteristics of octahedrally substituted montmorillonite (Schultz, 1969). The differentiation of the 1.38 and 1.7-1.8 nm spacings with depth (Figure 4.1) suggests a change in the distribution of these smectite phases within the profile. Whereas the beidellite/nontronite phase with the 1.38 nm spacing is dominant in the Ae horizon, and present in only minor amounts in the Ck horizon, the montmorillonite phase with the 1.7-1.8 nm spacing is dominant in the Ck horizon. Based on the criteria defined by Schultz (1969), approximately 90% of the net layer charge of the beidellite-like species of the Ae1 is in the tetrahedral layers, whereas approximately 25% of the net charge is in the tetrahedral layer for the expandable species in samples from the Ck horizon.

Infrared absorption spectra obtained for crystalline fine clay minerals of the $<0.2 \mu\text{m}$ separates from the Ae, Bt and Ck horizons display strong Al-O-Al vibrations in the $910\text{-}920 \text{ cm}^{-1}$ region. This $910\text{-}920 \text{ cm}^{-1}$ band is characteristic of the tetrahedrally-substituted beidellite (Farmer, 1974). The intensity of the band is stronger in the separates from the upper Ae

horizon, further supporting the interpretation of a higher proportion of beidellite based on the XRD analysis. The presence of strong Fe-Fe-OH absorption bands in the 810-820 cm^{-1} region in the infrared spectra from all horizons results from Fe in the octahedral layer of minerals in the smectite-rich $<0.2 \mu\text{m}$ separates (Goodman et al, 1976). The presence of a up to 10% Fe in the fine clay ($<0.2 \mu\text{m}$) fraction supports this suggestion. This Fe-rich inherited smectite was detected in clay separates throughout the sola, and has previously been documented in soils of the Interior Plains (Arshad and Pawluk, 1966; Pawluk and Bayrock, 1969; Spiers et al, 1984, 1985), although Mermut et al (1984) indicate that, in their examination, the Fe-rich smectite is an Fe-montmorillonite.

Diffraction and chemical analyses of clay ($<2.0 \mu\text{m}$) magnetic separates (Figure 4.2) were utilized to further elucidate the nature of the iron-bearing phyllosilicate minerals. These separates have an Fe content of between 12 and 15 %, and are comprised of an admixture of, in order of relative abundance, chlorite, smectite, trioctahedral clay mica, vermiculite and hydroxy-interlayered vermiculite. With the exception of the hydroxy-interlayered vermiculite relative enrichment in the Ae, there was minimal variability in content of the individual species with pedon depth. The Fe-bearing smectite phase, when intercalated with glycerol vapour, expanded to the 1.416 nm characteristic of nontronite, indicating that this may be the mineral species which is negatively enriched by the lessivage processes in the Luvisolic pedons examined.

The difference in diffraction behaviour of the tetrahedrally substituted smectites with profile depth, while not consequent to dissolution and neoformation of authigenic species (Spiers et al, 1985), may, however, result from oxidation/reduction of Fe within the actual mineral structure by protonation-deprotonation reactions (Badaut et al, 1985; Decarreau and Bonnin, 1986; Scott and Amonette, 1987; Stucki, 1987; Stucki et al, 1990), or from the weathering of

interlayer material from the micaceous minerals (Somasiri et al, 1971; Churchman, 1980; St Arnaud and Sudom, 1981). Oxidation of octahedral iron, and subsequent migration from the crystal lattice, would have only very minor effects on the b-axis spacings of the smectite minerals (Rozenson and Heller-Kallai, 1978), although it would cause a decrease in the exchange capacity. X-ray powder camera patterns of clay separates ($<0.2 \mu\text{m}$) dominated by the smectite group minerals showed that b-axis spacings remained essentially unchanged at 8.94 - 9.00 nm for samples from throughout the profile.

Mössbauer spectroscopy was utilized to examine the variability of the valence state of, and the structural site occupancy by, iron within the homionic fine clay ($<0.2 \mu\text{m}$) fraction minerals with depth in an attempt to resolve which, if any, of the above possible reactions has occurred in the sola to produce the variability in diffraction behaviour. The room temperature fitted Mössbauer spectra recorded over a velocity range of $\pm 3.7 \text{ mm sec}^{-1}$ for untreated fine clay ($<0.2 \mu\text{m}$) separates indicate that there are essentially no observable differences with depth.

The experimental spectra show a broadened Fe^{3+} resonance, with two prominent Fe^{3+} doublets having an I.S. and Q.S. values of 0.36, 0.50 (outer) and 0.35, 0.90 (inner) mm sec^{-1} respectively. There is also a Fe^{2+} doublet with an I.S. of 1.16 and Q.S. of 2.48 mm sec^{-1} . The three fitted doublets (Table 4.2) indicate that 96 % of iron in both the Ae and Ck fine clay separates is Fe^{3+} , with about 4% being Fe^{2+} . The values are consistent with the Fe^{3+} being in octahedral O,OH co-ordination within the phyllosilicate structure (Cardile and Johnston, 1985, 1986; Cardile, 1989; Dickson and Cardile, 1986; Goodman et al., 1988; Johnston and Cardile, 1985), with the linewidths of 0.40 and 0.54 mm sec^{-1} being intermediate between those documented for iron-bearing montmorillonites (0.48 and 0.77 mm sec^{-1}) and nontronites (0.32 and 0.40 mm sec^{-1}). The inner doublets comprised between 52% to 73% of the overall resonance area of the Ae and Ck fine clay respectively, with the outer doublets varying from 44 to 23%

of the area. There is no evidence of tetrahedral substitution by Fe^{3+} in the fine clay separates (Cardile, 1989). Although the broadening of the linewidths is indicative of a degree of structural disorder or differing environment around the respective Fe^{3+} ions in the structure, the Q.S. values (0.50 and 0.90 mm sec⁻¹) compare with those (0.56 and 0.96 mm sec⁻¹) assigned primarily to trans-octahedral sites in reference montmorillonites (Johnston and Cardile, 1986), with the smaller Al^{3+} ion being assumed to occupy the cis- sites. The minor Fe^{2+} doublet (Q.S. 2.48 mm sec⁻¹) is also in trans-octahedral co-ordination (Heller-Kallai and Rozenson, 1981).

Thus there is no relative change in site occupancy or net surface charge density apparent with depth. The X^2 values of 557 and 580 for the Ae and Ck fine clay separates, respectively, indicate that there is no change in the degree of crystal order. This may be interpreted as suggesting that there has been no alteration, or weathering, of the minerals.

Table 4.1. Computed Mössbauer parameters at 293 K for the fine clay separates from selected major genetic horizons of an Orthic Grey Luvisol from the upper slope of the catenary sequence.

Sample		I.S. ¹	Q.S. (mm sec ⁻¹)	P.W.	A (%)
Ae	Fe^{3+}	0.36 (1)	0.50 (1)	0.40 (1)	52 (5)
		0.35 (1)	0.90 (3)	0.54 (2)	44 (5)
	Fe^{2+}	1.16 (4)	2.48 (8)	0.39 (4)	4 (1)
Ck	Fe^{3+}	0.36 (1)	0.51 (1)	0.38 (1)	73 (8)
		0.34 (1)	0.92 (11)	0.52 (1)	23 (8)
	Fe^{2+}	1.16 (4)	2.67 (12)	0.35 (6)	4 (1)

¹I.S. = isomer shift; Q.S. = quadrupole splitting; P.W. = peak width at half height; A = relative area of component; (x) = x is uncertainty in last figure.

4.3.2. Micromorphological Analysis

Micromorphological examination indicated that the isoband fabric (Dumanski and St. Arnaud, 1966) of the Ae horizon consisted of a dense porphyric fabric between well developed horizontal joint planes. The plasma fabric was skelsepic to weak insepic, with a significant proportion of an isotropic noncrystalline or amorphous groundmass, shown by EDS microanalysis to be comprised primarily of Al and Si, present in the numerous vughs. The Si:Al ratio was between 1.5:1 and 2.1:1, similar to that described for Solodized Solonetzic soils (Spiers et al, 1984). There were common aggotubules containing mullgranic units (35-45 μm diameter). Sporadic zones of organic plasma concentration with a weak humic component occurred throughout the plasma. Mullgranic faecal pellets of small earthworms, probably of either the *Octolasion spp* or *Apporectodea turgida* observed during field sampling, were common in the upper 1-4 cm of the Ae horizons. Common opaque concentrations of varying size which were frequently enriched in Mn and P were observed at the base of the Ae horizon, probably representing a zone of periodic saturation caused by the sealing of the smectite-rich Bt horizons (Matlack et al, 1989) following significant periods of rainfall. Electron optical examination of the structural units indicated that the skeletal grains were loosely packed, with a minor amount of clay material bridging and binding the individual grains, with the iron oxyhydroxide material forming grain bridges.

The banded porphyric fabric of the Ae graded through the AB horizon to a dense porphyric fabric in the Bt horizons, with common vughs and widely spaced vertical joint planes. The plasma fabric was comprised dominantly of omnisepic zones randomly intermixed with skelsepic zones. The well-developed void argillans observed in the channels and vughs resulted from the translocation of clay material from the overlying horizons. The X-ray diffractograms of excised cutanic material (Figure 4.3) suggest considerable depth variability in relative

abundance of smectite species. The Ae, Bt1 and Ck horizon cutans have a higher relative proportion of mica and kaolinite than the Bt2 horizon. The dominant smectite species in the argillans has the diffraction behaviour of montmorillonite, further supporting the hypothesis of differential movement within the smectite species during lessivage. In situ microchemical analyses of argillans in thin section indicate that the content of mica remains relatively constant with depth at between 15 - 17%. The smectite content, based on $\text{Fe}_2\text{O}_3 + \text{MgO}$ data, reached a maximum at 90 cm. Kaolinite content, from diffraction intensity, is highest in cutanic features in the upper Bt1 horizon. The presence of significant contents of mica in argillanic features was also suggested by Howitt and Pawluk (1985b), who documented active translocation of mica suspended in the soil solution from the upper Bt horizons.

Electronoptical examination of the argillans in both plan and cross-section indicated considerable variation in the submicroscopic arrangement of the plasma with depth in the pedon (Plate 4.2(a,f), probably in part consequent to the mineralogical differences indicated above.

4.3.4. Colloidal Suspension Analysis

Solutions were collected from the series of gravity lysimeters over a 6 year period from below the Ae and AB horizons of pedons at three locations within the catena, with many collections (29) having visible colloidal material which was filtered with a $0.2 \mu\text{m}$ filter. The lessivage pattern of the colloidal material appears to be controlled by antecedent moisture conditions of the soils prior to the onset of long duration repetitive rainfall events, with translocation peaks in early spring following snowmelt and thaw, late June through mid July, and occasionally in late fall. For active lessivage in summer and fall it appears that the LFH horizons must be at, or near saturation, to provide sufficient flow to transport the colloidal material. Prior to the saturation period colloidal yields were enhanced if the upper mineral solum (Ae and AB horizons) had been relatively dry.

Table 4.3: Total chemical analyses of the colloidal leachates from a series of gravity lysimeters installed at three slope positions of a catenary sequence below the AB horizons.

	Al	Si	K	Fe	Mg	Ca
Bulked Spring Colloid Collection	(%)					
Upper slope	23.6	58.3	3.8	9.5	2.1	2.7
Mid slope	25.4	67.0	2.4	1.1	3.1	1.0
Lower Slope	25.6	66.0	2.2	2.1	2.7	1.4
Bulked Summer Colloid Collection						
Upper slope	26.2	67.5	2.1	0.9	2.4	0.9
Mid slope	26.5	66.7	2.1	2.4	1.2	1.1
Lower slope	27.2	67.7	1.3	0.2	3.0	0.6
Bulked Fall Colloid Collection						
Upper slope	25.9	68.3	2.4	0.2	2.1	1.1
Mid slope	28.2	65.5	1.8	0.5	3.0	1.0
Lower slope	24.5	68.1	2.8	1.1	2.3	1.2

Although the fall collections of colloidal material were more infrequent over the sampling period, the actual amount tended to be greater. This latter observation is in agreement with the findings of Howitt and Pawluk (1985b).

Table 4.4: Oxalate and pyrophosphate extractable Al, Si, Fe and C contents of the colloidal leachates from a series of gravity lysimeters installed at three slope positions of a catenary sequence below the AB horizons.

	Al _{ox}	Si _{ox}	Fe _{ox}	Al _{py}	Fe _{py}	C _{py}
Bulked Spring Colloid Collection	(%)					
Upper slope	7.93	3.25	1.37	0.34	0.27	1.78
Mid slope	9.52	2.97	1.12	0.09	0.15	1.32
Lower Slope	8.47	5.13	0.86	0.23	0.35	1.99
Bulked Summer Colloid Collection						
Upper slope	5.63	2.76	1.37	0.28	0.73	5.27
Mid slope	3.65	1.08	0.93	0.38	0.92	4.65
Lower slope	4.99	1.76	1.03	0.43	1.13	5.98
Bulked Fall Colloid Collection						
Upper slope	4.51	2.02	0.57	0.39	0.96	4.78
Mid slope	3.98	1.50	0.51	0.29	0.16	3.93
Lower slope	5.42	1.97	0.74	0.67	0.53	4.99

Subsamples of the colloidal leachate were then bulked by season of collection for subsequent mineralogical and chemical analyses. Further subsamples were examined directly by

SEM-EDS and FTIR spectroscopy. X-ray diffraction analyses indicated that the phyllosilicate component was comprised of an admixture of, in order of abundance, kaolinite, dioctahedral clay mica and smectite (Figure 4.3). Although only partially resolved by the high background consequent to radiation absorption and scattering by the amorphous and organic component of the colloidal leachate, the smectite component appears to be an admixture of high charge and low charge species. The low charge montmorillonite species is more abundant than the higher charge beidellite. This interpretation is based on the 1.4 and 1.7 nm spacing following vapour absorption of glycerol by the samples. The active translocation of kaolinite has not previously been observed in Luvisolic soils. Howitt and Pawluk (1985a) reported movement of micaceous clays, but were unable to differentiate the different smectite species.

Total chemical analyses of the colloidal separates show some seasonal variation, with higher K and Fe contents for the spring samples (Table 4.3). If all the K is in micaceous minerals approximately 16 -30 % of the colloidal material is clay mica. The seasonal pattern of the data from selected extraction of poorly crystalline aluminosilicate and organically complexed Fe and Al in Table 4.4 indicates that there is a far greater seasonality in the organo-complexes than for the inorganic components. The content of $Al_{(ox)}$, $Fe_{(ox)}$ and $Si_{(ox)}$ reflects a significant component of poorly crystalline components such as allophane and ferrihydrite in the mineral phase of the colloidal leachates. The higher than expected $Si_{(ox)}$ for allophanic components is a result of the high number of siliceous stomatocysts present in nearly all collections (Plate 4.3). These stomatocysts, or vegetative resting stages of Chrysophyceae or golden brown algae, have previously been described primarily from cool oligotrophic lake sediments (Smol, 1988; Duff and Smol, 1988a,b), appear to exhibit a marked seasonality, with highest numbers in spring and fall collections. The organisms have also been recently observed by Arocena and Pawluk (1990).

The maximum pyrophosphate extractable carbon content is found in the summer colloidal leachates. This is probably a reflection of maximum decomposition rate being associated with maximum faunal and floral activity, coupled with the leaching of constituents such as polysaccharides, polyuronides and carbohydrates from the canopy and shrub layers (Sanborn and Pawluk, 1983; Howitt and Pawluk, 1985b). The content of Al and Fe, although much lower than extracted from Podzolic soils, explains, in part, the presence of up to 0.4% (Al+Fe) documented in Luvisolic Bt horizons (Howitt and Pawluk, 1985a). This 'active iron' (Duchaufour and Souchier, 1978) has been suggested as being responsible for linking translocated phyllosilicates and humic components to promote the strongly developed structure common to the Bt horizons.

Infrared spectroscopic analysis of the colloidal leachates held over P_2O_5 for 24 hours prior to analysis supports the interpretation of the mobile phyllosilicate minerals suggested by X-ray diffraction. Specifically the 912-915 cm^{-1} band of the Al—O—H vibrations characteristic of tetrahedrally substituted Al was present in all spectra (Figure 4.4). The band at approximately 820 cm^{-1} was only present in samples from spring collections, suggesting that the major mobilisation of the Fe-smectite follows the seasonal snowmelt flush. The content of Fe of the spring colloidal material (Table 4.2) supports this observation. Presence of quartz, shown by scanning electron microscopy of selected collections to range in size from about 1.5 to 10 microns (Plate 4.3), was confirmed in all samples by the 779 and 799 cm^{-1} doublet. The dominant kaolinite mobilization, recognised by characteristic bands at 3620 and 3695 cm^{-1} , was also consistently found in samples collected following the spring melt. The band at 348 cm^{-1} , common to kaolinite, allophane and imogolite, was generally enhanced in the fall collections, coincident with higher levels of extractable aluminosilicate material.

The total mobile colloidal carbon content was shown by pyrophosphate extraction

(Table 4.3) to be at a maximum in collections from summer and fall. The infrared spectra illustrated confirm this observation. Further, the infrared spectra (Figure 4.3) of the colloidal leachates from the lysimeters also display a marked seasonality in both the relative amount of individual spectral bands of specific organic components and in the absolute amount of colloidal and absorbed organic material being mobilized with the phyllosilicate material. The strong broad band at 3300 - 3400 cm^{-1} , shown to be associated with 'fulvic acids' by Tan (1977), is at a maximum in the collections following long summer rain periods and must be associated with a flush of soluble or absorbed low molecular weight organic materials produced by faunal and floral decomposition processes in late spring to early summer. The relative intensity of this band always decreased in the late fall samples. The intensity of the aliphatic ν_{as} CH_3 and ν_{as} CH_2 bands (van der Marel and Beutelspacher, 1976) about 2930 and 2980 cm^{-1} also followed a similar pattern, with the ν_s CH_2 band at about 2850 cm^{-1} being of similar intensity throughout the year. Carbonyl absorption at 1733 cm^{-1} was only observed in the summer leachates. The broad band at ca 1730 - 1650 cm^{-1} associated with the ν $\text{C}=\text{O}$ of ketones and carboxylic acids (van der Marel and Beutelspacher, 1976) of fulvic acid components (Tan, 1977) displayed little seasonal variability in relative intensity.

Perhaps the most marked seasonal variability in the infrared spectra are observed in the 1500 to 1200 cm^{-1} region, where bands are weak in spring samples and very strong in late fall samples. Specifically, the 1384 cm^{-1} band associated δOH of low molecular weight $\text{R}-\text{COOH}$ acids attains maximum intensity in the fall colloidal samples. There is an associated ν $\text{C}=\text{C}$ 1554 cm^{-1} vibration, probably from aromatic compounds, observed in summer and fall collections. The 1270 - 1280 cm^{-1} (ν_{as} $=\text{C}-\text{O}-\text{C}$) vibration observed most intensely in fall and spring sample leachates may be associated with either phenols and alcohols, or aromatic ketones. These compounds may represent the degradation products of the lignin material from litter-fall. Any

vibrational bands resulting from organic components in the spectral region from 1100 to 1000 cm^{-1} are masked by the SiO_2 from the phyllosilicates.

The pronounced seasonal pattern of the infrared spectra of the organo-mineral colloidal material described above provides an insight into the seasonal variability of lessivage process. The colloidal material mobilized in the spring following snowmelt has a lower content of organic matter (Table 4.3). As biological activity and associated decomposition processes reach a seasonal maximum in early summer the leachates mobilized by intense summer rains contain a higher content of aromatic low molecular weight organics, probably primarily mobilised as organo-mineral complexes. The aliphatic compounds apparently are translocated with the fall rains. The relatively high content of mobile colloidal organic material is the source of both the bulge of total carbon commonly documented in the lower Bt horizons and the dark colour of the cutanic material at depth.

4.4. CONCLUSIONS

Static pedological physical, chemical, mineralogical and micromorphological properties of the pedons of a Luvisolic catenary sequence clearly indicate that lessivage has been a dominant soil forming process. Smectite and, to lesser extent, mica have accumulated in the Bt horizons of the pedons, whilst kaolinite has been negatively enriched in the Ae horizons. Within the smectite group a distinct zonation was observed within the pedon as a result of selective mobilization. The montmorillonite was enriched in the Bt horizon, with a mineral of the diffraction behaviour of beidellite or nontronite being more prevalent in the Ae horizons. Powder camera and Mössbauer spectroscopic analyses of fine clay separates indicated that there is no apparent change in either hexa spacing or oxidation state of iron in the clay structure which could, perhaps, cause a misinterpretation of the negative enrichment of beidellite in the Ae horizons by the lessivage process.

The dominance of montmorillonite in excised cutanic material further supports the difference in relative mobility of the individual smectite species. The montmorillonite content of cutans was greatest in the Bt2 horizons, with relative amount of mica being constant with depth. Kaolinite, however, was more abundant in Bt1 horizon cutans indicating a higher relative mobility of kaolinite in more recent pedohistory. This may reflect the negative enrichment and kaolinite platlet physical disintegration to form fine clay material in the Ae horizon.

Dynamic studies over a six year period using a series of gravity lysimeters installed below the Ae and AB horizons of the catenary sequence provided considerable information on the nature of the contemporary mobile colloidal phase. Kaolinite, mica and smectite were all shown to be present in the phyllosilicate fraction, with a considerable quantity of 1.5 to 10 μm quartz and feldspar grains being present in spring colloid collections. There were also significant numbers of siliceous algal stomatocysts present in almost all colloid samples. Chemical extractions indicated presence of poorly crystalline aluminosilicate and ferrihydrite species, along with a significant component of organically complexed Al and Fe. Pyrophosphate-extractable C contents of the leachates was as high as 5% by weight, perhaps explaining the poor peak resolution during diffraction analysis of untreated inorganic components.

Infrared spectroscopic analysis of seasonal samples of the colloidal material confirmed the mineralogical interpretations of the diffraction analyses and also indicated a marked seasonality of individual organic components. Specifically, contents of the low molecular weight aromatics are low in all spring collections and increase in content with the summer precipitation events, reflecting both leaf wash and increased soil faunal and floral decomposition activity. Maximum levels of degradation products of lignins are found in the late fall samples.

4.5. BIBLIOGRAPHY

- Arocena, J.M. and Pawluk, S. (1990) Development of microstructures in Cryorthods from Alberta. (in prep).
- Arshad, M.A. and Schnitzer, M. (1988). Chemical characteristics of humic acids from five soils in Kenya. *Z. Pflanzenernaehr. Bodenk.* 152: 11-16.
- Arshad, M.A. and S. Pawluk (1966). Characteristics of some solonchic soils in the Glacial Lake Edmonton basin of Alberta. II. Mineralogy. *J. Soil Sci.* 17: 48-55.
- Badaut, D., Besson, G., Decarreau, A., and Rautureau, M. (1985). Occurrence of a ferrous trioctahedral smectite in recent sediments of Atlantis II Deep, Red Sea. *Clay Min.* 20: 389-404.
- Belousova, N.I. (1979). Lysimetric studies in the Taiga zone genetical interpretations. *Coll. Int. du C.N.R.S* 303: 281-289.
- Bound, W.J. (1986). Illuvial band formation in a laboratory sand. *Soil Sci. Soc. Am. J.* 50: 265-267.
- Brewer, R. and Haldane, A.D. (1957). Preliminary experiments on the development of clay orientation in soils. *Soil Sci.* 84: 301-309.
- Brewer, R. and S. Pawluk (1975) Investigations of some soils developed in hummocks of the Canadian Sub-Arctic and Southern Arctic regions. *Can. J. Soil Sci.* 55: 301-309.
- Cardile, C.M. and J.H. Johnston (1985). Structural studies of nontronites with different iron contents by ^{57}Fe Mössbauer spectroscopy. *Clays Clay Min.* 33: 295-300.
- Cardile, C.M. and J.H. Johnston (1986). ^{57}Fe Mössbauer spectroscopy of montmorillonites: a new interpretation. *Clays Clay Min.* 34: 307-313
- Cardile, C.M. (1989). Tetrahedral iron in smectite: a critical comment. *Clays Clay Min.* 37: 185-188.
- Dickson, D.P.E. and Cardile, C.M. (1986). Magnetic ordering in a montmorillonite observed by ^{57}Fe Mössbauer spectroscopy at 1.3K. *Clays Clay Min.* 34: 103-104.
- Davis, R.I. (1971). Relation of polyphenols to decomposition and the pedogenic process. *Soil Sci.* 111: 80-85.

- Decarreau, A., and Bonnin, D. (1986). Synthesis and crystallogenesi at low temperature of Fe(III)-smectites by coprecipitated gels: experiments in partially reducing conditions. *Clay Min.* 21: 861-877.
- Dixit, S.P. (1978). Potential mobility of clay in soils as measured by electrophoretic mobility. *Agrochimica* 22: 25-31.
- Duff, K.E. and Smol, J.P. (1988). Chrysophycean stomatocysts from the postglacial sediments of a High Arctic Lake. *Can. J. Bot.* 66: 1117-1128.
- Duff, K.E. and Smol, J.P. (1989). Chrysophycean stomatocysts from the postglacial sediments of Tasikutaq Lake, Baffin Island, N.W.T. *Can. J. Bot.* 67: 1649-1656.
- Gagarina, E.I. and Chizhikova, N.P. (1984). Clay migration in soils on calcareous moraines. *Pochvovedeniye* 10: 5-17.
- Greene-Kelley, R. 1953. The identification of montmorillonoids. *J. Soil Sci.* 4: 233-237.
- Ghabru, S.K., St Arnaud, R.J. and Mermut, A.R. (1988). Use of high gradient magnetic separation in detailed clay mineral studies. *Can. J. Soil Sci.* 68: 645-655.
- Goodman, B.A., Russell, J.D., Fraser, A.R. and Woodhams, F.W.D. (1976). A Mössbauer and I.R. spectroscopic study of the structure of nontronite. *Clays Clay Min.* 24: 53-59.
- Goodman, B.A., Nadeau, P.H. and Chadwick, J. (1988). Evidence for the multiphase nature of bentonites from Mössbauer and EPR spectroscopy. *Clay Min.* 23: 147-159.
- Heller-Kallai, L. and Rozenson, I. (1981). The use of Mössbauer spectroscopy of iron in clay mineralogy. *Phys. Chem. Minerals* 7: 223-238.
- Holm Jakobsen, B. (1989). Evidence for translocations into the B horizon of a subarctic Podzol in Greenland. *Geoderma* 45: 3-17.
- Howitt, R.W. and S. Pawluk (1985) Genesis of a Gray Luvisol in the Boreal Forest zone. I. Dynamic pedology. *Can. J. Soil Sci.* 65: 1-8.
- Howitt, R.W. and S. Pawluk (1985) Genesis of a Gray Luvisol in the Boreal Forest zone. II. Dynamic pedology. *Can. J. Soil Sci.* 65: 9-19.

- Jenny, H. and Smith, G. (1935). Colloid chemical aspects of clay pan formation in soil profiles. *Soil Sci.* 39: 377-389.
- Johnston, J.H. and Cardile, C.M. (1985). Iron sites in nontronite and the effect of interlayer cations from Mössbauer spectra. *Clays Clay Min.* 33: 21-30.
- Johnston, J.H. and Cardile, C.M. (1986). Iron substitution in montmorillonite, illite, and glauconite by ^{57}Fe Mössbauer spectra. *Clays Clay Min.* 33: 21-30.
- Komadel, P., Lear, P.R. and Stucki, J.W. (1990). Reduction and re-oxidation of nontronite: extent of reduction and reaction rates. *Clays Clay Min.* 38: 203-208.
- Loveland, P.J. and P. Digby (1984). The extraction of Fe and Al by 0.1M phosphate solution: A comparison of some techniques. *J. Soil Sci.* 35: 243-250.
- Levy, G.M., Quaglia, A., Lazure, R.E. and McGeorge, S.W. (1987). A photodiode array based spectrometer system for inductively coupled atomic emission spectroscopy. *Spectrochim. Acta* 42B: 341-351.
- McKeague, J.A. (1979). Organo-mineral migration: some examples and anomalies from Canadian soils. *Coll. Int. du C.N.R.S.* 303: 341-348.
- Matlack, K.S., Houseknecht, D.W. and Applin, K.R. (1989). Emplacement of clay into sand by infiltration. *J. Sed. Pet.* 59: 77-87.
- Mehra, O.P., and M.L. Jackson (1960). Iron oxide removal from soils and clays by a dithionite-citrate system buffered with sodium bicarbonate. *Clays Clay Min.* 7: 317-327.
- Mermut, A.R., Ghebre-Egziabhier, K, and St.Arnaud, R.J. (1984). The nature of smectites in some fine textured lacustrine parent materials in Southern Saskatchewan. *Can. J. Soil Sci.* 64: 481-494.
- Meunier, A., and B. Velde (1982). X-ray diffraction of oriented clays in small quantities. *Clay Min.* 17: 255-262.
- Parfitt, R.L. (1989). Optimum conditions for the extraction of Al, Fe, and Si from soils with acid oxalate. *Comm. Soil Sci. Plant Anal.* 20: 801-816.

- Pawluk, S. (1961). Mineralogical composition of some Gray Wooded soils developed from glacial till. *Can. J. Soil Sci.* 41: 228-240.
- Pawluk, S. and M.J. Dudas (1978). Reorganisation of soil materials in the genesis of an acid Luvisolic soil of the Peace River region, Alberta. *Can. J. Soil Sci.* 58: 209-220.
- Pawluk, S. and M.J. Dudas (1982). Pedological investigation of a Gray Luvisol developed from eolian sand. *Can. J. Soil Sci.* 62: 49-60.
- Ransom, M.D., Bigham, J.M., Smeck, N.E. and Jaynes, W.F. (1988). Transitional vermiculite-smectite phases in Aqualfs in Southwestern Ohio. *Soil Sci. Soc. Am. J.* 52: 873-880.
- Russell, J.D., Birnie, A., and Fraser, A.R. (1984). High gradient magnetic separation (HGMS) in soil clay mineral studies. *Clay Min.* 19: 771-778.
- St. Arnaud, R.J. and M.D. Sudom (1981) Mineral distribution and weathering in Chernozemic and Luvisolic soils from central Saskatchewan. *Can. J. Soil Sci.* 61: 79-89.
- Santos, M.C.D., St. Arnaud, R.J. and Anderson, D.W. (1986a). Iron redistribution in three Boralfs (Luvisols) of Saskatchewan. *Soil Sci. Soc. Am. J.* 50: 1272-1277.
- Santos, M.C.D., St. Arnaud, R.J. and Anderson, D.W. (1986b). Quantitative evaluation of pedogenic changes in Boralfs (Gray Luvisols) of east-central Saskatchewan. *Soil Sci. Soc. Am. J.* 50: 1013-1019.
- Schulz, D.G., and Dixon, J.D. (1979). High gradient magnetic separation of iron oxides and other minerals from soil clays. *Soil Sci. Soc. Am. J.* 43: 793-799.
- Scott, A.D. and Amonette, J. (1987). The role of iron in mica weathering. In: Stucki, J.W., Goodman, B.A. and Schwertmann, U. (eds), *Iron in Soils and Clay Minerals*. Reidel, Dordrecht.
- Singer, M., Ugolini, F.C. and Zachara, J. (1978). In situ study of podzolisation on tephra and bedrock. *Soil Sci. Soc. Am. J.* 42: 105-111.
- Smol, J.P. (1988). Chrysophycean microfossils in paleolimnological studies. *Palaeogeog. Palaeoclim. Palaeoec.* 62: 287-297.

- Spiers, G.A., Pawluk, S. and Dudas, M.J. (1984). Authigenic mineral formation by solodization. *Can. J. Soil Sci.* 64: 515-532.
- Stucki, J.W. (1987). Structural iron in smectites. In: Stucki, J.W., Goodman, B.A. and Schwertmann, U. (eds), *Iron in Soils and Clay Minerals*. Reidel, Dordrecht.
- Tan, K.H. (1977). Infrared spectra of humic and fulvic acids containing silica, metal ions, and hygroscopic moisture. *Soil Sci.* 123: 235-240.
- Ugolini, F.C., Dawson, H. and Zachara, J. (1977a). Direct evidence of particle migration in the soil solution of a podzol. *Science* 198: 603-605.
- Ugolini, F.C., Minden, R., Dawson, H. and Zachara, J. (1977b). An example of soil processes in the *Abies amabilis* zone of the Central Cascades, Washington. *Soil Science* 124: 291-302.
- van der Marel, H.W. and Beutelspacher, H. (1976). *Atlas of Infrared Spectroscopy of Clay Minerals and their Admixtures*. Elsevier Scientific Publishing, Amsterdam, 379pp.
- Vedy, J.C. and Buckert, S.B. (1982). Soil Solution: Composition and Pedogenic Significance. In: *Pedology. 2. Constituents and Properties of Soils*. Bonneau, M. and Souchier, B. (eds.), Farmer, V.C. (Trans. ed.). Academic Press. pp184-213.

Figure 4. X-ray diffractograms of clay separates ($<2.0\ \mu\text{m}$) from selected major genetic horizons of an Orthic Grey Luvisol.

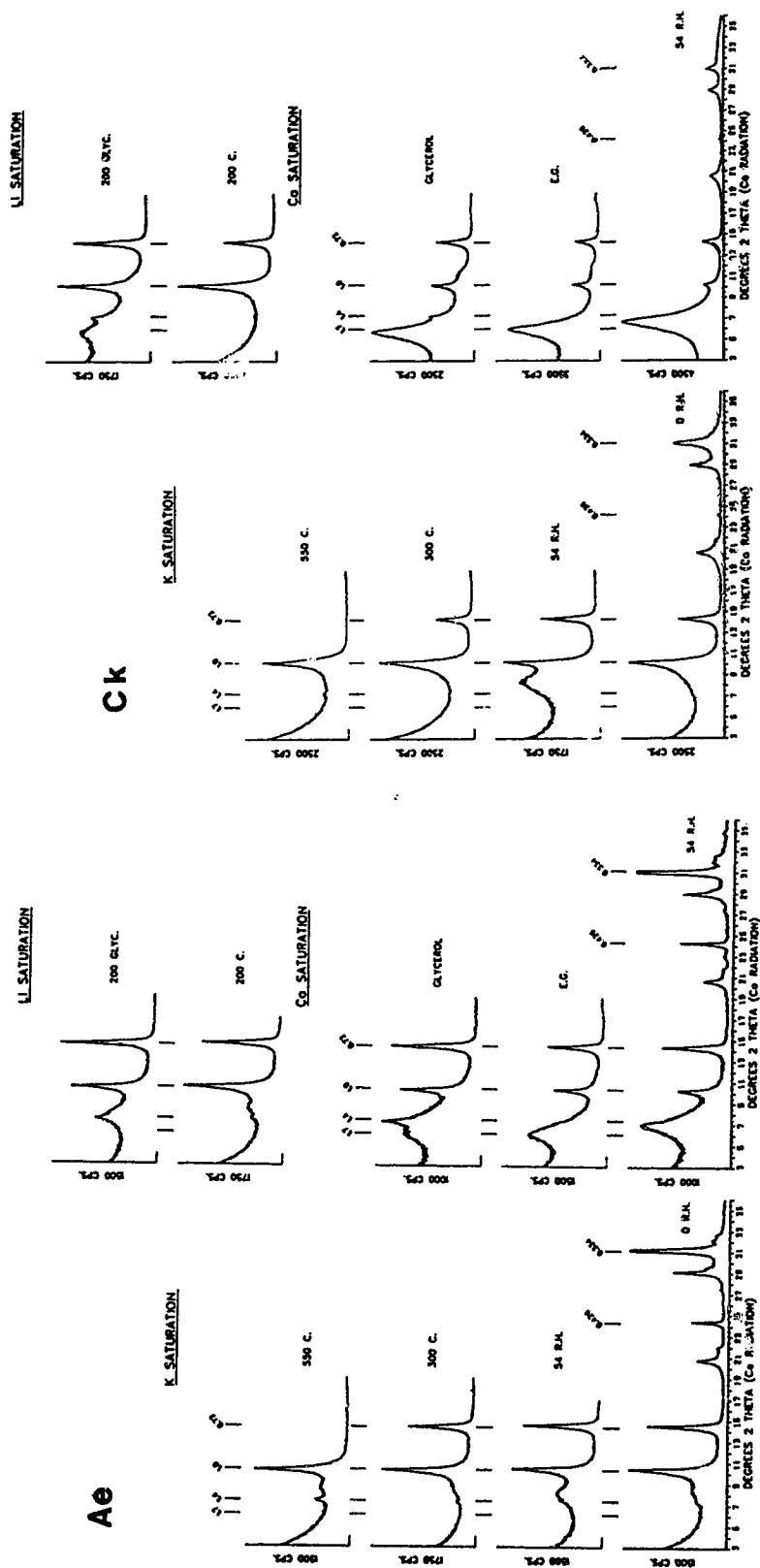
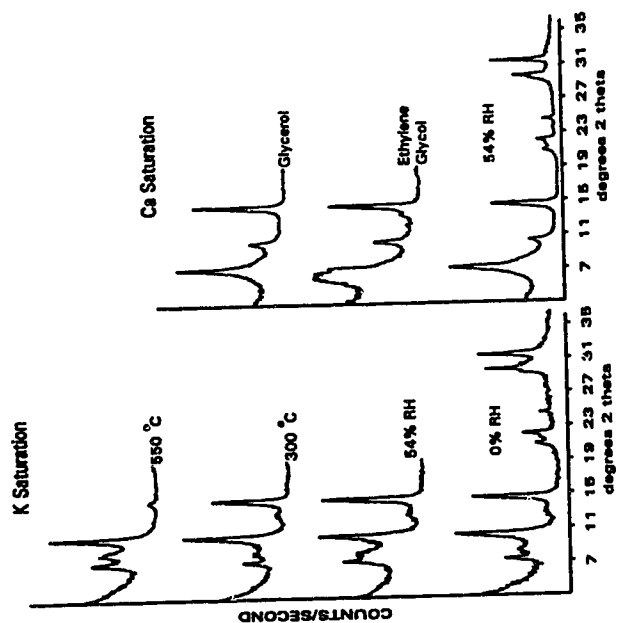


Figure 4.2: X-ray diffractograms of magnetic (1.7 T) clay separates from selected major genetic horizons.

X-ray diffractograms of magnetic clay separates from Ae.



X-ray diffractograms of magnetic clay separates from Ck.

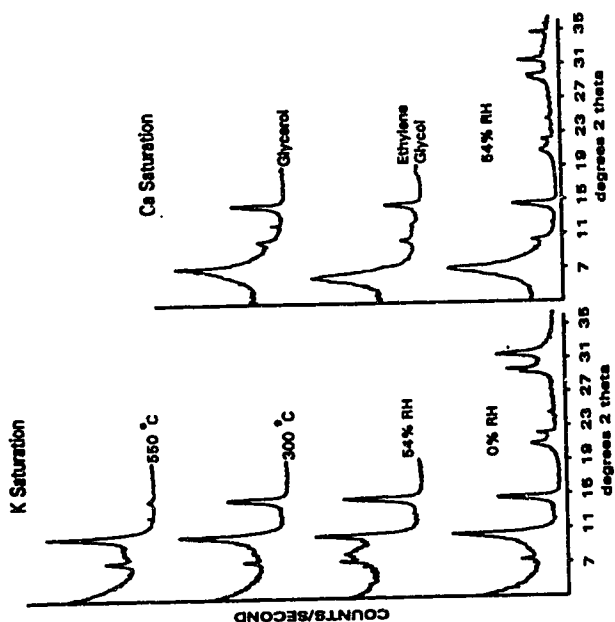
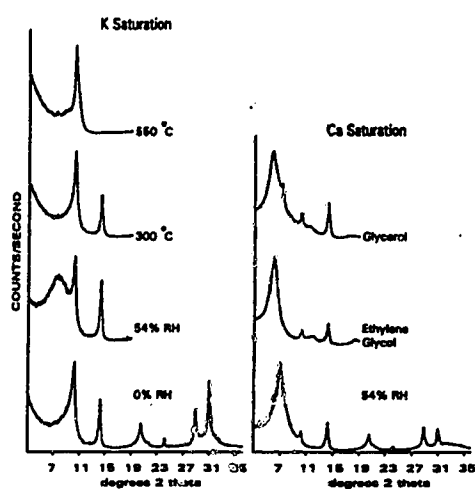
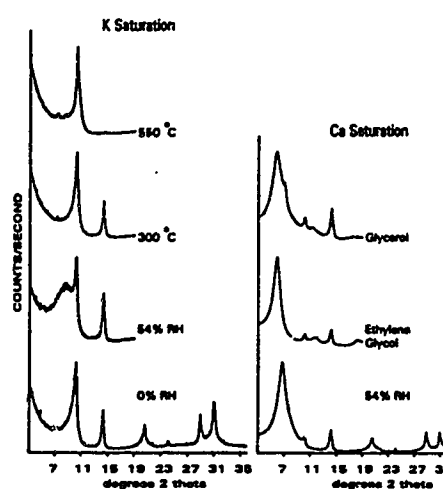


Figure 4.3: X-ray diffractograms of the cutanic clay material excised from peds sampled from the major genetic horizons of an Orthic Gray Luvisol.

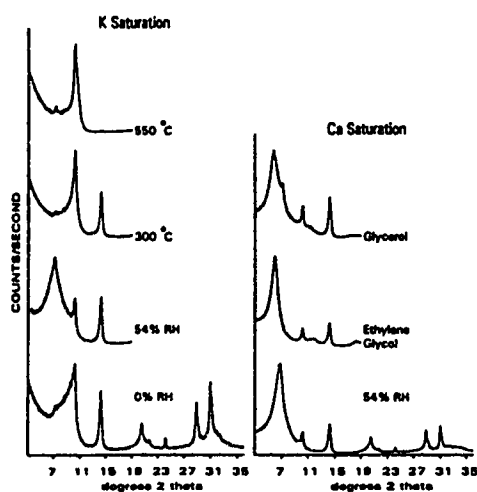
X-ray diffractograms of Bt1 (30 cm) cutan clays



X-ray diffractograms of BC (90 cm) cutan clays



X-ray diffractograms of Bt2 (65 cm) cutan clays



X-ray diffractograms of Ck (110 cm) cutan clays

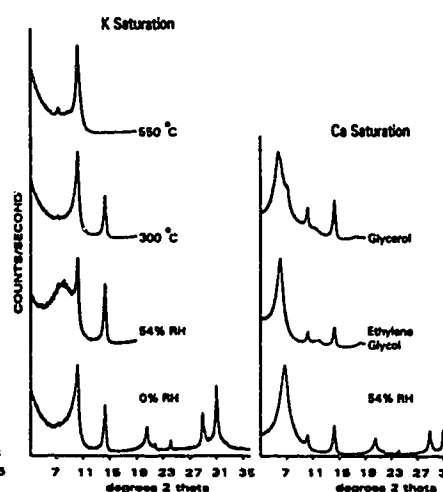


Figure 4.4: X-ray diffractograms of the untreated colloidal material filtered from the soil solutions collected in a series of gravity lysimeters installed below the AB horizons of a catenary sequence of soils.

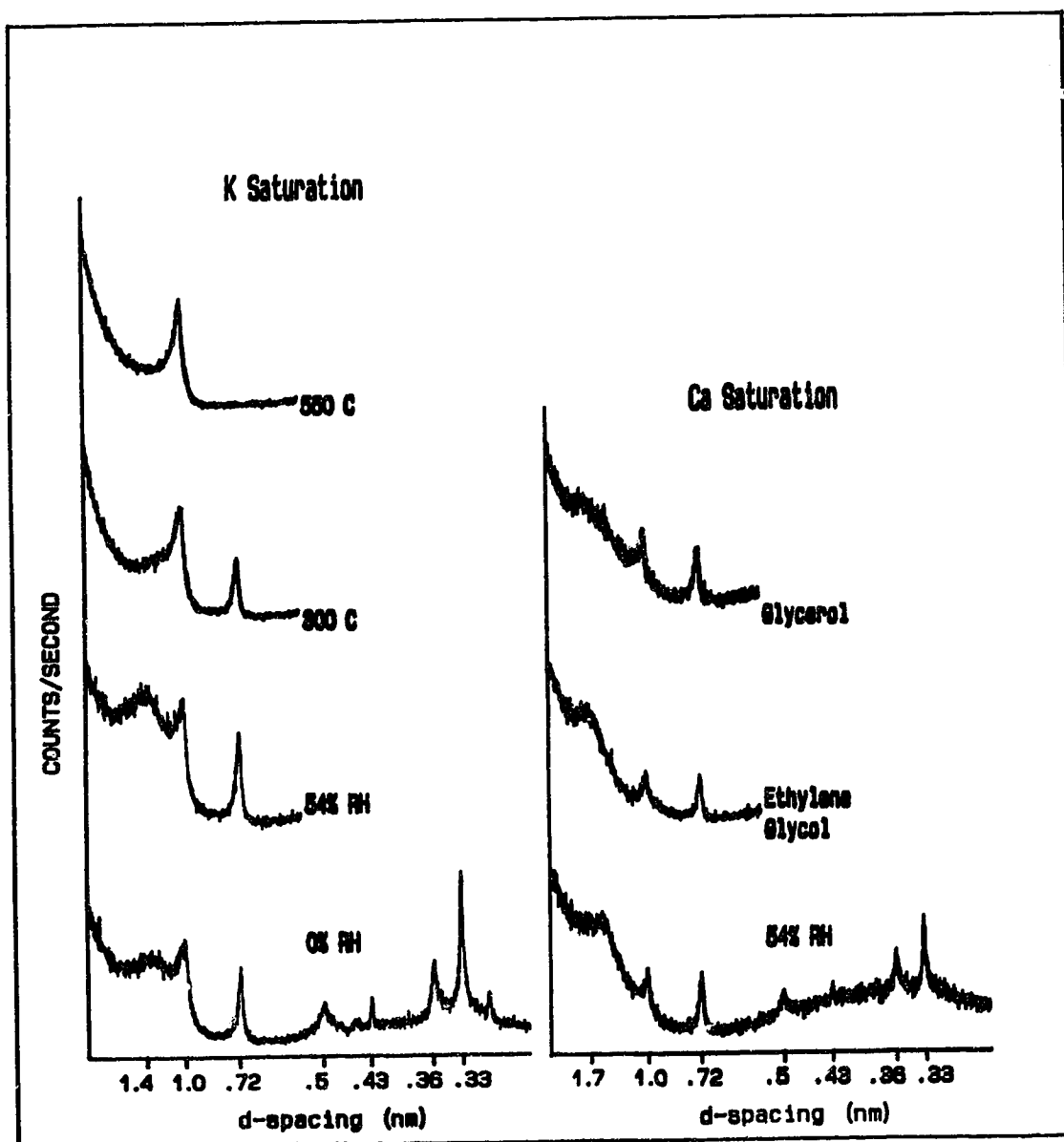


Figure 4.4: Infrared spectra of the untreated colloidal material from spring, summer and fall collections filtered from the soil solutions collected in a series of gravity lysimeters installed below the AB horizons of a catenary sequence of Luvisolic soils.

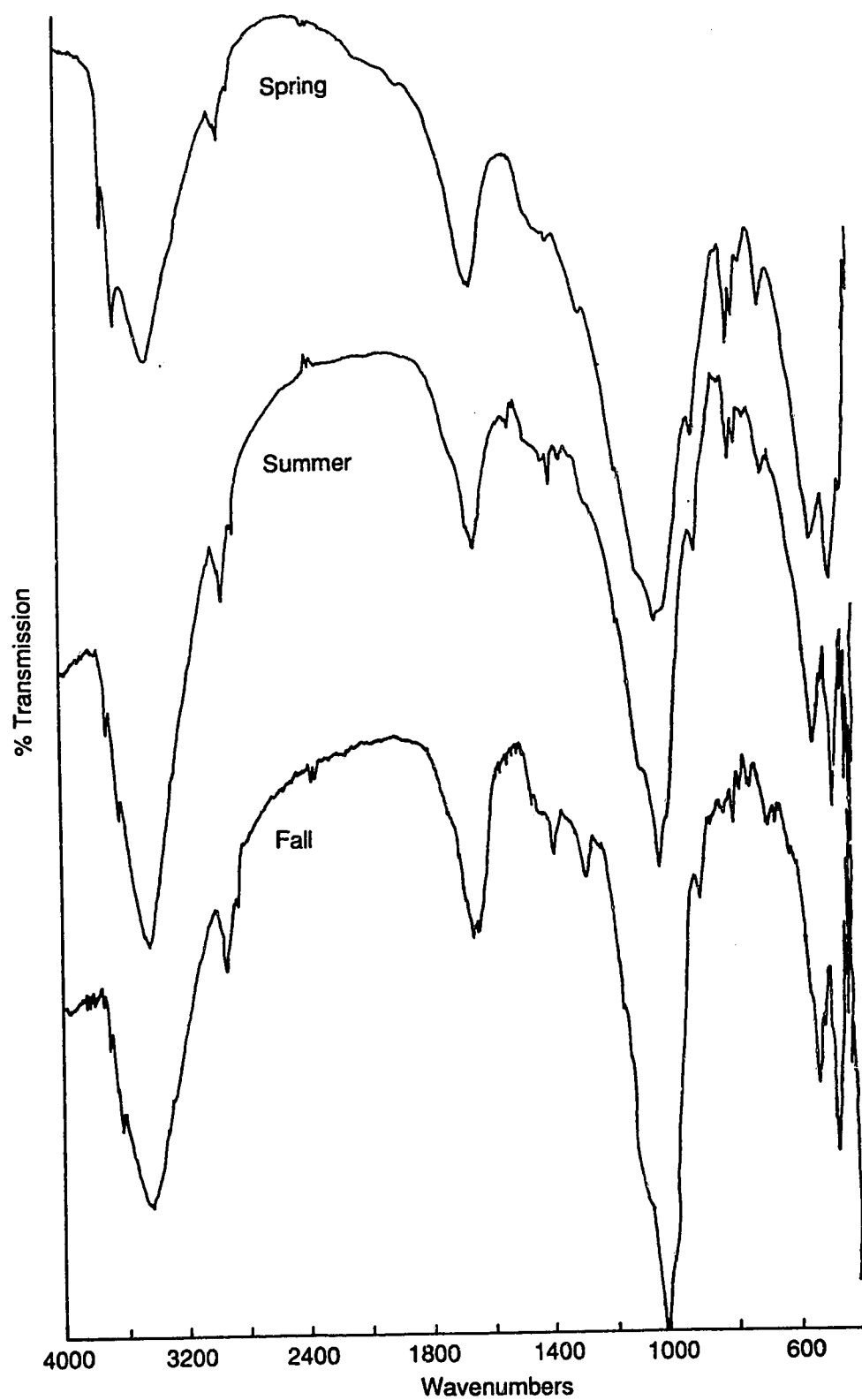


Plate 4.1: Scanning electron micrographs illustrating planar views of cutanic surfaces from the Bt and Ck horizons of an Orthic Grey Luvisol.

- a) Fungal hyphae on the surface of cutanic features from the Bt1 horizon.
- b) Smooth surface of the Bt1 cutans.
- c) Surface of a cutanic feature from the Bt2 horizon. Note the embedded fine silt grains on the surface.
- d) Stomatocysts, or vegetative resting stages, of Chrysophacean or golden brown algae on the surface of a cutan in the lower Bt2 horizon.
- e) Cross-section of cutan surface in upper Ck horizon illustrating the cementing of stomatocysts (see d) to the surface.
- f) Micaceous and kaolinitic clay platelets on the surface of cutans from the upper Ck horizon. Note the incipient 'card-house' stacking, possibly a result of flocculation in the higher ionic strength solutions of the deeper pedon.

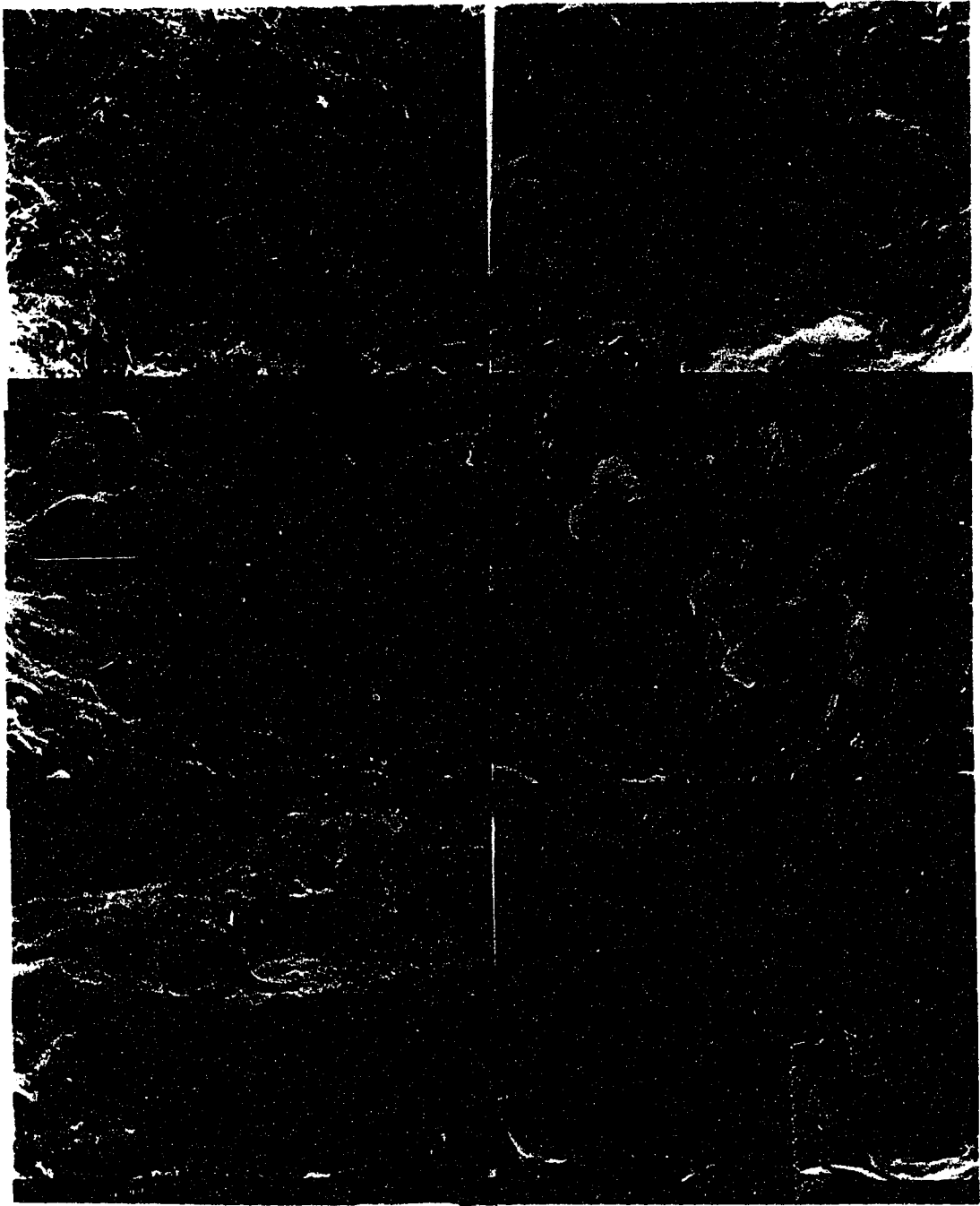


Plate 4.2: Scanning electron micrographs of cross-sections of selected cutanic features observed in the Bt and Ck horizons of an Orthic Grey Luvisol.

- a) Cross-section of randomly oriented clay material forming a cutan in the upper Bt1 horizon. Note the abundant fine silt quartz and feldspar grains comprising the cutanic matrix.
- b) Cross-section of less randomly oriented clay material forming a cutan in the Bt2 horizon. The amount of fine silt sized quartz and feldspar is less abundant at this depth.
- c) Cutanic cross-section from the Bt1 horizon, illustrating the layering of colloidal material around a 10 μm diameter pore. Note the numerous fine silt grains in the cutan groundmass, and the more dispersed arrangement of the clay.
- d) Cutanic cross-section from the BCk horizon illustrating the sequential layering of translocated colloidal material on flocculation in the higher ionic strength solutions of the lower pedon.
- e) Coarse silt quartz grain embedded in the outer layers of a cutanic feature from the lower Bt2 horizon.
- f) Layered clays surrounding the quartz grain depicted in (c).

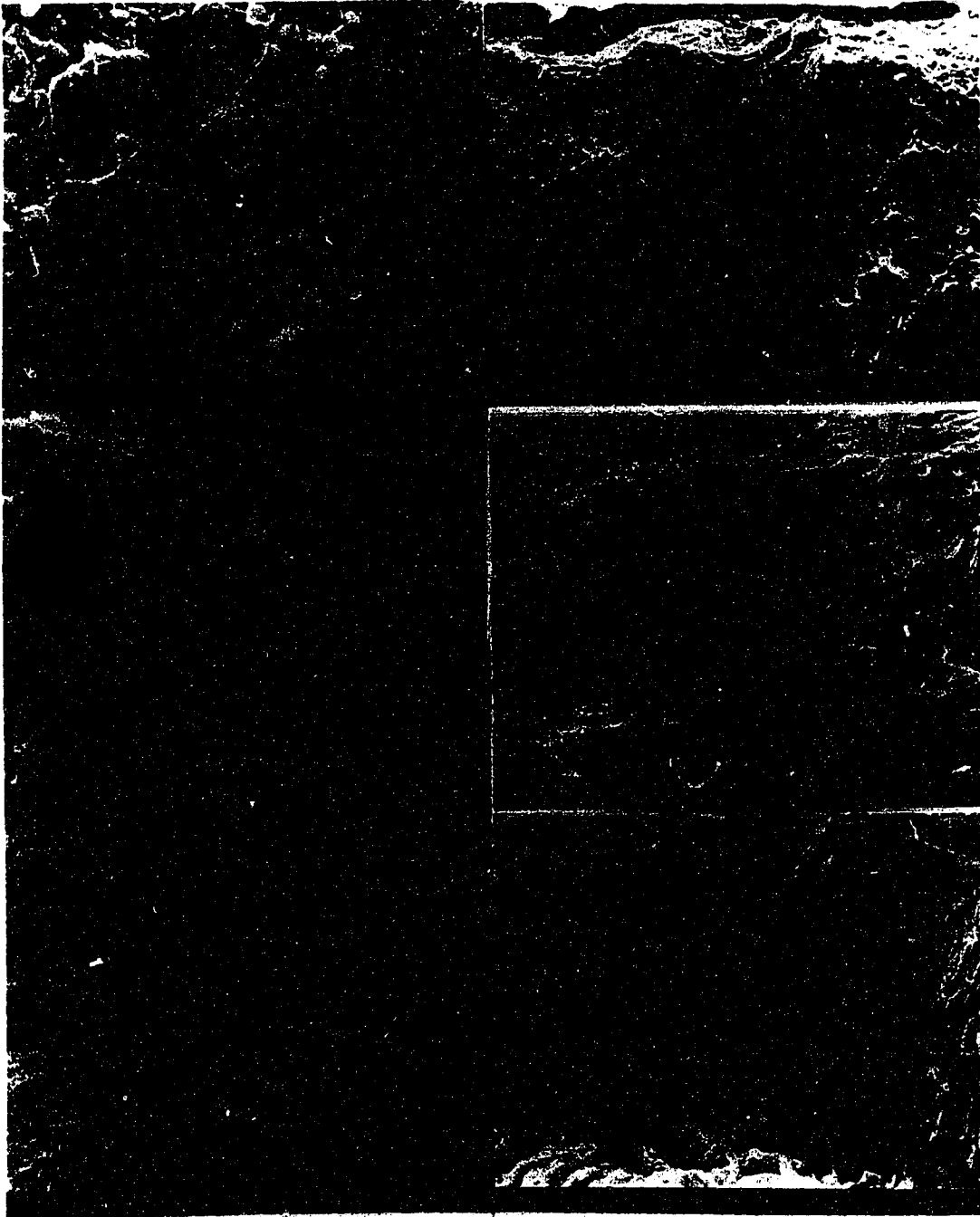
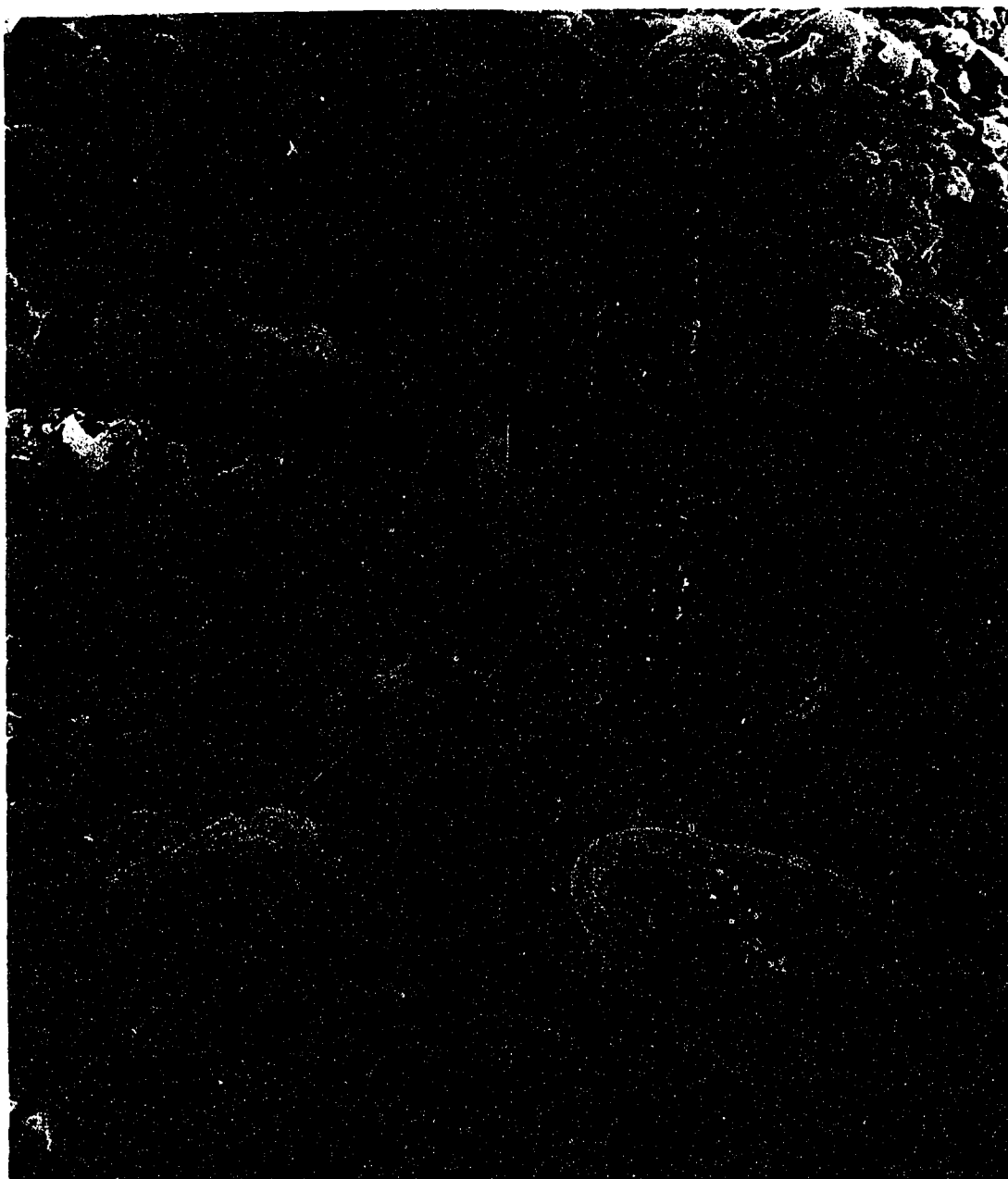


Plate 4.3: Scanning electron micrographs of selected colloidal material collected from a series of gravity lysimeters installed below the Ae and AB horizons of a catenary sequence of Luvisolic soils.

- a) Admixture of micaceous and kaolinite clay particles, with occasional fine quartz grains.
- b) Fine silt sized quartz and feldspar grains in the colloidal clay matrix.
- c) Rectangular phytoliths and mixed silt grains embedded in colloidal matrix.
- d) Small stomatocyst (rounded) and phytolith (rectangular) in coated with micaceous and kaolinite clay particles.
- e) Collared stomatocyst, or vegetative resting stage, of Chrysophacean or golden brown alga, previously described in oligotrophic lake sediments.
- f) A second common form of stomatocyst, or vegetative resting stage, of Chrysophacean or golden brown alga.



5. FERRIHYDRITE AT THE MINERAL-ORGANIC INTERFACE: AN EXAMINATION OF COMPOSITION AND FORM

5.1. INTRODUCTION

A variety of iron oxides can be formed in natural pedologic systems, with the precipitation of ferrihydrite being favoured where levels of Fe^{3+} are made available by the rapid oxidation of Fe^{2+} (Carlson and Schwertmann, 1981). Ferrihydrite is a poorly crystalline, hydrated ferric oxyhydroxide (Chukrov and Gorskov, 1981; Schwertmann and Fisher, 1973; Carlson and Schwertmann, 1981), with documented compositional range for synthetic ferrihydrite between $\text{Fe}_2\text{O}_3 \cdot 3\text{H}_2\text{O}$ and $\text{Fe}_2\text{O}_3 \cdot 2\text{H}_2\text{O}$ (Eggleton and Fitzpatrick, 1988), with the generally accepted formula being $\text{Fe}_5\text{O}_{12}\text{H}_9$.

Ferrihydrite precipitates on aeration of acid spring waters percolating through humiferous soils (Schwertmann and Fischer, 1973), forms in Podzolic (Chukrov et al., 1973; Kassim et al., 1984) and Oxic soils (Bigham et al., 1978), and in acid mine drainage environments (Brady et al., 1986) in association with various bacterial species (Jerris et al., 1989), and from volcanic springs (Childs et al., 1986). Ferrihydrite samples collected from drainage ditches have been described in terms of iron oxide-organic iron association (Schwertmann and Murad, 1988) or isostructural relationship with filamentous bacterial forms when drainage waters have high sulphate content (Wheatley, 1988). Earlier studies indicated the association of 'amorphous' iron oxide (probably ferrihydrite) in association with bog iron ores (Harder, 1919; Crerar et al., 1979) in acidic environments, or as massive concretions in gleysolic soils (Evans et al., 1978).

The observation during routine field surveys of thick (5-25 cm), essentially pure, bands of an iron oxyhydroxide material immediately above a calcareous mineral parent material at the base of a shallow, neutral to slightly alkaline, peat suggested a natural physicochemical

environment not previously described for the formation of poorly crystalline authigenic iron minerals. Descriptions of iron oxyhydroxide reaction products on calcitic surfaces and laboratory analogues have, however, been described (Loeppert et al., 1984, Clarke et al., 1985, Loeppert and Hossner, 1987). Accordingly the objective of this section is to provide a detailed description of the environment of formation, chemistry, morphology and structure of ferrihydrite from a deposit formed at the base of a shallow peat deposit immediately above a calcareous till/glaciofluvial deposit in central Alberta.

5.2. MATERIALS AND METHODS

The study site was located in a depressional area behind a small levee on the valley side of a regional drainage channel in a morainal landscape west of Edmonton, Alberta (Figure 1(a)). Samples were collected in the late fall from a series of shallow peat pedons (Terrestrial Fibrisols) developed under a closed canopy of *Picea banksiana*, air-dried and stored for analysis. At the base of the peat material, immediately above the calcareous mineral solum, was a 10-20 cm highly porous and saturated layer of an apparently pure iron oxy-hydroxide (Figure 5.1(b)).

Undisturbed samples of the iron-rich saturated layer were collected and stored frozen. Samples utilized for micromorphological examination were freeze dried prior to impregnation and production of 7x5 cm thin sections (Brewer and Pawluk, 1975) for petrographic examination. Porosity and shape factors were estimated using an automated Tracor 5000 image analysis system.

A series of shallow bore holes were drilled throughout the deposit in both May and November to enable sampling of the pore water percolating through the iron-rich layer for chemical and isotopic characterization. Water samples were also collected from a maarl encrusted spring and small pond which discharges into the small stream immediately below the sample site for the fall sample. Electrical conductivity, pH and oxidation potential (Light, 1972) were measured immediately on sampling, with the balance of the sample being frozen for subsequent analysis of dissolved ions by ion chromatography and photodiode array equipped inductively coupled plasma-atomic emission spectroscopy (ICP-AES) (Levy et al., 1987; McGeorge, 1987). The speciation of the resultant data was computed using the solution-mineral equilibrium program SOLMNEQ-PC (Kharaka et al., 1988). Analysis of the $^2\text{H}/^1\text{H}$ and $^{18}\text{O}/^{16}\text{O}$

contents of the water was by the methods of Coleman et al (1982) and Epstein and Mayeda (1953) respectively, with data being expressed relative to SMOW (Craig, 1961).

The elemental composition of the iron-rich material was determined by a combination of neutron activation and X-ray fluorescence (Norrish and Hutton, 1969). Total carbon content was determined with a LECO high frequency induction furnace, with carbonate content being determined by the method of Bundy and Bremner, 1972. The loss in weight of samples, pretreated with H_2O_2 to dissolve organic matter, on oven drying at 105 C ($\text{H}_2\text{O}^{(v)}$) was taken to represent the amount of absorbed water, and the loss on ignition at 1000 C ($\text{H}_2\text{O}^{(+)}$) to represent water derived from structural hydroxyls. Surface area was determined by solvation with ethylene glycol monoethyl ether (Carter et al., 1965). Oxalate- and DCB-extractable Fe, Al, and Si were determined by the methods described by Parfitt (1988), with the elemental measurements being completed ICP-AES.

X-ray diffractograms of the bulk material were obtained by step-scan analysis of powder mounts from 3 - 80° 2 θ with a Philips PW1730-PW1710 diffractometer system equipped with a curved crystal monochromator using $\text{CoK}\alpha$ radiation generated at 50 kV and 25 mA both before and after dissolution of the carbonaceous material phases in H_2O_2 , with quartz being used as an internal standard. Intensities of the broad diffraction bands were further examined by use of the Debye-Scherrer camera. Phase changes on heating to 1000 C were examined by both X-ray diffraction analysis and Fourier-Transform infra-red spectroscopy (FT-IR) of 1mg samples pressed in KBr pellets after holding samples at each 100 C rise for 3 hours. Differential thermal analysis (DTA) was completed at a heating rate of 15 C min⁻¹ in both oxygen and nitrogen atmospheres. Thermal gravimetry (TGA) was also completed in both oxygen and nitrogen atmospheres of subsamples both before and after removal of carbonaceous material.

Selected samples of both coarse (> 50 μm) and fine (< 50 μm) material were analysed at 293 K by Mössbauer spectroscopy on a 512-channel Cryophysics microprocessor-based instrument with a constant acceleration drive system and a sawtooth waveform. A $^{57}\text{Co-in-Rh}$ γ -ray source was used and sample sizes were chosen to give about 10 mg Fe cm⁻² or less in the beam. Velocity scales were calibrated with respect to natural iron at 293 K, with the midpoint of the magnetic hyperfine spectrum defining zero velocity. Spectra were deconvoluted, assuming overlapping Lorentzian peak lineshapes, using an iterative nonlinear regression X^2 minimization procedure (Childs et al., 1986).

X-ray photo-electron spectrochemical analyses (XPS) were conducted using a SSX-100

X-ray photoelectron spectrometer. Samples were mounted on copper grids and desiccated prior to insertion into the high vacuum chamber of the spectrometer. A monochromatized Al-K α X-ray exciting beam was used with a spot size of 150 μm^2 . Specimen charging was controlled with a low-energy electron flood gun. All binding energies were referenced to C (1s) at 285.0 eV.

Both air-dried and freeze-dried samples were coated with 20 nm Au and examined by scanning electron microscopy (SEM) on a Cambridge Stereoscan 250 instrument equipped with a Kevex energy dispersive X-ray detector and a Tracor 5000 microanalysis system (EDS). Whole mounts of unfixed material, both before and after sonification treatment, were prepared for transmission microscopy (TEM) by floating Formvar carbon-coated copper grids on small droplets of sediment suspended in deionized water, with excess material being removed from the grids after several seconds with filter paper. For thin sections, specimens were enrobed in 2.0% noble agar before dehydration and embedding in an epoxy resin. Sections (~ 150 nm) were cut with an ultramicrotome and also mounted on Formvar carbon-coated copper grids for microscopic examination. Selected sections were stained with uranyl acetate and lead citrate before TEM examination to enhance the electron contrast of any biological material. Specimens were examined using a Philips EM 400T equipped with an EDAX energy dispersive X-ray detector and a Tracor 5000 microanalysis system (EDS). EDS analysis was conducted using beam spot sizes of ~ 200 nm with 100 sec integration times, and selected area electron diffraction patterns (SAED) were calibrated against evaporated gold as a comparative standard.

5.3. RESULTS AND DISCUSSION

5.3.1. Water chemistry

The chemical composition of the waters percolating through the deposit and those of the permanent spring below the deposit site are listed in Table 5.1. Although temperatures at time of sampling were essentially constant, there was a significant difference in the pH of the interstitial solutions, ranging from 7.1 in the spring samples to 8.2 in the fall. The difference is probably due to recharge and flushing of the waters in the peat by acidic overland flow of snowmelt and rainfall to the midslope depression area during the spring. The ^2H and ^{18}O data of the spring waters support this suggestion (Maule, 1989), being essentially identical to the slightly evaporated waters found in the upper 1 metre of local soils. The differences in contents of both anions and cations in both the interstitial waters and the spring indicate that water sources are different, with the isotopic value ($\delta^{18}\text{O} = 18.41$) being that of shallow groundwater (Maule, 1989).

Table 5.1: Composition of seasonal interstitial percolating waters from the ferrihydrite band and from an adjacent groundwater discharge spring.

	Spring ¹	Fall	Groundwater
	$\mu\text{g ml}^{-1}$		
Ca	192	39	118
Mg	43	25	21
Fe	0.3	0.27	0.25
Mn	0.07	0.11	0.13
Al	0.57	0.59	0.57
Si	8.2	11.0	8.6
SO ₄ ⁻	415.0	262.0	87.0
Cl ⁻	10.8	4.8	14.6
CO ₃ ⁻	0.2	3.0	0.2
HCO ₃ ⁻	326.4	161.7	170.8
NH ₄ ⁺	8.5	1.4	1.3
PO ₄ ⁻	2.0	12.4	12.9
Temperature	2.5	4.5	3.0
pH	7.45	7.95	8.55
E.C. (dS m ⁻¹)	1.689	2.284	3.165
Eh (mV)	313	325	334
$\delta^{18}\text{O}$	-18.18	-17.98	-18.41
$\delta^2\text{H}$	-144.9		

¹ Data are means of 8 boreholes.

The rise in pH for the fall samples is a result of evapotranspiration processes drawing water equilibrated with calcite from the maarl layers immediately below the iron-rich band. Fall pH values of interstitial water in the band, although significantly increased over spring levels, are lower than that of the adjacent spring waters. This increase in fall pH is similar to the magnitude increase documented by Crerar et al (1979) for waters draining bog iron sites in New Jersey, although all their values were below 5.5. All data for Eh and pH plot in the stability field for Fe(OH)₃(am) (Figure 4.2), indicating that amorphous iron hydroxide precipitation is thermodynamically favoured from all waters sampled. The solubility product (K_{sp}) as refined by Fox (1989) for colloidal ferric hydroxide based on extensive literature and experimental values is defined by the following equation:

$$(\text{Fe})^*(\text{OH})^{2.35} = 10^{-31.7}$$

The means and standard deviations of the K_p and OH:Fe compositional ratio were documented as 31.7 ± 0.37 and 2.33 ± 0.07 respectively. The range in values of the ion activity product (pK_p) calculated for the waters percolating through the iron-oxyhydroxide deposit at the peat-mineral interface is 31.87 -32.65, consistent with the relationship in the above equation for colloidal ferric hydroxide (Fox , 1989).

In spite of the above relationships there was not any visible iron oxide precipitation associated with the alkaline spring discharge. Although both spring and iron deposit interstitial waters are supersaturated with respect to calcite, the calcite only precipitated from the spring waters on storage of subsamples in the laboratory. There was, however, carbonate effusion observable throughout the band matrix in the fall, and maarl deposits were forming in the spring-fed pond all year.

5.3.2. Chemical analysis

The elemental composition of the reddish-orange material (Table 5.2) are on an organic carbon free basis and are similar to values published for natural ferrihydrites published in the literature (Schwertman and Fischer, 1973; Henmi et al., 1980; Carlson and Schwertman, 1981; Childs et al., 1986), with only minor differences between the fine and coarse separates. Iron is the major component of both the coarse and fine material, ranging between 42 and 45 % of the total. Silicon (~5 %), Ca (~4 %), Mn (~1 %) and $\text{H}_2\text{O}^{(+)}$ (20 - 22 %) comprise the bulk of the remainder. The $\text{H}_2\text{O}^{(+)}$ values are in the range described for sythetic 2-line ferrihydrite by Eggleton and Fitzpatrick (1988), but are higher than those of natural ferrihydrite samples described from New Zealand (Childs et al., 1986) and Tonga (Childs and Wilson, 1988). The Ca values are much higher than generally recorded (Childs et al., 1986), and result from the inclusion of fine grained calcitic material, which may comprise up to 15% of the total deposit

of a late fall sample, in the sample matrix.

The $\text{Fe}_{(o)}/\text{Fe}_{(d)}$ ratios (Table 5.3) indicate that the material is very poorly crystalline, with essentially all the iron material being dissolved by oxalate. The low proportion of the total Si dissolved by the selective reagents is related directly to the amount of residue, a fine grained clear material which, on X-ray diffraction analysis, proved to be quartz. The low Si value dissolved by either oxalate or DCB further suggests that there is very little incorporation of Si into the structure, in agreement with the data of Carlson and Schwertmann (1981). The organic carbon (O.C.) content was determined as the difference between the total C as determined by induction furnace and the $\text{CO}_3\text{-C}$.

The surface area (EGME) values (Table 5.3) show little difference between the two particle separates.

Table 5.2. Elemental composition¹ of the ferrihydrite material sampled at the peat - mineral interface in late spring.

Element %	Content*		Element ($\mu\text{g gm}^{-1}$)	Content Whole Sample
	Fine	Coarse		
Fe	42.08	44.1	As	54
Mn	1.22	1.51	B	35
Al	<0.03	<0.03	Ba	750
Ca	4.18	3.74	Co	51
K	<0.01	<0.01	Cr	4
P	0.11	0.07	Mo	4
Mg	0.07	0.09	Sr	212
Si	5.34	5.79	U	5
Na	0.12	0.14	Zn	48
$\text{H}_2\text{O}^{(-)}$	16.2	15.6		
$\text{H}_2\text{O}^{(+)}$	22.9	20.1		

¹ Major elements determined by XRF, trace elements by INNA. Data expressed on a C free basis.

Table 5.3: Colour, surface area and some selected chemical values of the fall samples.

Property	Fine	Coarse
Colour		
S.A. ¹	616	560
	%	%
Fe _(o)	40.62	41.34
Al _(o)	0.20	0.23
Si _(o)	1.02	1.24
Fe _(dcb)	42.04	43.97
Al _(dcb)	0.214	0.24
Si _(dcb)	1.14	1.37
Fe _(o) /Fe _(dcb)	0.97	0.94
CaCO ₃	14.48	13.32
O.C.	8.98	7.35
Residue	4.76	4.89
S.A. ¹ (+C)	554	563
S.A. (-C)	626	648

¹ Surface area in m² gm⁻¹

However, removal of organic matter by oxidation with H₂O₂ causes an increase in surface area of ~70 m² gm⁻¹, an effect noted previously by Susser and Schwertmann (1983). A mean particle diameter, assuming a spherical particle and a mean density of 3.42 gm cm⁻³ (Henmi et al., 1980; Childs et al., 1986), of between 2.848-3.133 nm can be calculated. Based on the ferrihydrite formula of Fe₅O₁₂H₉ (Eggleton and Fitzpatrick 1988) both the total compositional (Table 5.2) and the oxalate extraction data (Table 5.3) indicate that the sample contains approximately 78 percent ferrihydrite based on 105 C weight, the balance being primarily organic carbon and calcium carbonate.

5.3.3. Thermal Analysis

The combined TGA-DTA curves for the ferrihydrite sample is illustrated in Figure 5.2. The TGA curves display the weight loss on heating for samples both before (+C) and after (-C) oxidation.

removal (-C) of organic carbon from the samples by oxidation with H_2O_2 , whereas the DTA curve is for an untreated sample run under an O_2 atmosphere. Both TGA curves gave a smooth and continuous weight loss, with the (+C) sample loss being 34.6% and the (-C) 27.8%, the difference of 6.8% being organic carbon. The O.C. value compares favourably with the average of the values in Table 5.3 of 8.2%. The total water loss (-C) compares with that of 19.65% and 25.0% for 6-linea and 2-line synthetic ferrihydrites respectively (Eggleton and Fitzpatrick, 1988), and 22.4% for a synthetic ferrihydrite (Saleh and Jones, 1984). At temperatures below 150 C the samples lost ~15% of the total weight loss, corresponding to the loss of adsorbed water of the endotherm of the DTA pattern. There are no exotherms observed during analyses in either O_2 or N_2 atmospheres which would correspond to phase transitions displayed by the DTA analysis of the material, either before or after organic carbon removal. This lack of exothermic peak, when documented by Carlson and Schwertmann (1981) in an N_2 atmosphere, was attributed to the possible incorporation of Si into the ferrihydrite structure. Based on the selective dissolution data (Table 5.3) the ferrihydrite in the current study has only minor incorporation of Si either in, or absorbed on, the mineral structure.

5.3.4. X-ray diffraction

The X-ray diffractograms (Figure 5.4) collected from powder mounts at 0.01° 2θ increments show that the air-dried material conforms to the diffraction characteristics described for ferrihydrite (Chukrov et al., 1973; Chukrov and Gorskov, 1981; Henmi et al., 1981, Childs et al., 1986; Schwertmann et al., 1982; Schwertmann and Murad, 1988; Lewis and Cardile, 1989). Although there are no sharp, discrete peaks, the broad bands centred at approximately 0.25, 0.22, 0.17, 0.15 nm are characteristic of 6-line ferrihydrite, with no indication of any other crystalline mineral phase being present in the samples. Although removal of adsorbed water by heating to 100 C does not enhance the intensity or resolution of the broad diffraction bands,

further heating to 200 and 600 C does improve the resolution of the weaker 0.17 nm band. Further heating at 100 C increments to 1100 C enabled examination of phase changes, with poorly differentiated hematite peaks being poorly resolved at 600 C, and full resolution not being reached until 900-1000 C. Removal of organic carbon with H_2O_2 did not change the rate of crystallinity change. Although there are reports of formation of maghemite from ferrihydrite on heating to ~ 300 C (Eggleton and Fitzpatrick, 1988), there was no diffraction evidence for neoformation of a maghemite phase from the ferrihydrite, either (+C) or (-C), until samples were heated to 1000 C. The resolution of the (206) line at 0.498nm enabled positive identification of maghemite.

Deconvolution of the 110 diffraction band at 2.5 nm enabled an estimate of the line width at half maximum (WHH_{110}) to be obtained. The value of $4.0^\circ 2\theta$ compared well with that obtained by measurement of the band width on the photographic film obtained with the Debye-Scherrer camera. The value enabled an estimate of the mean crystallite dimension (MCD_{110}) of the scattering domain perpendicular to the diffracting (110) plane by application of the Scherrer formula (Klug and Alexander, 1974). The value of 2.233 ± 0.4 nm compares favourably with the crystallite diameter (~ 30 nm) estimated from surface area data, and contrasts with the smallest particles resolved by SEM examination of approximately 20-50 nm diameter.

5.3.5. Infra-red spectroscopy

The infrared spectrum (Figure 5.5(a)) of the air-dried, but still hydrated, ferrihydrite sample show major absorption bands at 3432, 1625, 1400 and 985 cm^{-1} due to OH stretching, adsorbed and structural molecular water, carboxyl(?), and Fe-O stretching with some Si-O-Fe absorption at the molecule surface of partially polymerized Si (Carlson and Schwertmann, 1981). Removal of adsorbed water by heating subsamples prior to analysis as for the X-ray diffraction analyses confirms the presence of OH bonds within the natural ferrihydrite structure as described by

Russell (1979). The DTA analyses indicate loss of adsorbed water is essentially complete by 200 C, thus indicating that the more strongly defined 3430 and 1630 cm^{-1} infrared absorption bands (Figure 5.5(b)) result from structural OH and H_2O respectively.

The weight loss indicated by TGA (Figure 5.2) corresponds to the loss of structural OH and H_2O as indicated by the relative decrease in absorption in the 3400 and 1650 cm^{-1} regions (Figure 5.5(c)). The appearance of a sharp band at 3621 cm^{-1} (WHH 63 cm^{-1}) following heating to 600 C may be equivalent to that ascribed for free surface OH groups (Russell, 1979). The position of the Fe-O-Si band shifted from 985 to 959 at 300 C, and to 974 at 600 C. At higher temperatures (Figure 5.5(c,d,e)) absorption changed from one band at 1042 cm^{-1} to two bands at 900 C (at 1036 and 1077 cm^{-1} respectively) and four bands (at 1016, 1034, 1085 and 1162 cm^{-1}). There was a concomitant resolution of bands at 906 and 962 cm^{-1} following heating to 900 C, and at 790, 903, 945 and 962 cm^{-1} at 1000 C with the formation of hematite. These latter bands are attributed to Si-O stretching being resolved into a single phase, although no distinct crystalline Si phase is recognisable in the X-ray diffractograms (Figure 5.4(e)). The absorption bands at 790, 945, 962, 1016, 1034, 1085 and 1162 cm^{-1} are characteristic of a mixture of cristabolite and opal (Moenke, 1974; Drees et al., 1989). The separation into a single phase on heating suggests that the Si is not substituted within the ferrihydrite structure but is probably adsorbed on the mineral surface as a gel, a suggestion supported by the presence of small, but distinctive, absorption maxima in the 460 cm^{-1} region.

The structural reorientation was accompanied by the almost complete loss of the OH and H_2O bands in the 3400 and 1600 cm^{-1} regions of the spectra. The resolution of strong absorption bands in the 450 and 530 cm^{-1} region of the spectrum results from the conversion of the ferrihydrite to hematite and maghemite (Vempati et al. 1990b).

5.3.6. Mössbauer and X-ray Photoelectron Spectroscopy

The Mössbauer spectra for the fine and coarse ferrihydrite material illustrated in Figure 5.6(a and b) were collected at 295 K. The spectra are typical of high spin ferric iron in octahedral coordination to O and OH ligands (Bancroft, 1973), and are thus similar to those obtained at 295 K for iron oxyhydroxides when magnetic ordering is not present. The spectra are each fitted by two Lorentzian doublets (Table 5.4) which have the same isomer shifts (I.S. = 0.41), but different quadrupole splittings (Q.S. = 0.61 and 1.00). The I.S. values are higher than generally described for natural (Childs and Johnston, 1980; Henmi et al., 1980; Childs et al., 1986) or synthetic ferrihydrites (Lewis and Cardile, 1989). Such an increase is possibly related to the higher concentration of elements such as Si and Ca in the current samples, or the higher amount of $\text{H}_2\text{O}^{(+)}$.

As photoelectrons are only ejected from atoms within the surface 5 - 10 nm of a sample, with over 80% of the recorded energy being from the outer 0.2 nm (Bancroft et al., 1979), the illustrated XPS spectra (Figure 5.7) indicate that Ca, Mn, and Ti are probably surface adsorbed species on a ferrihydrite core. The Si(2p) peak centered at approximately 103 eV is similar to that of layer silicate minerals, and thus suggests the presence of tetrahedrally coordinated Si within the ferrihydrite structure (Vempati et al., 1990a). The Fe XPS spectra of the ferrihydrite material (Figure 5.7) displays evidence for several components. The main core line is broad (~ 3.5 eV), probably a consequence of sample charging, and asymmetric to the high energy side, with a major core line binding energies at ~ 710 eV (Fe2p1) and 723 eV Fe(2p3). The Fe(2p) spectra are similar to those documented for both $\alpha\text{-FeOOH}$, $\alpha\text{-Fe}_2\text{O}_3$ and $\gamma\text{-Fe}_2\text{O}_3$ (McIntyre and Zetaruk, 1975). The Fe(3p) and Fe(3s) envelopes, at 56eV and 93eV respectively, are also similar to $\alpha\text{-FeOOH}$, $\alpha\text{-Fe}_2\text{O}_3$ and $\gamma\text{-Fe}_2\text{O}_3$.

Table 5.4: Computed Mössbauer parameters at 293 K for the ferrihydrite material sampled from the peat-mineral interface in late spring.

Sample	I.S. ¹	Q.S. (mm sec ⁻¹)	P.W.	A (%)
Fine	0.41 (1)	0.61 (1)	0.34 (1)	51 (2)
	0.41 (1)	1.00 (1)	0.42 (1)	49 (2)
Coarse	0.41 (1)	0.61 (1)	0.34 (1)	48 (1)
	0.41 (1)	1.00 (1)	0.42 (1)	52 (1)

¹I.S. = isomer shift; Q.S. = quadrupole splitting; P.W. = peak width at half height; A = relative area of component; (x) = X is uncertainty in last figure.

These results confirm those from Mössbauer spectroscopy which indicate that all structural iron is Fe³⁺. The O(1s) spectrum (Figure 5.7) on deconvolution shows only a single component. The component is O²⁻ at 526.58eV, a binding energy some 3-4eV lower than found in any of the pure phase oxides and oxyhydroxides listed above (McIntyre and Zetruk, 1975). Further, there is no evidence for structural OH⁻ at, or in the outer few nanometers of the analysed material, from XPS examination. This latter observation is in conflict with structural information obtained by FTIR analyses, and may be a result of sample dehydroxylation from electron beam heating under the high vacuum.

5.3.7. Microscopy

The ferrihydrite deposit from the base of the peat deposit, apparently comprised of essentially amorphous material in hand specimen, displays a diversity of microstructure under both optical and electron-optical examination at magnifications from 5 to 50,000 times. On petrographic examination of thin sections (30 μ m) the ferrihydrite material was found to be reddish-brown in colour under plane light, to exhibit high negative relief ($n=1.52$), to be isotropic and non-pleochroic. The complex structure of the ferrihydrite band has a very porous vughy

microstructure, with estimates of total void area by full section image analysis ranging between 15 and 35%, with a minimum void area recognition of 0.001 cm^2 . Approximately 70 % of the porosity consisted of unrelated vughs less than $5 \times 10^{-3} \text{ cm}^2$ in area, with an aspect ratio of 2.04 ± 0.68 . The ferrihydrite itself, occupying between 80 and 60 % of the band area, falls into two broad area size classes. Of these size classes, approximately 20 % of the section is occupied by coalesced concentric vesicular spheroids from 20-60 μm in diameter. The smaller particles had a diverse structure ranging from tubiform structures formed from coalesced 2-10 μm diameter spheroids to bacterial rod shaped structures coalesced to a hollow hexagonal tube 20-40 μm in diameter. Similar, although somewhat larger, structures have been related to filamentous bacteria in drains from organic soils of near neutral pH (Wheatley, 1988).

The diversity of microstructure under high magnification (5,000 - 50,000 X) examination by SEM is illustrated in Plate 5.1(a-f). The material in Plate 5.1(a), for example, illustrates a mass of fine globular features coalesced together to create a relatively featureless microform, analogous to the hollow sphere structure of Eggleton, 1987. Plate 5.1(b), on the other hand, illustrates a series of large globular features edge-welded together, or linked by very fine sinuous tubiform filamentous and bacterial rod-like structures such as illustrated in Plate 5.1(c), suggesting that bacterial membranes may act as ferrihydrite nucleation sites (Ferris et al., 1989). The 25-50 nm diameter tubiform filaments (Plate 5.1(c)) commonly appear to intertwine about a central core to form a rope-like structure with a hollow core when examined in cross-section. The dichotomously branching random open mesh of hyphae-like filaments (Plate 5.1(d)), about 2-300 nm in external diameter with a 50 nm central pore, are comprised of welded globular forms between 20-50 nm in diameter (Plate 5.1(e)). The 4.0 μm diameter fungal hypha displayed for contrast in Plate 5.1(f) has a series of both microtubular and globular forms on the surface. These surface features are about 20 nm and 75 nm in diameter

respectively. Many of the forms are analagous in morphology to those described for calcified rods and filaments in calcretes (Philips et al., 1987; Philips and Self, 1987). Some of the rod-like forms (Plate 5.1(c)) suggest that bacterial cells may be serving as nucleation sites for the formation of the authigenic mineral (Ferris et al., 1986, 1987, 1989; Thompson et al., 1990; Thompson and Ferris, 1990).

Energy dispersive analyses of the microstructures observed by scanning electron microscopy (Plate 5.1(a-f)) indicate that the more tubular form of the ferrihydrite contains slightly more Si than the congealed globular form. The tubules also contain minor amounts of Al. The particle size is, however, too small to enable separation for detailed X-ray analysis to discern whether there are any atomic-level structural differences (Carlson and Schwertmann, 1981) between the morphological forms. The Ca present in the analytical spectra is assumed to be associated with the calcite microcrystals described below.

Examination by SEM of material retained on 0.2 μm filters from both spring and fall samples indicated a variety of microcrystalline materials, some of which appeared to be encrustations coating various bacterial forms (Plates 5.2, 5.4). The presence of calcite microcrystals (Plate 5.2(a-f)) within the colloidal material suspended in the interstitial waters support the prediction from the speciation modelling which indicated the solutions to be supersaturated with respect to calcite. The acicular form of the calcite crystals in Plate 5.2(a), when compared to the uncoated filamentous bacteria (Plate 5.2(b)), indicate a genetic relationship which suggests that the bacterial membrane provides a nucleation site for calcite precipitation from the percolating solutions. The accumulation of the acicular calcite into the incipient alveolar texture (Philips and Self, 1987) illustrated in Plate 5.2(b) is bounding a channel form. The common anastomizing form of the calcite is arrowed (Plate 5.2(c)), with the larger crystals displaying a serrated surface (Plate 5.2(d)) which commonly appears to serve as a nucleating

point for ferrihydrite precipitation. The coating of ferrihydrite (Plates 5.2(b-c) arrowed), based on EDS analysis, illustrates a chemical precipitative coating, possibly a product of a simple acid-base reaction between the dissolved Fe species and the calcite surface (Loeppert and Hosener, 1984; Clarke et al., 1985). The clusters (Plate 5.2(e-f)) of coated coccoid and rod-like bacterial morphological forms filtered from the interstitial waters are also coated and cemented together by a calcite precipitate with very small nodules of iron and manganese rich material on the surface.

In contrast the bacterial material illustrated in Plate 5.3 (a-f) all have ferrihydrite rich features precipitated on their surfaces. Plate 5.3 (a) illustrates a bacterium with a mucilagenous coating high in Fe, with much lesser concentration of Si and a trace of Al. The colony (Plate 5.3(b)), very similar in form to that in Plate 5.2(f), has a chemical composition essentially identical to that of the rod in Plate 5.3(a). In contrast the rod adhering to a calcite fibre (Plate 5.3(c)) is coated with a test enriched in both Fe and Mn, whilst that in Plate 5.3(d) has a coating of almost pure manganese oxide. The doughnut arrangement (Plate 5.3(e), possibly formed from coated coccoid bacteria (Plate 5.3(f)), is essentially pure ferrihydrite in composition with some interlaced calcite fibres.

The micrographs of the hematite and maghemite formed by heating the ferrihydrite at 1000 C for 5 hours in Plate 5.4(a-d) show a similar diversity of ultra-structural forms suggesting that the atomic-scale rearrangement and dehydration from the precursor ferrihydrite crystals to the more ordered crystal form of hematite is not necessarily accompanied by a structural or morphological rearrangement. The energy dispersive analyses of the individual structural features are essentially identical to those depicted in Figure 5.1(a-b) for the freeze-dried ferrihydrite samples. Plates 5.4(a) and 5.4(b) illustrate features essentially similar to those of the parent ferrihydrite, with well-defined 10-50 nm globules annealing to form either platelike

(5.4(a)) or tubiform (5.4(b)) microforms. The feature in Plate 5.4(c) is a cross-section of a 1 μm diameter tube formed from a series of 5-20 nm spherical units with a central 50-60 nm pore. This feature has both Si and minor amounts of Al associated in the EDS spectra with the dominant Fe, analogous to the tubiform ferrihydrite chemistry described above. Plate 5.4(d) depicts an open mesh-like structure of fine tubiform fibres which appear to possibly have formed from mineral-sheathed rod or coccoid bacterial precursors (Plate 5.4(e)). In contrast the hematite of Plate 5.4(f) appears to have formed from a more amorphous mucilage or gel-like precursor.

When examined by TEM, both samples grown in the laboratory at the air/water interface of solutions samples collected from within the ferrihydrite band in the field and from dried, impregnated band material, show a diversity of features. Some of the features are typical of highly aggregated ferrihydrites (Plate 5.5(a), 5.5(b)) and others are similar to those described for a fibrous microcrystalline goethite (Plate 5.5(c), 5.5(d)) (Nakai and Yoshinaga, 1980; Fordham et al. 1984). The coccoid form in Plate 5.5(c) is similar to that illustrated by Ferris et al (1989) as a nucleation site for ferrihydrite formation. Energy dispersive microanalysis (Figure 5.6(c-d)) of all observable microstructural forms of ferrihydrite revealed small differences in chemical composition as determined by a standardless analysis involving ZAF corrections, being composed primarily of Fe (80-90%), with lesser amounts of Si (10.0-11.0%) and Mn (0.2-2.5%), with the acicular crystals generally being higher in Si and Mn than the more aggregated forms, supporting the observations of the bacterial sheaths described above. There were also minor amounts of S (<3.0%) and Ca was always present as an adsorbed ion. The acicular crystals (Plate 5.5(e-f)) are similar in both form and size to those described for goethitic precursors formed at pH 10 in aged iron oxide gels (MacKenzie and Meldau, 1959).

The electron diffraction pattern (Plate 5.6(a)) for a ferrihydrite aggregate contrasts with

that of the electron dense material on the calcite fibre (Plate 5.6(b)). The diffuse ferrihydrite diffraction bands are superimposed on the diffraction lattice of the calcite. The ferrihydrite appears as to either be precipitating as an amorphous mucilagenous coating on the acicular calcite (Plate 5.6(c), or acting as a cementing material welding and dissolving the calcite (Plate 5.6(d)).

5.4. CONCLUSION

Chemical analyses of interstitial water, collected during both spring and fall, percolating through the 2-15 cm thick iron rich band found at depths of between 60 and 100 cm of the Terric Fibrisol sampled in this study indicate that the microenvironment is oxidising, with Eh/pH conditions being in the stability field for $\text{Fe}(\text{OH})_3(\text{s})$. Further, the calculated ion activity products indicate supersaturation with respect to amorphous $\text{Fe}(\text{OH})_3(\text{s})$ for the interstitial waters, but not for adjacent spring waters. Thus the interstitial solutions of the band probably result from a combination of overland and interflow waters flowing from the mineral soils upslope. These iron-charged solutions migrate through the acid peaty overburden to the relatively impermeable calcite-rich mineral boundary layer. The rapid pH increase at this layer causes precipitation of the dissolved iron as an oxy-hydroxide.

The chemical composition of the band was found to be dominated by Fe (43%), with lesser amounts of Ca (4%), Si (5%), H_2O (21%) and several trace elements (As, B, Ba, Co, Cr, Mo, Sr, U and Zn). X-ray diffraction analyses indicated the material to be 6-line ferrihydrite with a room temperature Mössbauer spectrum similar to that described for other natural samples. On heating, the combined results from XRD, DTA, TGA and FT-IR indicate an initial rapid water loss below 150 C, with a slow water and structural hydroxyl loss to 1000 C. At 1000 C XRD and FT-IR analyses indicate the ferrihydrite undergoes a phase change to form a mixture of hematite, maghemite, with the adsorbed silica forming a mixture of cristabolite and opal-CT.

The ferrihydrite deposit displays a diversity of microstructure under both optical and electron-optical examination at magnifications from 5 to 50,000 times. Petrographic examination of thin sections (30 μm) of the reddish-brown ferrihydrite material indicated an high negative relief ($n = 1.52$), isotropic and non-pleochroic mineral. The ferrihydrite band had a very porous vuggy microstructure, with estimates of total void area being between 15 and 35 %. Examination by SEM, with associated EDS microanalysis, demonstrated that the ferrihydrite was composed of a complex series of microstructures, including hollow microtubules between 200 and 300 nm in diameter, coalesced bacterial rod-like structures and small globular features. There were minor compositional differences between the microstructures, with the tubular form containing more Si and Al. Examination of colloidal material from the interstitial water indicated presence of a range of bacterial forms which appear to form nucleation sites for mineral precipitation, both of calcite and ferrihydrite. Manganese rich bacterial casings appear to be distinct from the Fe-rich casings, suggestive of a microbial species-mineral interrelationship.

Both impregnated and whole mounts, when examined by STEM and EDS, confirm the observations of the optical and scanning microscopical examination. Although some ferrihydrite encapsulated bacterial coccoid forms were observed in the impregnated and stained sections, there were no obvious encapsulated filamentous bacterial forms. The fresh whole mount material, at high magnifications, indicated that the abundant acicular calcite crystals were functioning as nucleation sites for a chemical precipitate of an iron rich material with the electron diffraction pattern of ferrihydrite.

5.6. BIBLIOGRAPHY

- Bancroft, G.M. (1973). *Mössbauer Spectroscopy: An Introduction for Inorganic Chemists and Geochemists*. McGraw-Hill, London.
- Bancroft, G.M., Brown, J.R., and Fyfe, W.A. (1979). Advances in, and applications of, X-ray photoelectron spectroscopy (ESCA) in mineralogy and geochemistry. *Chem. Geol.* 25: 227-243.
- Beveridge T.J. and Fyfe, W.S. (1985). Metal fixation by bacterial cell walls. *Can. J. Earth Sci.* 22: 1893-1898.
- Bigham, J.M., Golden, D.C., Bowen, L.H., Buol, S.W. and Weed, S.B. (1978). Iron oxide mineralogy of well drained Ultisols and Oxisols: 1. Characterization of iron oxides in soil clays by Mössbauer spectroscopy, X-ray diffractometry and selected chemical techniques. *Soil Sci. Soc. Am. J.* 42: 816-825.
- Brewer, R. and Pawluk, S. (1975). Investigations of some soils developed in hummocks of the Canadian Sub-Arctic and Southern Arctic regions. *Can. J. Soil Sci.* 55: 301-309.
- Bundy, L.G. and Bremner, J.M. (1972). A simple titrimetric method for the determination of inorganic carbon in soils. *Soil Sci. Soc. Am. Proc* 36:273-275.
- Carlson, L. and Schwertman, U. (1981). Natural ferrihydrites in surface deposits from Finland and their association with silica. *Geochim. Cosmochim. Acta* 45: 421-429.
- Carter, D.L., M.D. Heilman and C.L. Gonzales 1965. Ethylene glycol monoethyl ether for determining surface area of silicate minerals. *Soil Sci.* 100: 356-360.
- Childs, C.W. and Johnston, J.H. (1980). Mössbauer spectra of proto-ferrihydrite at 77 K and 295 K, and a reappraisal of the possible presence of akaganeite in New Zealand soils. *Aust. J. Soil Res.* 18: 245-250.
- Childs, C.W. and Wilson, A.D. (1983). Iron oxide minerals in soils of the Ha'apai group, Kingdom of Tonga. *Aust. J. Soil Res.* 21: 489-503.

- Childs, C.W., Wells, N. and Downes, C.J. (1986). Kokowai Springs, Mount Egmont, New Zealand: chemistry and mineralogy of the ochre (ferrihydrite) deposit and analysis of the waters. *J. Royal Soc. N.Z.* 16: 85-99.
- Chukhrov, F.V. and Gorshkov, A.I. (1981). Iron and manganese oxide minerals in soils. *Trans. Royal Soc. Edinburgh: Earth Sci.* 72: 195-200.
- Chukhrov, F.V., Zvyagin, B.B., Ermilova, L.P. and Gorskhov, A.I. (1973). New data on iron oxides in the weathering zona. In: *Proc. Int. Clay Conf., Madrid, 1970*. J.M. Serratosa, ed., Div. de Ciencias, C.S.I.C., Madrid, 333-341.
- Clarke, E.T., Loeppert, R.H. and Ehrman, J.M. (1985). Crystallization of iron oxides on static surfaces in static systems. *Clays Clay Min.* 33: 152-158.
- Coleman, M.L., Shepard, T.J., Durham, J.J., Rouse, J.E. and Moore, G.R. (1982). Reduction of water with zinc for hydrogen isotope analysis. *Anal. Chem.* 54: 995-998.
- Craig, H. (1961). Standard for reporting the concentration of deuterium and ^{18}O in natural waters. *Science* 133: 1702-1703.
- Crerar, D.A., Knox, G.W. and Means, J.L. (1979). Biogeochemistry of bog iron in the New Jersey Pine Barrens. *Chem. Geol.* 24: 111-135.
- Drees, L.R., Wilding, L.P., Smeck, N.E. and Senkayi, A.L. (1989). Silica in soils: quartz and disordered silica polymorphs. In: *Dixon, J.B. and Weed, S.B. (ed). Minerals in soils environments*, 2nd edition. Soil Sci. Soc. Am., Madison, Wisconsin.
- Eggleton, R.A. (1987). Noncrystalline Fe-Si-Al-Oxyhydroxides. *Clays Clay Min.* 35: 29-37.
- Eggleton, R.A. and Fitzpatrick, R.W. (1988). New data and a revised structural model for ferrihydrite. *Clays Clay Min.* 36: 111-124.
- Epstein, S. and Mayeda, T.K. (1953). Variations of ^{18}O content of natural waters. *Geochim. Cosmochim. Acta* 4: 213.
- Evans, L.J., Rowsell, J.G. and Aspinall, J.D. (1978). Massive iron formations in some Gleysolic soils of southwestern Ontario. *Can. J. Soil Sci.* 58: 391-395.

- Ferris, F.G., Beveridge, T.J. and Fyfe, W.E. (1986). Iron-silica crystallite nucleation by bacteria in a geothermal sediment. *Nature (London)* 320: 609-611.
- Ferris, F.G., Fyfe, W.E. and Beveridge, T.J. (1987). Bacteria as nucleation sites for authigenic minerals in a metal contaminated lake sediment. *Chem. Geol.* 63: 225-232.
- Ferris, F.G., Tazaki, K. and Fyfe, W.S. (1989). Iron oxides in acid mine drainage environments and their association with bacteria. *Chem. Geol.* 74: 321-330.
- Fordham, A.W., Merry, R.H. and Norrish, K. (1984). Occurrence of microcrystalline goethite in an unusual fibrous form. *Geoderma* 34: 135-148.
- Fox, L.E. (1989). Solubility of colloidal ferric hydroxide. *Nature* 333: 442-443.
- Henmi, T., Wells, N., Childs, C.W. and Parfitt, R.L. (1980). Poorly-ordered iron-rich precipitates from springs and streams on andesitic volcanoes. *Geochim. Cosmochim. Acta* 44: 365-372.
- Kharaka, Y.K., Gunter, W.D., Aggarwal, P.K., Perkins, E.H. and DeBraal, J.D. (1988) SOLMINEQ-88: a computer program for geochemical modelling of rock-water interactions. U.S. Geol. Surv. Water-Resources Investigations Report 88-4227.
- Levy, G.M., Quaglia, A., Lazure, R.E. and McGeorge, S.W. (1987). A photodiode array based spectrometer system for inductively coupled atomic emission spectroscopy. *Spectrochim. Acta* 42B: 341-351.
- Lewis, D.G. and Cardile, C.M. (1989). Hydrolysis of Fe^{III} solution to hydrous oxides. *Aust. J. Soil Res.* 27: 103-115.
- Light, T.S. (1972). Standard solution for redox potential measurements. *Anal. Chem.* 44: 1038-1039.
- Loeppert, R.H. and Hossner, L.R. (1984). Reactions of Fe(II) and Fe(III) with calcite. *Clays Clay Min.* 32: 213-222.
- Loeppert, R.H. and Hossner, L.R. (1987). Influence of pH, CO_2 and O_2 on reaction of Fe(II) and Fe(III) with calcite. *Clays Clay Min.*
- MacKenzie, R.C. and Meldau, R. (1959). The aging of sesquioxide gels. I. Iron oxide gels. *Min. Mag.* 32: 153-165.

- McIntyre, N.S. and Zetaruk, D.G. (1975). X-ray photoelectron spectroscopic studies of iron oxides. *Anal. Chem.* 49: 1521-1529.
- Maule, C.P. (1989). Snowmelt infiltration and seasonal groundwater interactions with the unsaturated zone. Unpubl. Ph.D. thesis, University of Alberta. Edmonton, Alberta.
- Moenke, H.H.W. (1974). Silica, the three dimensional silicates, borosilicates, and beryllium silicates. In: Farmer, V.C. (ed). *The Infrared Spectra of Minerals. Mongraph 4*, Mineralogical Society, London.
- Norrish, K. and Hutton, J.T. (1969). An accurate spectroscopic method for the analysis of a wide range of geological samples. *Geochim. Cosmochim. Acta* 33: 431-453.
- Philips, S.E., Milnes, A.R. and Foster, R.C. (1987). Calcified filaments: an example of biological influences in the formation of calcrete in South Australia. *Aust. J. Soil Res.* 25: 405-428.
- Philips, S.E. and Self, P.G. (1987). Morphology, crystallography and origin of needle-fibre calcite in Quaternary pedogenic calcretes of South Australia. *Aust. J. Soil Res.* 25: 429-444.
- Saleh, A.M. and Jones, A.A. (1984). The crystallinity and surface characteristics of synthetic ferrihydrite and its relationship to kaolinite surfaces. *Clay Min.* 19: 745-755.
- Schwertmann, U. and Fischer, W.R. (1973). Natural "amorphous" ferric hydroxide. *Geoderma* 10: 237-247.
- Schwertmann, U., Schulze, D.G. and Murad, E. (1982). Identification of ferrihydrite in soils by dissolution kinetics, differential X-ray diffraction, and Mössbauer spectroscopy. *Soil Sci. Soc. Am. J.* 46: 869-875.
- Schwertmann, U. and Murad, E. (1988). The nature of an iron oxide-organic iron association in a peaty environment. *Clay Min.* 23: 291-299.
- Susser, P. and Schwertmann, U. (1983). Iron oxide mineralogy of ochreous deposits in drain pipes and ditches. *Z. Kulturtechnik Flurbereneingung* 24: 386-395.
- Thompson, J.B., Ferris, F.G. and Smith, D.A. (1990). Geomicrobiology and sedimentology of the mixolimnion and chemocline in Fayetteville Green Lake, New York. *Palaios* 5: 52-75.

- Thompson, J.B. and Ferris, F.G. (1990). Cyanobacterial precipitation of gypsum, calcite, and magnesite from natural alkaline lake water. *Geology* (in press).
- Vempati, R.K., Loeppert, R.H., Dufner, D.C. and Cocke, D.L. (1990a). X-ray photoelectron spectroscopy as a tool to differentiate silicon-bonding state in amorphous iron oxides. *Soil Sci. Soc. Am. J.* 54: 695-698.
- Vempati, R.K., Loeppert, R.H., Sittertz-Bhatkar, H. and Burghardt, R.C. (1990b). Infrared vibrations of hematite formed from aqueous- and dry-thermal incubation of Si-containing ferrihydrite. *Clays and Clay Min.* 38: 294-298.
- Wheatley, R.E. (1988). Ochre deposits and associated bacteria in some field drains in Scotland. *J. Soil Sci.* 39: 253-264.

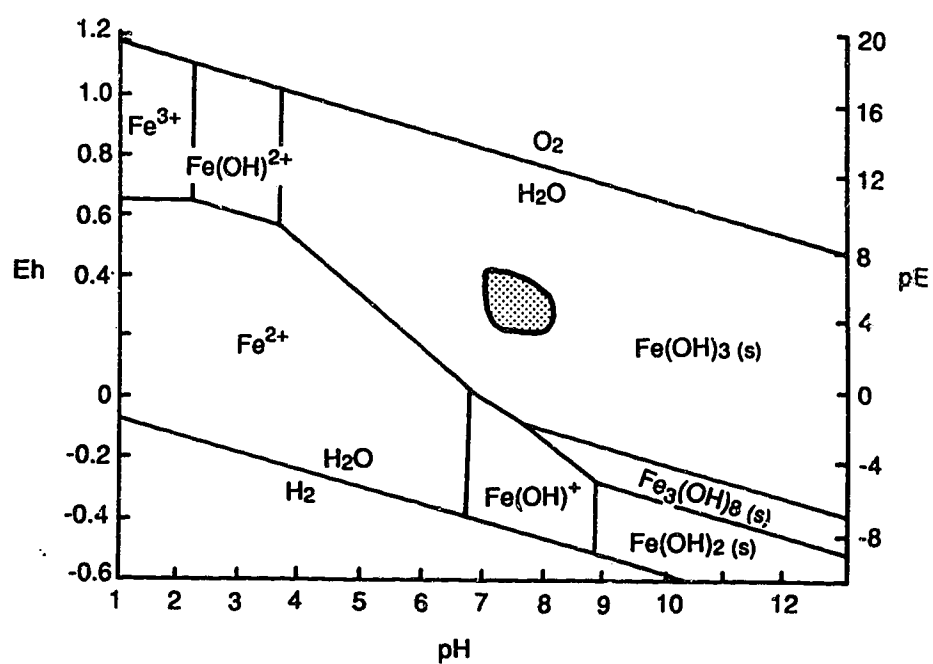


Figure 5.1. Eh-pH diagram displaying the measured parameters for the site waters displayed on an Eh-pH diagram of selected mineral phases for the system Fe_2O_3 - SiO_2 - H_2O .

Figure 5.1: Differential thermal analysis and thermogravimetric analysis patterns for the ferrihydrite samples, both before and after treatment with H_2O_2 to oxidize organic carbon.

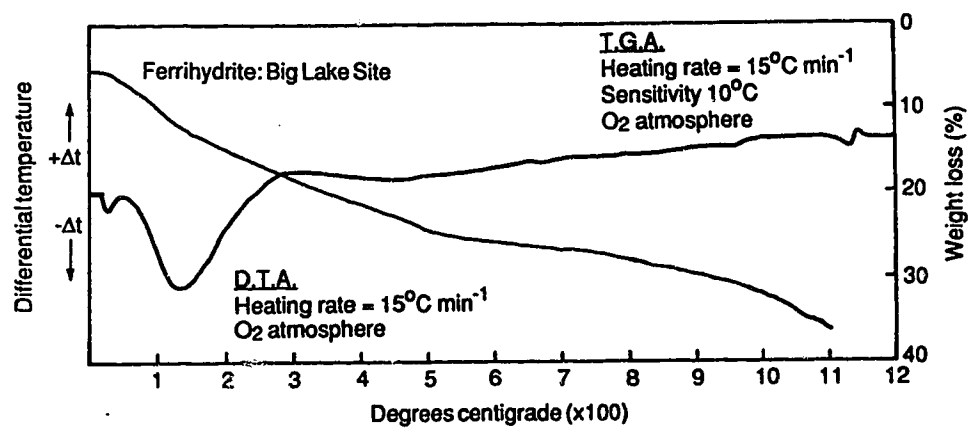


Figure 5.3: X-ray diffractograms obtained by step-scan analysis of powder mounts using CoK α radiation of ferrihydrite samples without dissolution of the carbonaceous material phases in H₂O₂, heated to selected temperatures between 25 C and 1000 C: a) 25 C; b) 200 C ; c) 400 C; 600 C; d) 800 C; e) 1000 C. Samples were held at each temperature for 3 hours prior to analysis analysis at 0% R.H.

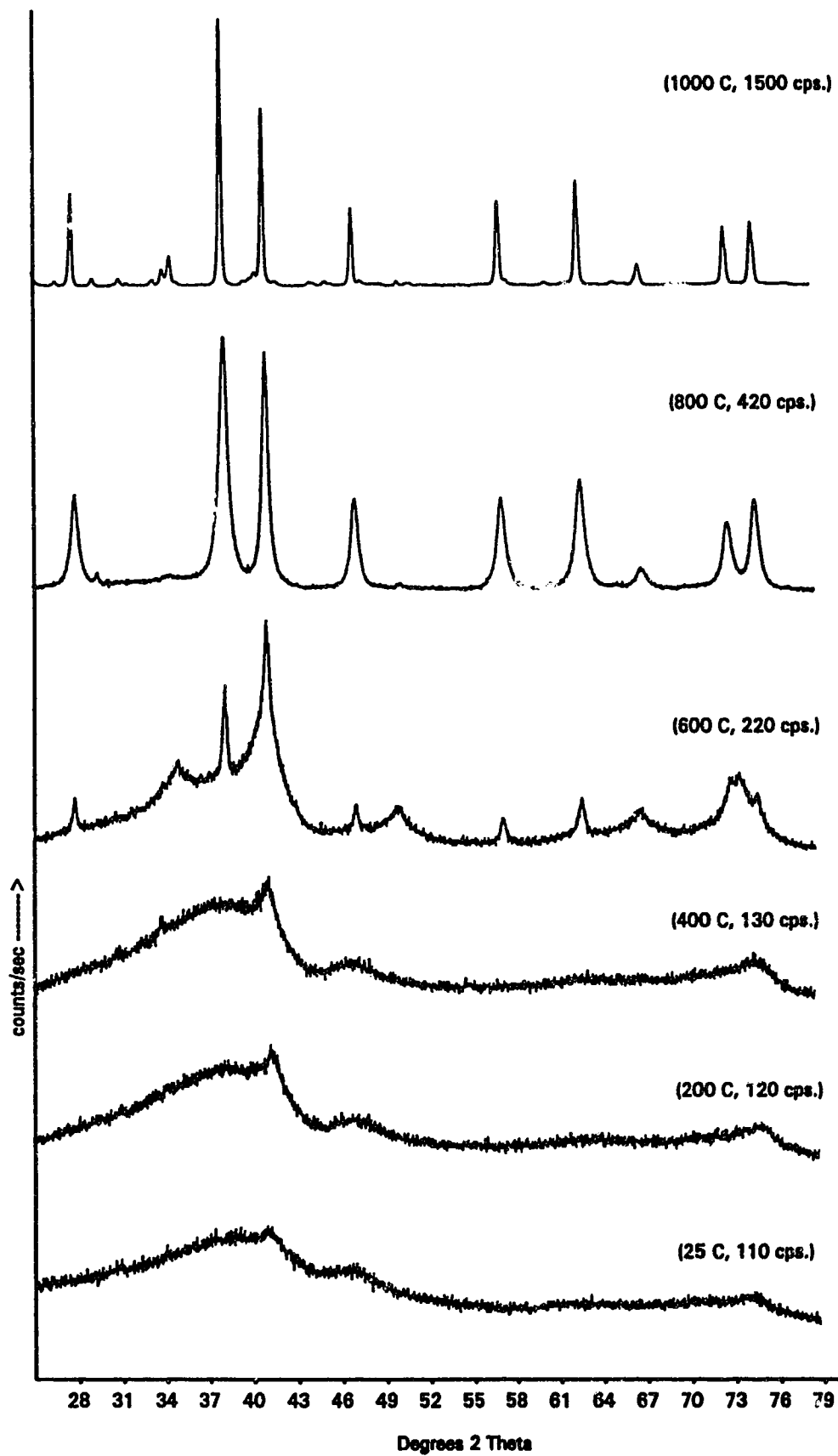


Figure 5.4. Fourier transform infra-red spectra of ferrihydrite samples heated to selected temperatures between 25 C and 1000 C: a) 25 C; b) 200 C ; c) 600 C; d) 800 C; e) 900 C; f) 1000 C. Samples were held at each temperature for 3 hours prior to analysis.

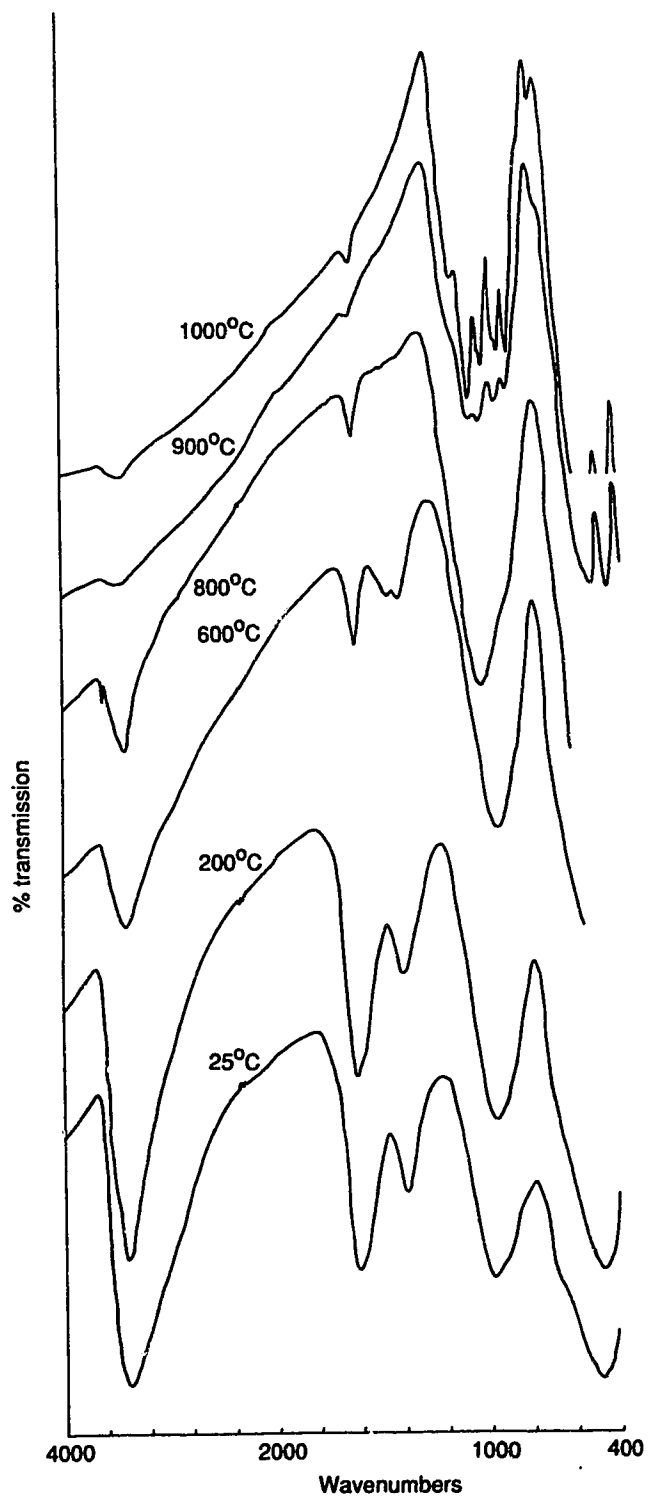


Figure 5.5. Room temperature Mössbauer spectra of ferrihydrite samples obtained without dissolution of the carbonaceous material phases in H₂O₂

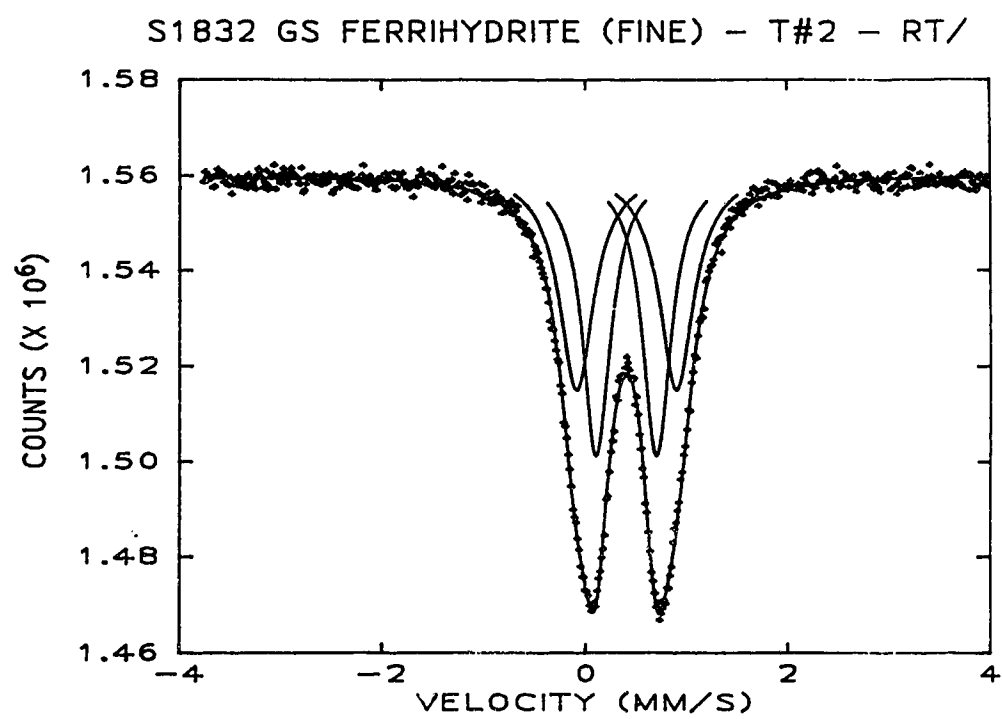


Figure 5.6. X-ray photoelectron spectra of ferrihydrite samples obtained following dissolution of the carbonaceous material phases in H_2O_2 .

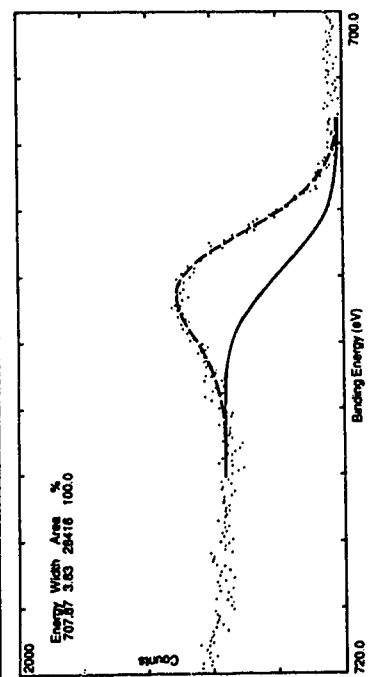
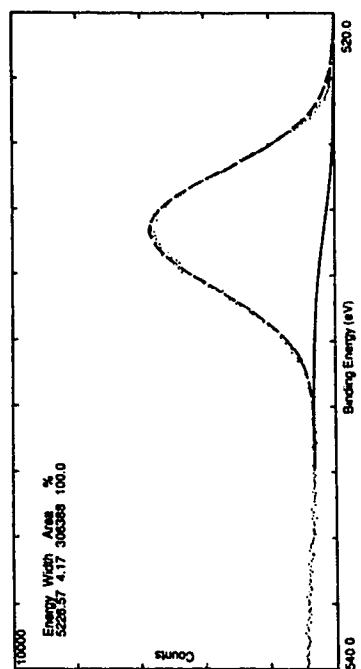
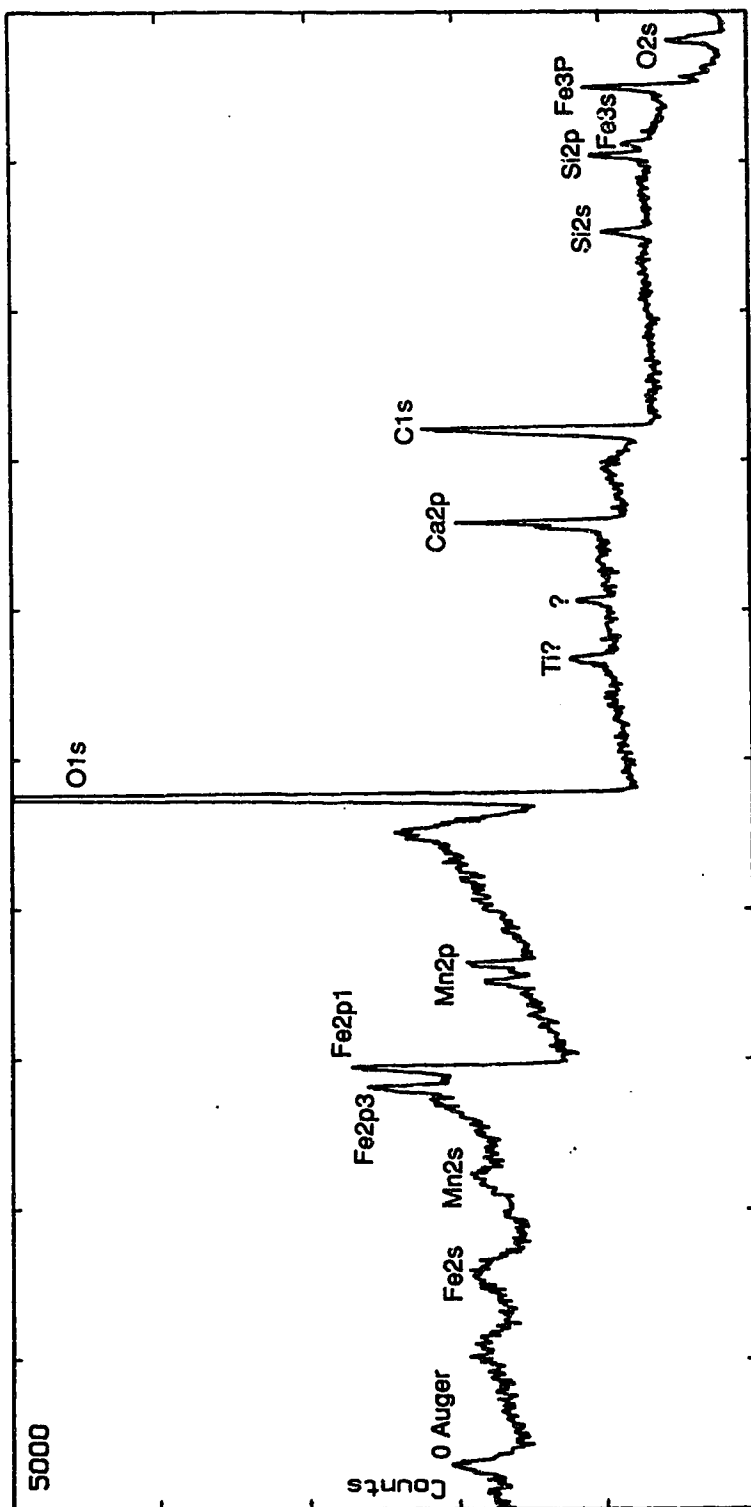


Plate 5.1. Scanning electrons micrographs of ferrihydrite microstructures within samples from the band sampled from the Terric Fibrisol pedon.

- a) Welded fine globular ferrihydrite crystallites forming a featureless hollow porous groundmass.
- b) Globular features edge welded together.
- c) Sinuous tubiform filamentous ferrihydrite intertwined to form a rope-like form.
- d) Diachotomously branching open mesh structure of 2-300 nm diameter hyphae-like filaments with hollow core.
- e) Hollow core (50 nm diameter) of ferrihydrite form illustrated in d)
- f) Fungal hyphae with both filamentous and globular hyphal forms on surface.

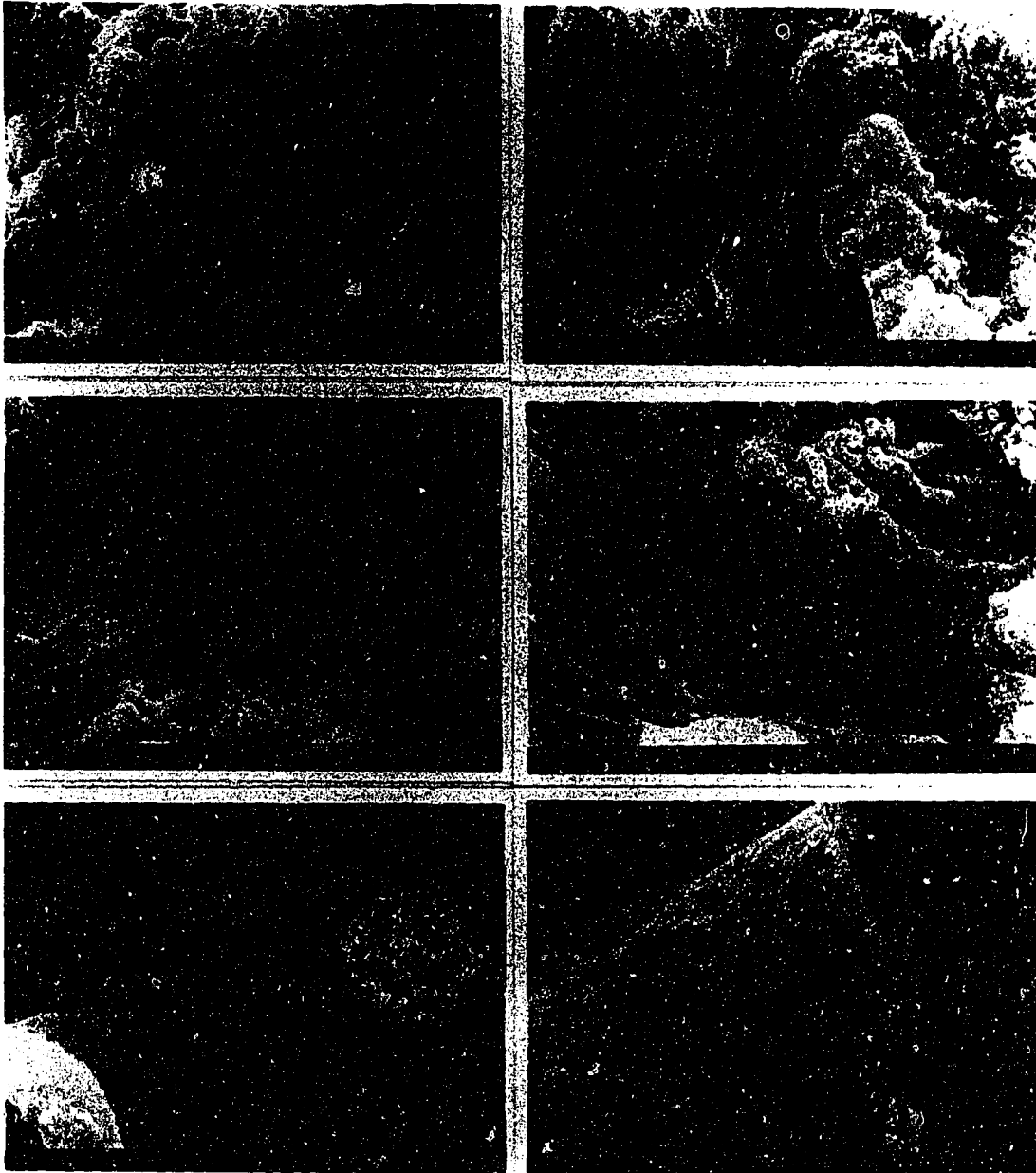


Plate 5.2. Scanning electrons micrographs of material retained on 0.2 μm filters from both spring and fall samples of interstitial waters from within the ferrihydrite band of a Terric Fibrisol pedon.

- a) Acicular calcite crystals.
- b) Uncoated bacterial form analogous to calcite crystals in a).
- c) Accumulation of acicular calcite to form an incipient aveolar texture.
- d) Serrated form of calcite crystal forming a nucleating site for ferrihydrite globules.
- e) Ferrihydrite coated coccoid form.
- f) Ferrihydrite coated rod form. This is higher in Mn than e).

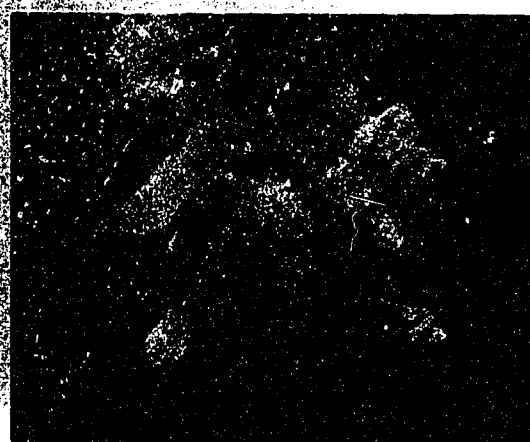
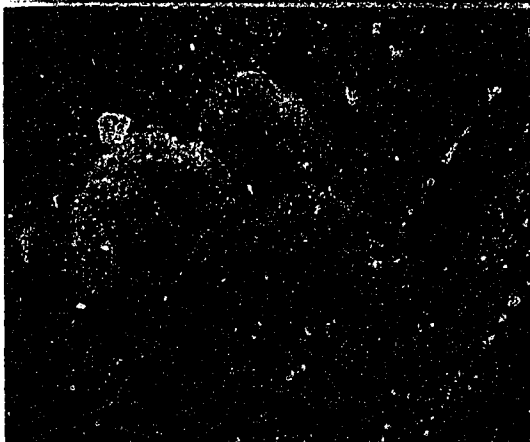
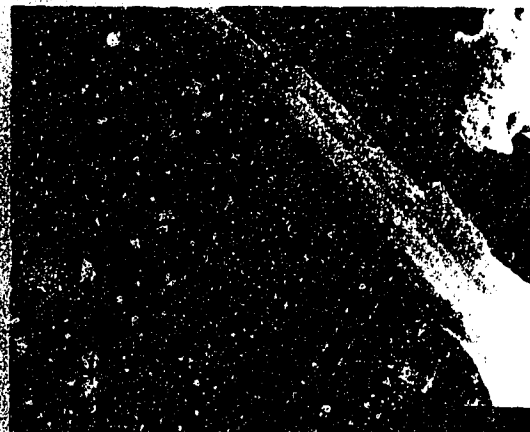
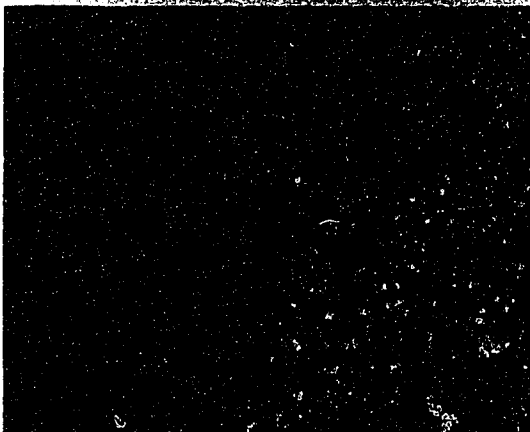
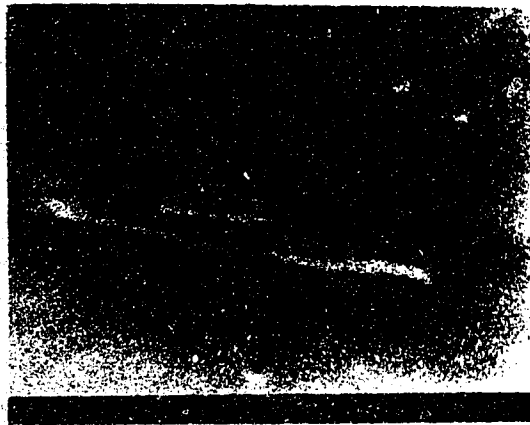


Plate 5.3. Scanning electrons micrographs of material retained on 0.2 μ m filters from both spring and fall samples of interstitial waters from within the ferrihydrite band of a Terric Fibrisol pedon.

- a) Bacterial form with a mucilagenous coating high in Fe, with minor amounts of Si and Al.
- b) Bacterial form with a mucilagenous coating high in Fe.
- c) Bacterial adhering to calcite fibres coated with almost pure ferrihydrite.
- d) Bacterial coating of almost pure Mn oxyhydroxide.
- e) Doughnut arrangement of ferrihydrite material possibly formed from a coated coccoid colony.
- f) Ferrihydrite coated bacterial rods welded into an incipient rope structure as illustrated in 5.1.

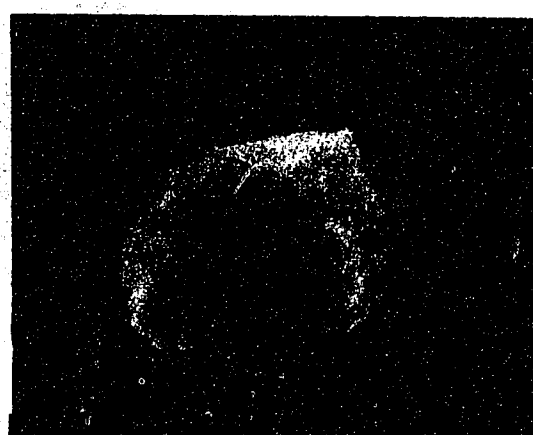
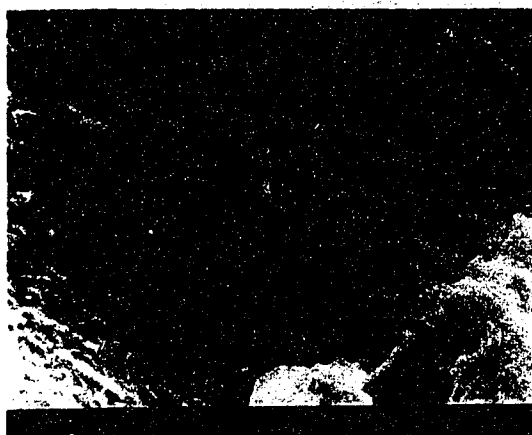
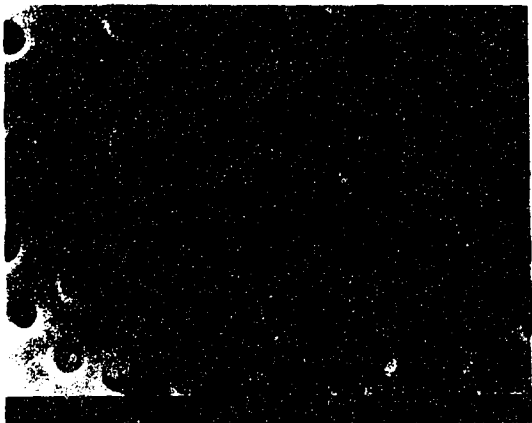


Plate 5.4. Scanning electrons micrographs of microstructures observed in the ferrihydrite material from the band sampled from the Terric Fibrisol pedon following heating to 1000 C for 5 hours in an oxygen atmosphere.

- a) Globules of annealed 10-50 nm globules of iron oxide.
- b) Globules of annealed 10-50 nm globules of iron oxide forming a tubiform structure.
- c) Cross-section of a 1 μm diameter tube comprised of welded 5-20 nm spherical structural units.
- d) Open mesh-like structure of fine tubiform filaments.
- e) Fine rod feature which may be precursor of mesh structure in d).
- f) Hematite formed from more muciligenous or gel-like precursor.

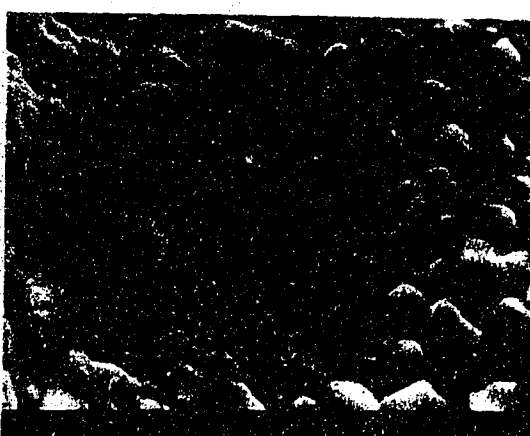
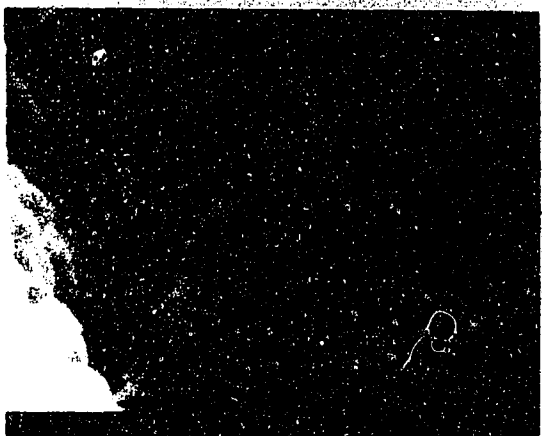
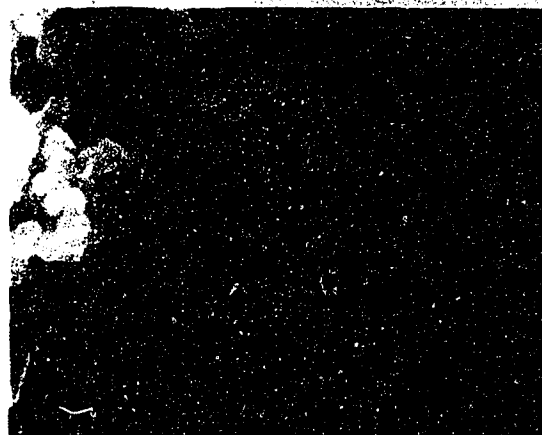
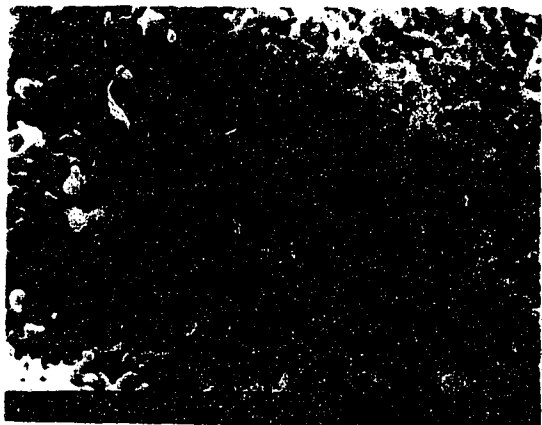


Plate 5.5. Transmission electron micrographs of both impregnated, stained ferrihydrite and fresh whole mounts of material grown at the water-air interface in the laboratory from interstitial solutions sampled from the band sampled within the Terric Fibrisol pedon.

- a) Mixture of small (5-20nm) ferrihydrite globules and acicular forms.
- b) Amorphous groundmass, with 5-10 nm fibrils present on upper edge.
- c) Coccoid form appears as nucleating point for ferrihydrite precipitation, with the groundmass structure being similar to that documented for imogolite and fibrous microcrystalline goethite.
- d) Acicular ferrihydrite crystals, with coccoid form as nucleating site (right).
- e) Hollow tubules of ferrihydrite (20-40nm diameter), with small globules forming groundmass (5 nm diameter).
- f) Acicular ferrihydrite crystals.

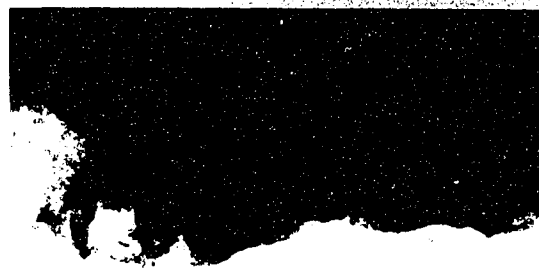
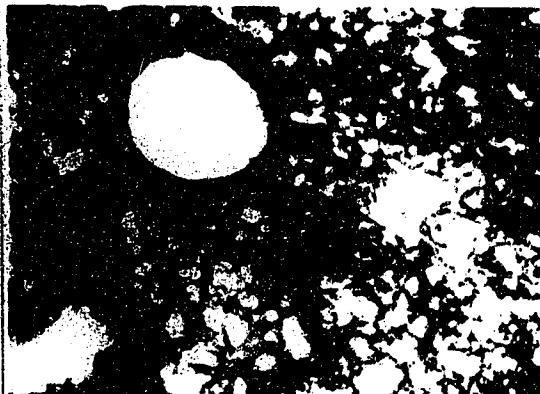
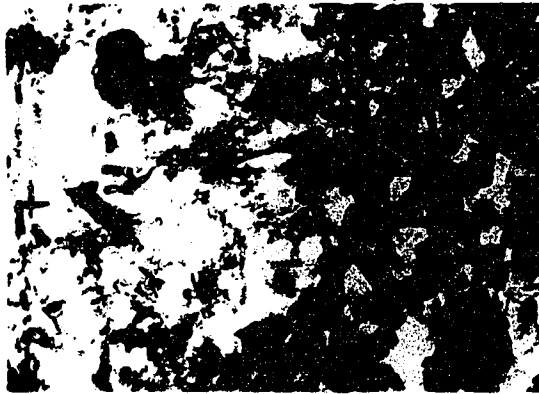
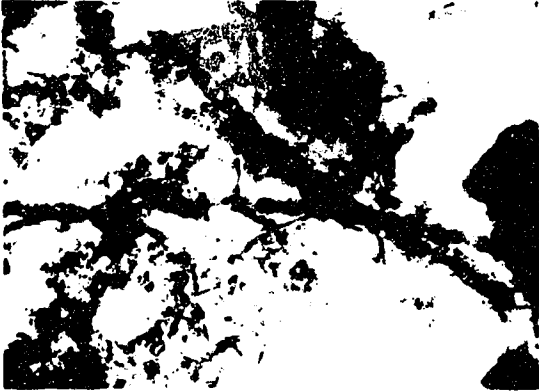
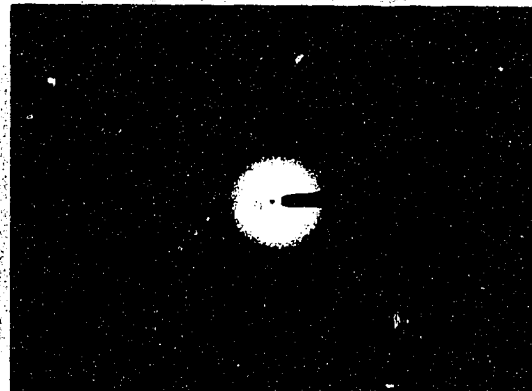
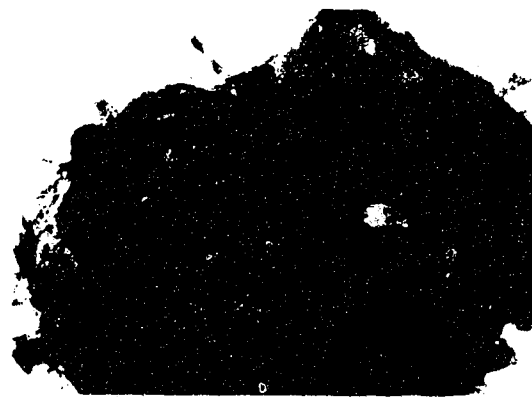
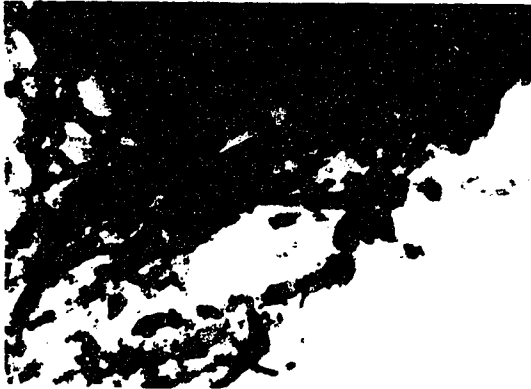


Plate 5.6. Transmission electron micrographs and electron diffraction patterns of fresh whole mount material grown at the water-air interface in the laboratory from interstitial solutions sampled from the band sampled within the Terric Fibrisol pedon.

- a) Electron diffraction pattern of pure ferrihyrite.
- b) Electron diffraction pattern of pure ferrihyrite superimposed on a calcite lattice.
- c) Location of a).
- d) Mixture of secondary calcite crystallites with ferrihydrite globules and coccoid host forms.
- e) Ferrihydrite encasing a tube of calcitic fibres, with some small globules (5-10 nm) of material adjacent fibre.
- f) Ferrihydrite tubular forms without a calcitic core.



6. OVERVIEW OF THESIS

6.1. CONCLUSIONS:

The results of the individual research chapters may be summarized as follows:

6.1.1. Authigenic Mineral Formation During Solodization.

In this chapter the transformations and translocations occurring during pedogenesis within the solodized zones of both a Black and a Brown Solodized Solonetz pedon were examined. Mineralogical, solution chemical and micromorphological data were discussed in terms of preferential translocation of individual phyllosilicate minerals, and neo-formation of both crystalline and poorly crystalline aluminosilicate minerals.

Specifically, mineralogical and micromorphological examination of Solodized Solonetz pedons show the presence of both crystalline and non-crystalline authigenic minerals in the Ae horizons and the solodized zones of the columnar Bnt horizons. A zeolite mineral with the characteristics of clinoptilolite was detected in the coarse clay (1.0-2.0 μm) separates and was the mineral species dominant in the <2.35 specific gravity separates of the fine (2.0-5.0 μm) and medium (5.0-20.0 μm) silt fractions. Measurement of pH (1.0M NaF) of whole soil samples from the solodized zone of these pedons indicated the presence of high levels of active aluminum. Treatment with acid ammonium oxalate and hot 0.5M KOH indicated that the poorly crystalline material was composed predominantly of silicon, aluminum and iron. Differential FT-IR analyses of these clay fractions before and after the chemical extractions indicated that components of this phase have characteristics reported for both opaline silica and allophane.

6.1.2. Isotopic Evidence For Clay Mineral Weathering And Authigenesis In Luvisolic Soils.

This chapter focuses on the phyllosilicate mineralogy of two Luvisolic pedons with parent materials of different provenance. The objectives were to compare and contrast the

relative mobilities of the individual phyllosilicate species both within and between the pedons, and to utilise the ^{18}O geochemistry to decipher the possibilities for both crystalline and poorly crystalline aluminosilicate authigenesis.

Clay mineral distribution and weathering were studied in two Cryoboralf pedons developed on texturally different tills in northeastern Alberta, Canada, to elucidate authigenic mineral formation in these soils. The crystalline clay minerals were identified by X-ray diffraction analyses, and quantified by analyses for cation exchange, surface area and elemental content. The total non-crystalline clay component was determined using selective dissolution treatments. The crystalline clay suite of the parent materials consisted of an admixture of smectites, kaolinite, dioctahedral mica, and chlorite. Beidellite and montmorillonite were both identified as components of the smectite group. Kaolinite was negatively enriched in the Ae horizons in all clay size separates, whereas mica and smectites were enriched in the Bt horizons as a result of lessivage. Routine chemical and mineralogical characterization suggested apparent neoformation of beidellite in the Ae horizons of these pedons. As the detrital crystalline clays in these soils are isotopically distinct from any neoformed clay species, the ^{18}O content of both crystalline and poorly-crystalline clay species was used to explain the observed clay mineral variations within the soils. The ^{18}O content of the crystalline clay separates indicated the observed inter-horizon variability in content of the individual phyllosilicate mineral species was a result of physical translocation rather than authigenesis. The interpretation of neoformation of a high charge smectite (beidellite?) in Ae horizons was not supported by the ^{18}O data. Changes in measured ^{18}O content of clay separates following selective dissolution provided evidence, however, of authigenic poorly crystalline components. Intra-profile variation in the ^{18}O signature of the authigenic clays was explained in terms of evaporative effects on ^{18}O enrichment of the soil water.

6.1.3. An Examination Of The Mobile Colloidal Phase In A Luvisolic Catenary Sequence.

Both static and dynamic approaches to the study of soil genesis were combined in this chapter in an endeavour to define the pedogenic mineralogic translocations that have occurred within soils of a Luvisolic catenary sequence, and to establish the exact nature of the contemporary mobile colloidal phase.

Clay mineral distribution was examined within pedons from a Luvisolic (Cryoboralf) catenary sequence by X-ray diffraction analysis, and quantified by analyses for cation exchange, surface area and total elemental content. The crystalline clay suite of the parent materials, as typical of Alberta soils, consisted of an admixture of smectites, kaolinite, dioctahedral mica, and an iron-rich chlorite. The minerals of the smectite group consist of an admixture of high- and low-charge species, with the iron-rich phase isolated by magnetic separation having the diffraction characteristics of nontronite. The characteristics are analogous to the 'beidellite-phase' suggested in the earlier chapters of this document. Kaolinite was negatively enriched in the upper pedon (Ae horizons), with dioctahedral clay mica and smectites were enriched in the Bt horizons. X-ray diffraction, in-situ microchemical and micro-structural analyses of the cutanic materials from throughout the pedons indicated that montmorillonite, mica and kaolinite were all equally mobile within the modern soils. Montmorillonite is, however, the most abundant phyllosilicate species present in the modern cutans.

Examination of the solid material in leachates collected from a series of gravity lysimeters installed below the Ae and AB horizons provided an insight into the nature of the contemporary phases. Kaolinite, mica and smectite were all shown to be present in the phyllosilicate fraction, with a considerable quantities of 1.5 to 10.0 μm diameter quartz and feldspar grains. The silt grains were most abundant in spring collections, and were commonly observed in microstructural examination of cutanic features in the Bt2 and BC horizons. The

ubiquitous occurrence of algal stomatocysts in colloidal leachate materials from the lysimeters has not previously been observed in soil waters to the author's knowledge. Chemical extractions indicated the presence of both poorly crystalline aluminosilicate and ferrihydrite species, along with a significant component of organically-complexed Al and Fe.

Infrared spectroscopic examination of the colloidal material in the leachates suggested a marked seasonality in the migration of individual organic compounds or organo-clay complexes. The contents of low molecular weight aromatics were low in all spring collections, increasing with increasing content with summer precipitation events. Maximum levels of lignin degradation products, for example, were consistently found in late fall samples. The seasonality of movement of the specific organic groups is assumed to reflect the dynamism of faunal and floral decomposition processes in the Boreal ecosystem.

6.1.4. Ferrihydrite At The Mineral-Organic Interface: An Examination of Composition and Form.

During a series of field surveys small areas of Terric Fibrisol were mapped on levées several metres above modern drainage channels. Bands of an iron oxyhydroxide material were consistently observed at the interface between the peaty material and the underlying calcareous mineral parent material, an environment not typically described for the occurrence of ferrihydrite. Accordingly the objective of the final research chapter was to provide a detailed description of the environment of formation, coupled with the chemistry, morphology and structure of the ferrihydrite deposit.

X-ray diffraction analyses indicated that the band was a 6-line ferrihydrite with a 25 C Mössbauer spectrum similar to that described in the literature. On heating to 1000 C the ferrihydrite was converted to a mixture of hematite and maghemite. These mineralogical transformations with heating may, in part, support suggestions that presence of maghemite in

Prairie soils is a product of periodic fire. The adsorbed silica phase formed a mixture of cristabolite and opal-CT. Chemical analyses of water collected from the within the ferrihydrite band indicated an oxidizing microenvironment, with calculated ion activity products indicative of supersaturation with respect to amorphous $\text{Fe}(\text{OH})_3$. In addition to Fe (43%), the ferrihydrite contains Ca (4%), Si (5%) and is enriched in several trace elements, namely As, B, Ba, Co, Cr, Mo, Sr, U and Zn. The porous, vughy ferrihydrite displayed a diversity of microstructures, under both optical and electron optical examination, which were associated with minor compositional variations. The hollow tubular forms, for example, contained more Si and Al, based on EDS analyses, than the bacterial rod-like forms and globular structures. Examination of colloidal features from the interstitial waters indicate presence of a range of bacterial forms which serve as nucleation sites for precipitation of calcite and ferrihydrite. The manganese-rich bacterial casts were distinct from iron-rich forms, indicative of a microbial species-mineral inter-relationship.

Examination of mounts by STEM confirmed both a bacterial-mineral and mineral-mineral interaction in the formation of constituents of the ferrihydrite band. Although encapsulated bacterial coccoid forms of ferrihydrite were observed, there were no obvious encapsulated filamentous bacterial forms. Acicular calcite needles were observed to be functioning as nucleation sites for a chemical precipitate of ferrihydrite.

6.2. SYNTHESIS:

Much of the research component of the current thesis has been directed at elucidating the differential mobility of phyllosilicate mineral phases within selected lessivage soils. These soils fall into two distinct orders based on the nature of their parent materials, namely the Solonetzic and Luvisolic Orders. Sites sampled for soils of each Order range from over two distinct Albertan soil-climate zones. The Solonetzic soils were, for example, sampled from both the

Brown and Black soil-climate zones. The Luvisolic soils, whilst being all Orthic, or a Gleyed catenary associate, were sampled from sites several hundred kilometres apart. Much of the region of northern Alberta where the soils bordering the Kinosis and Legend map units are Organic Cryosols of the discontinuous permafrost zone. Within a few kilometres of the Legend site, at essentially the same elevation, were mineral soils with ice at depth during the sampling season, and associated upland peats over permafrost.

Interestingly, the relative mobility of the individual phyllosilicate minerals within all the pedons examined over this relatively extensive climatic range developed on diverse parent materials, ranging from acidic to calcareous to saline-calcareous, was essentially identical. All of the B(n)t horizons were enriched in smectite species relative to the parent materials. The surface mineral, or Ae, horizons were negatively enriched in kaolinite and micaceous species. This was, however, not merely a reflection of relative mobility of the fine clay ($<0.2 \mu\text{m}$) fraction as there was a significant variation with depth of relative species abundance within the fine clay in the Ae, B(n)t and C(sa)(k) horizons. Although distinct high- and low- charge smectite phases were identified in all parent materials, these phases exhibit an apparent differential mobility during soil development. The low-charge (or montmorillonite-like) species are more mobile than the high-charge (or beidellite- / nontronite-like). Evidence from Mössbauer spectroscopy, coupled with X-ray diffraction and infrared spectroscopy of magnetically separated clay separates, indicates the presence of a smectite phase which tends towards a nontronite. Chemical microanalysis demonstrated that the total magnetically separated phase had about 12 - 20 % iron, with separation of a pure smectite phase not being attempted.

Although such a depth diversity in diffraction behaviour on which the preceding interpretations are based has been assigned by other researchers to mineral weathering and/or authigenesis, the isotopic chemistry data obtained in one phase of the current thesis definitively

discounts such an hypothesis. The isotopic data did, however, provide information on the evaporative controls on the formation of the minor amounts of authigenic poorly-crystalline aluminosilicates present in the pedons. These authigenic poorly crystalline aluminosilicates were identified in all of the lessivage soils examined.

The mineralogic data obtained from the longterm dynamic study of the catenary Luvisolic sequence added considerably to that obtained in a previous dynamic study in the region. The mineralogic data reported in the thesis provide evidence for the migration of both phyllosilicate and non-phyllosilicate phases in the colloidal component of modern throughflow. Under current climatic conditions kaolinite, dioctahedral mica and smectite are all mobile, as are fine silt sized quartz and feldspar grains. The latter observation explains the reported presence of such grains in cutans of lessivage soils. The relative higher abundance of the high-charge over the low-charge smectite species in the colloidal leachates is in contrast to all the static data presented in the chapters of this thesis. However, as the Ae horizons are now depleted in the low-charge species, perhaps the low ionic strength of the modern soil solution encourages the dispersion of the high-charge species.

The recognition of stomatocysts, or resting stages of Chryosphyaceae, of essentially pure amorphous silica composition in the lysimeter colloctions may suggest a mechanism for the translocation of weathering products within a pedon previously unrecognized. The recent observations of related organisms in Podzolic systems tends to reinforce the suggestion. Perhaps the models of Si-Fe-Al translocations as either inorganic or organic complexes may be expanded to include the profound influence of organisms observed in the dynamic studies of the current thesis.

The genesis of authigenic crystalline aluminosilicate minerals has not previously been examined in the lessivage soils of the Canadian Prairies. Data presented in the preceding

chapters presents unequivocal evidence for the both the formation and the weathering of clinoptilolite, a zeolite mineral previously considered to be an allogenic soil mineral in studies documenting occurrence in saline soils elsewhere in the world. It appears, however, based on both modelling of soil solution data from long term incubations and from electronoptical observation that the zeolite mineral precipitates at the Bnt-Ae interface and dissolves in the Ae-Ahe horizons. The recognition of the presence of the clinoptilolite may aid in explaining anomalous response to fertilization of Solonchaks soils because the NH_4^+ ions are adsorbed within the hollow zeolite structure. Thus the routine acid extractions for fertility determinations do not measure the true N-fertility status of the soil. The problem is, however, further compounded when an alkaline extractant is used for fertility assessment. An alkaline extractant (eg. NaHCO_3) could partially dissolve some of the zeolite mineral and, again, provide anomalous estimates of the N-fertility status. Complete dissolution of clinoptilolite in a low density medium silt concentrate was achieved in both warm NaHCO_3 and KOH as part of the characterization of the mineral. A similar problem must also exist with acid and/or alkaline extractants in the assessment of P-status, because of the fixation by the poorly-ordered aluminosilicate of the PO_4^{3-} . The latter problems in fertility assessment must also exist because of the significant component of poorly-ordered aluminosilicates estimated to be present in Luvisolic soils.

In recent years, since the initial definition of ferrihydrite as a distinct mineral phase by Chukrov, there have been numerous reports in the literature of occurrence in soils. There have been techniques developed, such as differential X-ray diffraction or Rietveld diffraction profile reconstruction, to enable the routine identification of small (<5%) quantities in soil and geologic materials. Ferrihydrite is now assumed to be a precursor the pedogenic neoformation of minerals such as hematite and goethite. Much of the ferrihydrite research has, however, focussed on synthetic material for use in, for example, crystallographic or ion (eg As, Cd, Cu, Pb) adsorption studies

in order establish complexation constants to enable the modelling of the fate of pollutants in natural ecosystems. The material described in the current thesis has been, or is being, used as a natural analogue in adsorption studies in at least three universities at present.

In spite of such a flurry of activity in the ferrihydrite arena, there is a paucity of detailed examination of natural material, of the environment of formation, of the composition especially as related to adsorbed and/or structural inclusions of trace elements, or of detailed particle morphology. This thesis attempts to address this deficiency by presenting a detailed examination of the morphology of natural ferrihydrite. The morphological examination provided evidence of at least two distinct forms of the mineral at the sites examined, namely one of apparently chemical origin, and one of microbiogeochemical origin. The chemical form precipitates directly on fine acicular calcite lathes, whereas the biological form encapsulates bacterial rods to form sinusoidal hollow tubules. Such biological forms have recently been observed in very acid environments characteristic of acid mine drainage.

6.4. RESEARCH RECOMMENDATIONS:

The objective of this section of the thesis is to briefly overview 'gaps' in our knowledge of the genetical processes of the leaching soils of Western Canada, or in general, and suggest how the knowledge barrier may be lifted. In hindsight, the major facet of information lacking to aid in the elucidation of the genetical processes related to the movement of clay minerals in the soils of Western Canada is the paucity of knowledge of the actual crystal, or compositional, chemistry of the individual clay minerals present in the soil parent materials.

The coupling of differential X-ray diffraction with detailed structural analysis using techniques such as Rietveld analysis could be utilized to obtain information on the nature of the kaolinite minerals, which are known to be b-axis disordered, for example. Comparison of the differential pattern with calculated diffraction profiles for structural models based on defect

structures should provide information on the structural integrity of the kaolinite species. Such analysis may indicate a depth phase differentiation within the kaolinites analogous to that documented in this thesis for smectites.

Data on the surface charge density of the clay mineral phases would be very useful in aiding in the differentiation of the apparent high-charge and low-charge smectite phases, especially if obtained on phases separated on the basis of their magnetic susceptibility. As the chlorite in the soils is known to be iron-rich, magnetic purification of small quantities would enable definition of crystal chemistry, and thus elucidation of structure and surface charge characteristics.

Detailed lysimetric studies with both gravity and tension lysimeters placed at a greater range of depths than employed in the current study are needed to enable further differentiation of the relative mobilities of individual species with depth. The added chemical information obtained from the tension lysimeters could be utilized for geochemical prediction of mineral precipitation / dissolution reactions. Such information could be coupled with that obtained by immiscible displacement to enable a simulation model of the processes of pedogenesis. Lysimetric studies would also enable the detailed definition of the seasonality of movement of silica in the stomatocysts. Ongoing submicroscopic examinations in which quantification is being completed, numbers as high as 200 organisms per 1000 μm^2 have been observed. Over pedogenic time this must account for the mobilisation of a considerable amount of silica. High resolution electron microscopic and EDS examination of the colloidal organo-clay complexes could also be initiated.

Laboratory analogue studies utilizing calcareous and saline-calcareous parent materials could help explain the apparent differentiation of the smectite phase mobility. The effect of seasonal surface horizon saturation on the relative mobility of individual phyllosilicate species

could be examined by utilizing such controlled laboratory experiments in which redox potential was monitored. The effect of surface acidification by either fertiliser or precipitation in analogue studies could also provide information which will prove crucial to the understanding of the processes maintaining an evolving soil resource. Studies of soil solution chemistry following fertiliser amendment must, in the long term, provide a more accurate measure of soil fertility status, as the soil solution provides the nutrient pool from which the plant must obtain necessary supply.